Air Motion and Thermal Environment in Pig Housing Facilities with Diffuse Inlet

Jacobsen, Lis

Air Motion and Thermal Environment in Pig Housing Facilities with Diffuse Inlet

PhD Thesis
Defended in public at the Danish Institute of Agricultural Sciences
Research Centre Bygholm
(131206)

Lis Jacobsen

ISSN 1901-7294
DCE Thesis No. 15

AALBORG UNIVERSITY
Department of Civil Engineering

Aalborg University
Department of Civil Engineering
Architectural Engineering

DCE Thesis No. 15

Air Motion and Thermal Environment in Pig Housing Facilities with Diffuse Inlet

**PhD Thesis defended in public at the
Danish Institute of Agricultural Sciences
Research Centre Bygholm
(131206)**

by

Lis Jacobsen

December 2006

Scientific Publications at the Department of Civil Engineering

Technical Reports are published for timely dissemination of research results and scientific work carried out at the Department of Civil Engineering (DCE) at Aalborg University. This medium allows publication of more detailed explanations and results than typically allowed in scientific journals.

Technical Memoranda are produced to enable the preliminary dissemination of scientific work by the personnel of the DCE where such release is deemed to be appropriate. Documents of this kind may be incomplete or temporary versions of papers—or part of continuing work. This should be kept in mind when references are given to publications of this kind.

Contract Reports are produced to report scientific work carried out under contract. Publications of this kind contain confidential matter and are reserved for the sponsors and the DCE. Therefore, Contract Reports are generally not available for public circulation.

Lecture Notes contain material produced by the lecturers at the DCE for educational purposes. This may be scientific notes, lecture books, example problems or manuals for laboratory work, or computer programs developed at the DCE.

Theses are monograms or collections of papers published to report the scientific work carried out at the DCE to obtain a degree as either PhD or Doctor of Technology. The thesis is publicly available after the defence of the degree.

Latest News is published to enable rapid communication of information about scientific work carried out at the DCE. This includes the status of research projects, developments in the laboratories, information about collaborative work and recent research results.

Published 2008 by
Aalborg University
Department of Civil Engineering
Sohngaardsholmsvej 57,
DK-9000 Aalborg, Denmark

ISSN 1901-7294
DCE Thesis No. 15

Air Motion and Thermal Environment in Pig Housing Facilities with Diffuse Inlet

Dissertation By Lis Jacobsen

Danish Institute of Agricultural Science, Bygholm, Denmark.

Preface

Production conditions of livestock animals have changed very much over the last century regarding housing conditions, heard size and production level. Also the working conditions for stockmen have developed from part time to full-time occupation.

New production methods that imply large production units, more wet conditions in the animal houses and the absence of bedding materials increase the need for climate control to provide acceptable climatic conditions and air quality for comfort and welfare of the animals. The working environment for the stockmen also has to be taken into consideration in terms of dust load and air contaminant concentrations. Some of the control problems of different ventilation systems have been related to the spatial and temporal variance in thermal conditions due to location and regulation of the ventilation equipment. Downfall of cold inlet air from ventilation inlet openings into the occupational zone of the animals and inadequate mixing or supply of fresh and uncontaminated air was some of the problems addressed. The subject of this thesis is the diffuse ceiling ventilation system that was based on a demand for stable thermal climate over time and space.

The present Ph.D thesis, including 5 supporting papers and 2 appendices, is submitted in partial fulfilment of the requirements for a Doctor of Philosophy (Ph.d.) degree. This thesis covers documentation of the environmental conditions in a diffuse ceiling ventilated pig housing facility. The methods used is both experimental and numerical. The work has been performed on Danish Institute of Agricultural Sciences (DIAS) under supervision of Prof. P.V.Nielsen Aalborg University and Senior Scientist S.Morsing, DIAS. I thank senior scientists Guo-Qiang Zhang and lector Bjarne Bjerg

for valuable comments to the manuscripts. Also thanks to friends, family and the colleges at Bygholm for support and encouragement.

Summary

A ventilation system with ambient air supply through diffuse ceiling used in pig production facilities is presented. The climatic conditions were examined both experimentally and numerically in an full scale experimental room and the inlet boundary conditions of the diffuse inlet were examined in a wind tunnel model.

In the full scale experiments the focus has been on the correlation between variations in ambient climatic conditions and changes in environmental condition in the occupational zone. It was found that the environmental conditions in the occupational zone were independent on changes in ambient temperature and air exchange rate.

The effect of housing equipment on environmental conditions has been examined both experimental and numerically and it was found that impervious housing equipment has a significant effect on the climatic conditions close to the wall in the occupational zone.

The wind tunnel experiments show that the diffuse material works as a heat exchanger and preheats the inlet air if the temperature in the room is higher than the inlet air. The result of the experiment is that the heat exchanging function of the inlet boundary surface is dependent on flow velocity and radiative conditions in the room. The experiments show that a wall boundary condition of no-slip does not apply at the surface of the diffuse material, since there can be some penetration depth of the boundary layer into the porous material.

The preheating effect is significant to the correct estimation of thermal comfort in terms of the operative temperature of the occupational zone. A model of the boundary

condition of the diffuse inlet is necessary because the inlet is a conglomeration of an inlet and a wall boundary condition. Two methods of modelling can be chosen, a model based on the determination of radiative and convective material properties of the diffuse material, or a model based on empirical determination of the inlet surface temperature. The latter is chosen because it gives a better understanding of the physical interactions between the room climate conditions and the inlet flow velocity and temperature. A linear approach has been taken to develop a model of the surface temperature from experimental data of the independent parameters of flow through the diffuse material and flow and radiation properties in the occupational room.

Sammenfatning (Danish Summary)

I talrige danske svineproduktionsanlæg anvendes et ventilationssystem med friskluftindløb gennem et diffust materiale i loftet.

Denne afhandling undersøger de klimatiske forhold en fuldskala model af en diffust ventileret svinestald ved numerisk simulering (CFD) og eksperimentelt. I et vindtunnelforsøg er undersøgt de termiske forhold ved det diffuse indløb, som funktion at de termiske og strømningsmæssige forhold i indløbet og lokalet.

I fuldskalamodel forsøget har fokus været sammenhængen mellem ændringer i omgivelsernes klima og klimaændringer i staldlokalet med diffus ventilation. Resultaterne viser at klimaforholdene i lokalet er uafhængige af ændringer i omgivelsernes temperatur og luftskiftet i det diffuse ventilerede rum.

Effekten på klimaforholdene i lokalet fra en delvis ruminddeling i stiafsnit er blevet undersøgt både eksperimentelt og med CFD. Resultaterne viser at ruminddeling kan have en statistisk signifikant forskellig effekt på de klimatiske forhold i lokalet.

En detaljeret undersøgelse af de fluidmekaniske og termiske omgivelsers effekt på de termiske forhold ved det diffuse indløb er blevet udført i en vindtunnel. Forsøgene viser at det diffuse materiale virker som en varmeveksler og forvarmer indløbsluften, hvis rumtemperaturen er højere end indløbstemperaturen. Varmeveksler effekten, og dermed den termiske randbetingelse for det diffuse indløb, er afhængig af lufthastighed og -temperatur i både indløb og i lokalet samt termisk stråling fra lokalet. Ud fra målingerne kan det konkluderes at en no-slip randbetingelse i det diffuse materiale ikke kan antages og at der vil være en indtrængning af luft fra lokalet ind i det diffuse materiale, selvom det er modsat den af ventilationsanlægget dikterede gennemløbsretning.

Iagttagelse af ovenstående forvarmning af indløbsluften i det diffuse materiale er en grundlæggende forudsætning for korrekt estimering af dyrenes termiske komfort i lokalet. En simulering af den termiske komfort forudsætter ligeledes at randbetingelsen for det diffuse indløb er korrekt defineret. Randbetingelsen kan defineres på to måder: en deterministisk metode baseret på fastlæggelse af termiske, konvektive og strålingsfysiske materiale parametre for det diffuse materiale, og en empirisk model af indløbstemperaturen. I projektet er det valgt at udvikle en empirisk model for randbetingelsen ved det diffuse indløb fordi en model giver en bedre forståelse for samspillet mellem de fysiske variable. En lineær model for overfladetemperature på det diffuse materiale er udviklet.

Table of Contents

1 Introduction

The diffuse ceiling ventilation system is a ventilation technology that has successfully been used in agriculture in Denmark for a decade. Until now very few investigations of the environmental conditions in the occupational zone of the animals and the characteristic function of the diffuse ceiling has been performed and published.
The diffuse ceiling ventilation room has the potential of more widespread utilization among which examples could be: open landscape office buildings, schools, utility stores, indoor sport arenas etc. Knowledge about the environmental conditions and thermal regulation performance of the diffuse ceiling ventilation system is prerequisite to the introduction of the system in new environments.

1.1 Objectives of the study

The aim of this study was to examine the environmental conditions in the occupational zone of the animals in a room with a diffuse inlet ventilation system. The objective of a swine housing ventilation system is to keep environmental conditions in the occupational zone at predefined levels of temperature, humidity and air contaminants (CO_2) independent on the ambient climate conditions. The diffuse ventilation system capacity to meet these requirements are examined in terms of keeping the room temperature setpoint in the animal occupational zone. The reproducibility of the experimental results with simplified numerical models was examined. The inlet boundary conditions of the diffuse material was examined experimentally. A stochastic model of the thermal inlet boundary condition was developed based on the experimental results.

1.2 Materials and methods

The diffuse inlet ventilated room was examined both experimental and numerically. The numerical part was based on deterministic modelling of the mass- energy- and momentum relations in the room. The accuracy of numerical models is primarily restricted by the adequate and accurate description of boundary conditions of the calculation domain. In a diffuse inlet ventilation system, like the diffuse inlet ceiling, the boundary conditions of the diffuse inlet are dependent on thermal- and air velocity- conditions in the room. Hence it was difficult to formulate the boundary conditions of the diffuse inlet without knowing the climatic conditions in the room. The calculation domain could be expanded to include the diffuse material, but the geometrical complexity of the diffuse inlet matrix makes it impossible to include the diffuse material as a part of the calculation domain. An approach where either material parameters are included in a deterministic model or a model of the boundary condition based on stochastic modelling or empiric data must be pursued. In the following paragraph some of the attempts in literature to develop a deterministic model based on material parameters are discussed. The experimental part of this study was focused on the effect of the diffuse ventilated room on climate conditions in the occupational zone and the development of a stochastic model of the diffuse inlet boundary condition. The experiments are performed in a full scale room and in a wind tunnel system.

1.3 Outline of the dissertation

The dissertation is a collection of papers of the experiments and simulations conducted during the research period. To avoid extensive repetition of the material presented in the papers a short resume of the content and conclusions of each paper is

presented in the relevant chapters of this dissertation with reference to the paper in concern.

The detailed objective for the included papers were:

Paper 1:

To investigate the relations between the selection of environmental setpoints and the resulting energy consumption and indoor environment, through a simulation of energy- and mass-balances in the room. What are the annual effects on air quality and energy consumption of changing the temperature setpoints?

Paper 2:

To compare the energy consumption of a pig house in different climatic zones dependent on the selection of environmental setpoints formulated as a sum of temperature (ºC) and relative humidity (%RH).

To investigate the effect of humidity and temperature conditions on energy consumption. What is the change in energy consumption for ventilation and heating when changing the setpoint sum of temperature and humidity?

Paper 3:

To investigate the thermal conditions close to the floor and ceiling in a diffuse ventilated room with pig- and supplemental heating sources in a fullscale experimental room.

To compare the measuring results with simulations on a similar room with simplified boundary conditions. How does the simulations results compare to the measuring results in locations close to the floor and ceiling?

Paper 4:

To investigate the effect of changes in inlet velocity, inlet temperature and pen partitions, on the thermal conditions in the occupational zone. Is the thermal

environment in the diffuse ventilated room dependent on the inlet conditions? Does pen partitions effect the thermal conditions in the occupational zone?

To compare the measuring results with simulations on a similar room with simplified boundary conditions.

Paper 5:

To investigate the thermal boundary condition of a diffuse inlet as a function of the inlet velocity and temperature, room velocity and temperature and thermal radiation sources. Does the non-slip boundary condition apply to the surface of the duffuse inlet? How is the downstream surface temperature dependent on inlet and room velocity and temperature

2 Background

This study concerns the diffuse ceiling ventilation system for pig housing. Diffuse ventilation with a clean air supply through the entire ceiling, is installed in more than 60% of the finishing pig housing in Denmark. An inlet diffuser covers the entire ceiling in the occupational room, inlet air flows vertically through the diffuse material supplying the upstream surface of the diffuse inlet with “unconditioned” fresh ambient air. The flow through the diffuse material is controlled through regulating the negative pressure in the diffuse room relative to the ambient pressure. Thermal conditions and air motion patterns in the occupational room influence the downstream surface boundary condition of the diffuse material.

The exhaust air is typically extracted through a central axial fan with a inlet opening 2-3 meters above the housing floor and a discharge above the roof . Other types of forced exhaust ventilation could also be utilized. Inside the housing, the room is divided in pens with the sectioning wall more or less diffusive.

The heating facility can be floor heating, irradiative topheating or strategically placed convection heating or a combination

The purpose of ventilation is to provide suitable environmental conditions in the occupied region for both livestock and personnel.

In the description of the diffuse ventilation it is feasible to separate the ventilation system into 3 separate regions Figure 2.1

- plenum
- diffuse ceiling
- ventilated room volume

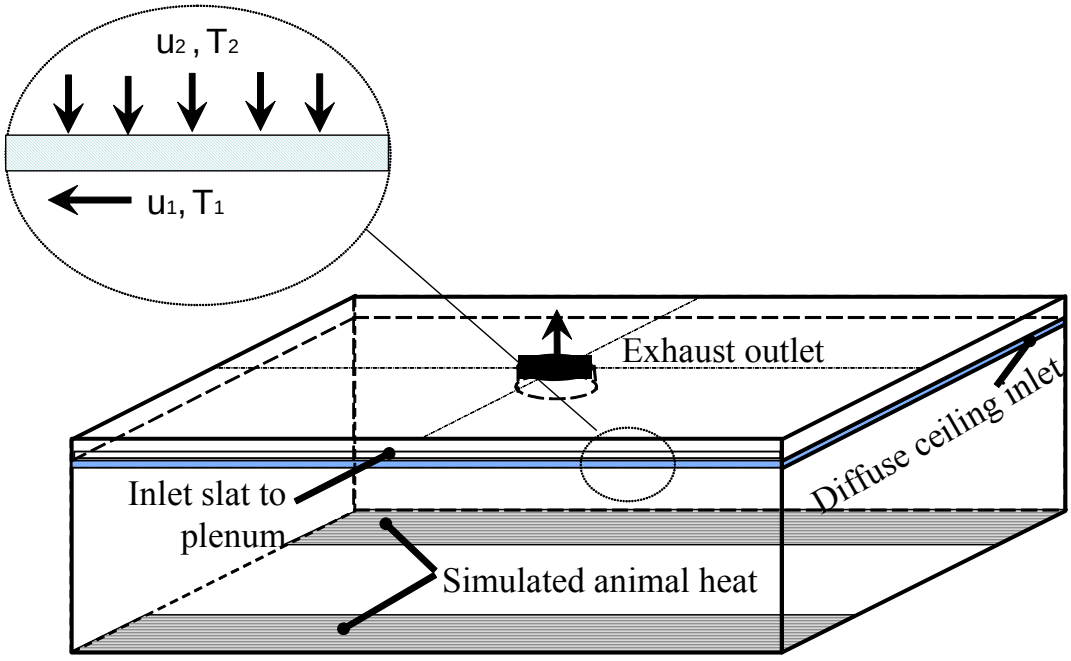

Figure 2.1: Diffuse ventilated room showing inlet to plenum, diffuse ceiling, animal heat simulators and exhaust outlet.

Plenum

The plenum is the space between the roof and the diffuse ceiling. The plenum have inlet openings to the ambient air. The inlet openings usually do not have mechanically driven air flow and the presence of air jets are limited to the forces associated with ambient air speed momentum and the negative pressure gradient from the diffuse

ceiling. The pressure difference over the diffuse ceiling regulates the ventilation air flux through the ceiling from the plenum.

Diffuse ceiling

The diffuse ceiling is the diffuse material that separates the plenum from the ventilated room volume. The diffuse ceiling should have a uniform pressure difference on the entire surface and uniform pressure resistance to allow a uniform air flux through the entire ceiling. The flow are governed by the negative pressure difference between the plenum and the ventilated room volume. The diffuse ceiling should prevent the presence of cold surfaces which could give an elevated radiation temperature difference between the animals and the ceiling surface.

Ventilated room volume

The ventilated room volume is characterized by very low inlet air velocity. In the diffuse ventilated room there is a absence of air jet momentum to move the fresh air flow, thus the air circulation in the occupation zone is dependent on the buoyancy forces. The flow velocity is low, except at the exit opening to the exhaust fan. The formation of large scale turbulence is dominant. The buoyancy forces level can depend on both activation of the heating system but also on the activity level and density of livestock and the potential thermal energy consuming processes (evaporation).

2.1 Animal housing

Animal housing systems consist of

- House envelope
- Environmental conditioning system

- Internal housing facilities (feeding-, cleaning-, pen partition- and management-system).

The house envelope is the building construction that physically is the demarcation between ambient and occupational zone in the building.

The configuration of the environmental conditioning system in a animal housing system is dependent on the species of animal and the production stage of the animal in the housing confinement. Some animal species are well adapted to unsteady environmental conditions through their physical properties while others are poorly equipped either by nature or from adaptation to production optimization requirements, such as low fat content in pig. Animals that are tolerant to environmental changes are kept in houses that comply with these conditions if this is economically profitable to the farmer. The heat loss from the animal is proportional to the energy consumption the animal has to consume to maintain its optimal body temperature (Pedersen and Sällvik, 2002). Heat energy loss from the animals is not a quantitative exploitable productivity parameter and therefore an economical loss to the farmer. All other parameters equal the heat loss is dependent on the age and weight of the animal (Strøm and Feenstra, 1980). Young animals emit relatively more heat energy pr. kg. weight than older animals. All though it could be economically attractive it is difficult to keep the animals under non heat loss conditions, and this would be in contradiction to the environmental conditions that comply with the thermal comfort requirements of the animals. The animals would die from hyperthermia under these conditions.

Thermal comfort

Thermal comfort is that condition of the mind that expresses satisfaction with the thermal environment and no regulatory response are required (Benzinger, 1978). Thermal comfort is controlled through the thermoregulatory system. The purpose of

the thermoregulatory system is to keep a constant internal temperature through the heat balance (Fanger, 1970). If the heat balance is dissatisfied the sensory organs will send impulse to the brain that will generate a response to correct the environment by behaviour.

The heat loss from the animals, like humans, determines the thermal comfort of the subject. Thermal comfort principles for humans can readily be transferred to pigs with few amendments. The thermal comfort principles for humans and animals are based on satisfying a energy balance where the variables to be taken into consideration are (EN ISO 7730, 1997; Fanger, 1970; Farge, 1972; Xin, 2005):

- Metabolic rate (activity),
- External work
- Thermal resistance of the clothing and the clothing rate
- Air temperature
- Mean radiant temperature
- Relative humidity
- Relative air velocity
- Partial water vapour pressure

From the above parameters it is possible to calculate the predicted mean vote (PMV) and the predicted percentage of dissatisfied individuals (humans) (PPD)(Fanger, 1970). The PMV is a index that predicts the mean value of votes of a large group of persons on a 7-point scale (from -3 to +3) and the PPD predicts the percentage of individuals that feel uncomfortably cool or warm. If all other parameters are equal the operative temperature can be used to evaluate the thermal environment at certain conditions (EN ISO 7730, 1997). The operative temperature is defined as the uniform temperature of a radiantly black enclosure in which an occupant would exchange the

same amount of heat by radiation and convection as in an actual non uniform environment. The operative temperature can be calculated as the mean value of air and mean radiant temperature:

$$t_o = At_a + (1 - A)\bar{t}_r$$

/ 2.1

Where t_o is the operative temperature, t_a is the air temperature and mean radiant temperature $\bar{t}_r$ and A is a function of the relative air velocity u_{ar} [m/s] where A=0.5 if $u_{ar}<0.2$, A=0.6 if $0.2<u_{ar}<0.6$ and A=0.7 if $0.6<u_{ar}<1.0$.

The heat energy is emitted from the animals as radiation, convection and conduction from the body surface and by respiration, hence the surrounding air and surface temperatures and velocities are important for the energy balance to be satisfied and to the animals perception of thermal comfort. The body heat energy balance can be expresses with:

$$Q_H = Q_{Esw} + Q_{Ere} + Q_R + Q_C + Q_D$$

/ 2.2

where Q_H is the internal heat production, Q_{Esw} is the energy loss through transpiration and evaporation, Q_{Ere} is the latent and dry respiration loss, Q_R is the radiative loss, Q_C is loss through convection and Q_D is loss through conduction. All the variables that influence the thermal sensation of the pigs can be regulated through the environmental control system or the construction of the occupational room of the pigs.

The difference between pigs and humans is primarily that pigs do not have the perspiration function and the clothing ability. Perspiration is a temperature regulatory function by evaporation that humans have, that is dysfunctional at elevated levels of relative humidity (Benzinger, 1978; Olsen et al., 2001; Sako et al., 2002). Pigs use

their dunging or wetting behaviour to create a evaporational temperature regulation, if pigs do not have the wetting facilities they are more sensitive to elevated temperatures than humans(Olsen et al., 2001). Pigs have a clothing ability of thermoregulation by increasing the fat content of the skin sub layer, but from a production perspective this is undesired, this means that the equivalent of a thermal clothing parameter should be a constant for pigs in a confined production facility.

Environmental conditioning systems

The environmental regulation system in pighouses consist of:

- ventilation system
- heating facilities
- cooling systems

Ventilation

Different ventilation systems like displacement-, mixing- and diffuse inlet ventilation systems are applied in pig housing facilities. .

Displacement ventilation systems seek to avoid any mixing of the air within the room and to rely on the buoyancy forces to establish a piston like movement of the air in the vertical direction. Rather than maintaining uniform air temperature and contaminant concentration in the room, vertical gradients of both temperature and contaminant concentration are allowed to develop.

Mixing ventilation consist of outlet fans to create underpressure in the room and inlet slots or side openings to provided the fresh air necessary to comply with the environmental requirements. The high momentum jet of uncontaminated inlet air through the inlet slots penetrates into the room and mixes with the contaminated air with the purpose to create a spatially constant temperature and contaminant concentration throughout the occupational zone to comply with the given

requirements of air quality. The problems related to a mixing ventilation system (MVS) and displacement ventilated system (DVS) are found to be temporal and spatial gradients of temperature and air contaminants (Bjerg et al., 2000; Gan, 2000; O'Shaughnessy et al., 2002; Wilhelm and McKinney, 2001; Zhang et al., 2003). Comparing the diffuse ceiling inlet ventilation system (DCV), (Aarnink and Wagemans, 1997; Wagenberg and Smolders, 2002) to the displacement and mixing ventilation system, the diffuse ventilation system is not as efficient to improve its air quality; it takes higher ventilation rates to reach the same contaminant level in the occupational zone with the DCV system than with the DVS. In a system comparison of the three above mentioned ventilation systems performed by Wagenberg and Smolders (2002) temperature in the occupational zone were less dependent on the air exchange rate in the room in the diffuse ceiling ventilation system than in the displacement or mixing ventilation system. Consequently the air exchange rate in the DCV system had to be increased compared to the DVS and MVS to meet the temperature demands of the climate controller. The temperature setpoints and the number and size of the animals were the same in all three systems.

Comfort and heating/cooling panel systems

The heat energy balance of a subject is dependent on conduction, convection and radiation. If there is a temperature difference between the object and the surrounding opaque surfaces there is a radiative heat energy transport. If there is a temperature difference between the object and the surrounding air there is a convective heat energy transport. And if the object is in physical contact with a solid surface of another temperature there is a convective heat energy transport. Dependent on the temperature difference between the surface of the room and the radiation emitting subject, the radiative energy transport can be of the same magnitude as the convective

energy transport. Where the energy exchange by convection between a object and the surrounding air varies linearly with the temperature difference, the radiative energy transfer between the object and the surrounding surfaces, through the Stefan-Boltzman law (Incropera and De Witt, 1990), varies with the 4. power of the temperatures. This means that particularly at low temperature differences the radiative energy transport becomes dominant compared to the convective energy transport (Holmberg et al., 2004). The diffuse ceiling has the same working fundamentals as cooling (or heating) panels. It must be assumed that the diffuse ceiling surface is colder than the other unheated surfaces in the room, because there is an inlet flow of cooler ambient air, hence the surface temperature of the diffuse ceiling is lower than the room temperature and the diffuse inlet works as a cooling panel. Cooling panels could have a beneficial effect on the climate in the pighouse that is not evident with a measurement of sensible air temperature. Several authors have examined the effect of utilizing radiant panels on thermal comfort. (Ardehali et al., 2004; Chen, 1990; Jiang et al., 1992; Kim et al., 2005; Rees et al., 2001). For cooling panels it was found that, compared to air conditioning with convective energy transport, the radiative energy transport gave better comfort (lower operative temperature,(EN ISO 7730, 1997)) at lower energy consumption. Other researchers (Kim et al., 2005).(Jiang et al., 1992) found that the cooling panels could reduce the vertical temperature stratification but also increase the air movement and contaminant dispersion in the room compared to a room ventilated by displacement.

2.2 Environmental control strategies

The climatic comfort in the pig house is regulated with environmental control strategies that consist of setpoints of climatic parameters.

Environmental control in pig hosing facilities was examined in Morsing et al.,(2003) and Morsing et al., (2005) (**paper 1 and 2**), using the program StaldVent to calculate mass- and energy balances within the pighousing envelope. A very important parameter in the prediction of energy consumption of a pighouse is the heat and moisture production from the animals. Pedersen and Sällvik(2002) presented algorithms for heat and moisture production in terms of sensible and latent heat production from pigs (and other livestock) depending on the feeding level and the animal weight. The CO_2 production can be directly related to the heat production both from the animals (Pedersen and Sällvik, 2002) but also from the decomposition of organic matter in the pighouse. Since the latter is usually not known the program StaldVent is primary applicable in housing systems without deep litter bedding. The temperature, moisture and CO_2 level in the pighousing facility is regulated through the heating and ventilating system. The ventilation rate is dependent on the setpoints of temperature, moisture and CO_2 concentration in the pighouse and the ambient conditions. Knowing the ambient temperature, relative humidity and CO_2 concentration StaldVent calculates the necessary ventilation rate or heating requirement to meet the setpoint values.

The setpoint parameters frequently have a priority order, eg. the temperature has first priority and the moisture or CO_2-concentration has second priority. The setpoint parameters are not independent hence there will be a effect of changing one setpoint parameter on the annual average value of another setpoint parameter. If the temperature setpoint is changed from a 22/20°C to a 18/16°C span the CO_2 concentration limit of 3000ppm will be exceeded 1000 hours per year to 50 hours per year, respectively (under Danish climate conditions) (**paper 1**). Reducing the setpoint temperature seem like a good tool to improve the air quality in the pighouse but the

effect of reducing the setpoint temperature may be a thermal discomfort of the animals and a 55% annual increase in energy consumption for ventilation (**paper 1**). The thermal discomfort of the animals can be reduced using covered creep areas, producing improved local thermal conditions under the covers. A combined setpoint strategy of sum of temperature (°C) and relative humidity (%) are used in many pighousing facilities (**paper 2**). When normal air quality and low energy consumption is first priority a sum of 90 is used when the air quality has higher priority a sum of 85 is used. Energy consumption for heating is very dependent on the setpoints of humidity and the wetness conditions in the house. Under Danish climate conditions a wet condition building with normal air quality (sum 90) and temperature setpoint 22/18°C will have a 84% annual decrease in energy consumption for heating if the conditions are changed to dry conditions (**paper 2**). If the wet building with normal air quality (sum 90) is changed to both dry conditions and good air quality (sum 85) the building will have a 48% annual decrease in heat energy consumption. The energy requirements for ventilation will be almost independent on these changes.

Conclusions

Changes in environmental control strategy will significantly effect the annual energy consumption for heating or ventilating in the closed envelope housing type. If high temperature conditions are required due to the well being of the animals a dry condition in the house must be aimed at to decrease the energy consumption for heating. If a lower temperature setpoint is chosen the annual energy consumption for ventilation increases. To keep the same local climatic comfort in the house at lower temperatures, covered creep areas can be used.

2.3 Physics of the diffuse ventilated room

Boundary conditions

Boundary conditions equivalent to both the boundary condition of an inlet and a wall apply to the surface of the diffuse inlet. Low momentum flow characterizes the inlet boundary condition. The air exchange rate of the room is under standard operation conditions between 10-25 1/h resulting in an inlet velocity of maximum 0.014 m/s (if the room height is 2m). The surface of the inlet interacts with the room thermal conditions like a wall, therefore there will be a radiative heat transfer mechanism between the diffuse inlet surface and the animals in the occupational room. Usually an inlet boundary condition does not have radiative properties unless the inlet fluid has opaque optical character. A wall boundary condition of no slip does not apply at the surface of the diffuse material since the material is diffusive and there can be some penetration debt of the boundary layer into the porous material.

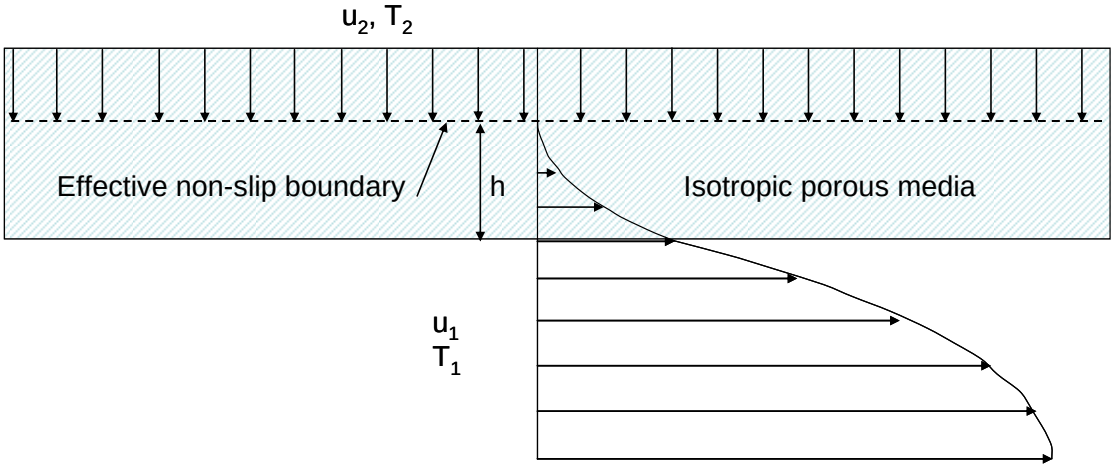

Figure 2.2: Illustration of the penetration depth and the effective non slip boundary surface at a flow situation in a porous material.

The penetration depth h, Figure 2.2, is dependent on the material properties on the surface and the local dynamic and static pressure difference between the inlet pressure and the boundary layer pressure. Under ideal conditions the fluid is assumed incompressible, the boundary layer flow pressure is constant on the entire ceiling surface and the porous material is assumed isotropic, the penetration depth will be

zero, h=0m, on the entire ceiling surface. Under non ideal conditions the dynamic and spatial changes in the boundary pressure induce local pressure conditions where the boundary layer flow u_1 displace the inlet flow u_2 and the local penetration depth h>0m in some locations. Convective heat transfer inside the boundary layer is possible if temperature differences between the inlet fluid, boundary layer fluid and the diffuse material exist. If the conditions are ideal the inlet air will be heated by convective heat transfer between the solid matrix of the porous material heated by radiation and the inlet air. If the conditions are non ideal, (non isotropic and compressible) both convection heat transfer, between the inlet fluid and the boundary layer fluid and the solid matrix, and mixing heat transfer, between the inlet fluid and the boundary layer fluid, take place within the effective boundary volume of the porous material. The effective boundary volume is defined as the volume where both mixing and convection heat transfer pertain and is delimited by the effective non-slip boundary and the downstream boundary of the porous material. These conditions that differentiate the diffuse inlet boundary conditions from the boundary conditions of both a traditional open inlet and a wall is most significant to the thermal and fluid dynamical properties of the diffuse inlet. These conditions determine the perception of comfort by the subjects in the diffuse ceiling inlet ventilated occupational room.

3 Theoretical background

Modeling of the diffuse ventilation of livestock building is not found in literature at this moment. Therefore the attempts to successfully simulate the flow regime in a diffuse ventilation system must draw from the experience of related areas of research. In this chapter we will draw out the results of research in related areas and discuss

how these findings can be used in the mathematical modelling of the flow behaviour in diffuse ventilated livestock buildings.

Initally the fundamental equation and general equations of mass-, momentum- and heat conservation in a fluid medium is presented.

3.1 Background of fluid mechanical movement and energy transport

The description of thermal and fluid motion in a room is based on the conservation formulation of mass, momentum and energy in a control volume. Indoor airflow is often assumed incompressible turbulent airflow of a Newtonian fluid. In the present case the effects of buoyancy is important hence the exemption of the compressibility assumption is accounted for by using the Boussinesq approximation and assuming isothermal incompressibility. In the porous medium the solid and fluid temperature are different. Non equilibrium conditions between the fluid and the porous medium is accounted for by considering separate energy equations for the two phases. The two equations are coupled through the convective heat transfer term that accounts for the convective heat exchange between the two phases (Talukdar et al., 2004). The porous medium is considered homogeneous and isotropic. The radiative properties of the porous material is assumed to be gray and to emit, absorb and scatter radiation isotropically, gaseous radiation is neglected.

The general transport equations are expressed in Cartesian coordinates using tensor notation, initially assuming laminar conditions.

Conservation of mass, (the continuity equation) states that, under the assumption of incompressibility, that the amount of mass entering the control volume will also leave the control volume for constant property:

$$\frac{\partial u_i}{\partial x_i} = 0 \qquad / 3.1$$

where x_i is the position vector in the i-th coordinate direction, u_i is the instantaneous fluid velocity component in the i-th coordinate direction.

Conservation of momentum (Navier –Stokes equations(NS)). The first term represent the rate of increase of momentum pr. unit volume in the control volume. The second term represent the rate of momentum lost by convection per unit volume through the control surface. The next two terms represent the surface forces applied by the external stresses per unit volume, pressure and shear stresses respectively. The change in density is considered a change in external stresses contributed by the gravitational force. The next term (Boussinesq) represents the body force due to gravity and thermal expansion of the fluid. The last term is the source term.

$$\frac{\partial(\rho u_i)}{\partial t} + \frac{\partial(\rho u_i u_j)}{\partial x_j} = -\frac{\partial p}{\partial x_i} + \frac{\partial}{\partial x_j}\left(\mu\left(\frac{\partial u_i}{\partial x_j} + \frac{\partial u_j}{\partial x_i}\right)\right) + \beta g_i \rho(T_0 - T) + S_m \qquad / 3.2$$

where u_j is the instantaneous fluid velocity component in the j-th coordinate direction, ρ is the fluid density, p is the instantaneous pressure, μ is the dynamic viscosity, g_i is the component of gravitational acceleration, T_0 is the reference temperature and T is the instantaneous local temperature, S_m is the momentum source/sink term and β is the isobaric thermal expansion coefficient defined as

$$\beta = -\left(\frac{1}{\rho}\right)\left(\frac{\partial \rho}{\partial T}\right)_p \qquad / 3.3$$

assuming ideal gas conditions $\beta=1/T$.

For most fluids $\beta \approx 10\text{-}3$ to 10-4 1/K and for small variations in temperature (<10K) the variations in density are less than 1%. Density is therefore treated as a constant in all terms in the equations except in the buoyancy term. This assumption is the Boussinesq approximation (Arpaci and Larsen, 1984).

The equation of *conservation of energy* is derived from the first law of thermodynamics applied on a control volume.

Assuming ideal gas conditions $dh=C_p dT$.

$$\rho\frac{\partial T}{\partial t}+\frac{\partial(\rho u_i T)}{\partial x_i}=\frac{\partial}{\partial x_i}\left[\frac{k}{C_p}\frac{\partial T}{\partial x_i}\right]+u_i\frac{\partial p}{\partial x_i}+S_T \qquad / 3.4$$

Where k is the thermal conductivity coefficient [W/mK] and Cp is the specific heat at constant pressure [J/kgK]. Assuming incompressibility

/ 3.4 reduces to:

$$\rho\frac{\partial T}{\partial t}+\rho\frac{\partial(u_i T)}{\partial x_i}=\frac{\partial}{\partial x_i}\left[\frac{k}{C_p}\frac{\partial T}{\partial x_i}\right]+S_T \qquad / 3.5$$

4 Computational fluid dynamics (CFD) modelling

Solving the above partial differential equations analytically is only possible for a few simple problems. A numerical method to solve these non-linear and coupled partial differential equations is referred to as Computational Fluid Dynamics or CFD. In CFD the Navier-Stokes equations are solved by discretizing the equations using either finite difference, finite volume or finite element techniques so that the continuous problem is transformed into a discrete problem that can be solved numerically.

The application of a turbulence model to account for the fluctuating motion of the fluid is compulsory after time averaging the momentum equations.

The task of modelling convection and radiation inside a porous material is very complicated. Two lines of treatment can be chosen: the direct simulation or the continuum simulation. When working with fine resolution complicated structures the cost of computation becomes considerable when working with a direct simulation. A continuum approach must therefore be pursued in most cases. If the solid matrix of porous material consists of structures that are complex to break down into simple

geometrical elements as cylinders or spheres, the radiative and convective properties of the material must be determined experimentally.

The aim of the present project is not to determine the physical properties of the porous material. But for the understanding of the physical connection among the constituents of the diffuse ventilated room, a brief description, as found in literature, of the definition of material parameters and their importance in the governing equations, follows appropriately.

4.1 Turbulence

The consequence of discretization is that flow phenomena of dimensions smaller than the grid resolution are not accounted for in the solution. And because the small scale motion affects the large scale motion this loss of information must be added to the model artificially. This is done with adding a turbulence model. The turbulence model used is the two equation k-ε eddy viscosity model of (Launder and Spalding, 1974). This model relates the eddy viscosity to the transport equation of turbulent kinetic energy, k and the transport equation of turbulent dissipation of kinetic energy ε.

With equation / 3.2 and / 3.4 it is possible to solve laminar flow problems and if the computational cells were smaller than the smallest spatial and temporal turbulent flow eddy turbulent problems could be solved too. This technique is called a Direct Numerical Solution DNS and requires a large computer. To overcome this problem the equations are simplified through a process of Reynolds time averaging Navier Stokes (RANS). The technique is to consider the flow to be composed of a mean flow with random fluctuation flow components superimposed in it. Each instantaneous dependent component φ (velocity, pressure, temperature,

concentration) in the NS equations is decomposed into a mean $\overline{\varphi}$ and a fluctuating φ' component where the relation is:

$$\varphi = \overline{\varphi} + \varphi' \qquad / 4.1$$

Where the line superscript denotes time averaging

$$\overline{\varphi} = \frac{1}{\Delta t \int_t^{t+\Delta t} \varphi(t) dt} \qquad / 4.2$$

With these decompositions the conservation equations are time averaged and the new system of equation are the RANS equations:

$$\frac{\partial \overline{u_i}}{\partial x_i} = 0 \qquad \mathbf{/ 4.3}$$

$$\rho \frac{\partial (\overline{u}_i)}{\partial t} + \rho \frac{\partial (\overline{u}_i \overline{u}_j)}{\partial x_j} = -\frac{\partial \overline{p}}{\partial x_i} + \frac{\partial}{\partial x_j}\left(\mu \left(\frac{\partial \overline{u}_i}{\partial x_j} + \frac{\partial \overline{u}_j}{\partial x_i} - \rho \overline{u_i' u_j'} \right) \right) + \beta g_i \rho (T_0 - \overline{T}) + S_m$$

/ 4.4

$$\rho \frac{\partial \overline{T}}{\partial t} + \rho \frac{\partial (\overline{u}_i \overline{T})}{\partial x_i} = \frac{\partial}{\partial x_i}\left[\frac{k}{C_p} \frac{\partial \overline{T}}{\partial x_i} - \rho \overline{u_j T'} \right] + \frac{\partial \overline{p}}{\partial t} + u_i \frac{\partial \overline{p}}{\partial x_i} + S_T \qquad / 4.5$$

The time averaging produces a number of new terms in the conservation equations. In the momentum equation the $\overline{u_i' u_j'}$ represents the transport of momentum due to the fluctuating motion of the flow in other words the turbulent Reynolds stresses. The Reynolds stresses has to be modelled in order to close the system of equations. In a first order model the common approach is the Boussinesq (1877) approximation to imitate the constitutive relation of the isotropic Newton-Stokes fluid (Arpaci and Larsen, 1984). The known constitution that viscous stresses in a laminar flow is proportional to the velocity gradient is assigned to the turbulent stresses assuming that turbulent stresses are proportional to the velocity gradient. The coefficient of proportionality in the incompressible case is the turbulent (eddy) viscosity μ_t that is

not a property of the fluid but depends on the turbulent fluid motion (Arpaci and Larsen, 1984):

$$-\rho\overline{u_i'u_j'} = \mu_t\left(\frac{\partial\overline{u_i}}{\partial x_j}+\frac{\partial\overline{u_j}}{\partial x_i}\right)-\frac{2}{3}\delta_{ij}\rho k \qquad \textbf{/ 4.6}$$

Where μ_t is the turbulent dynamic viscosity, $\mu_{eff}=\mu_t+\mu$, δ_{ij} is the Kronecker delta ($\delta_{ij}=0$ when $i\neq j$ and $\delta_{ij}=1$ when $i=j$) and k is the turbulent kinetic energy:

$$k = \tfrac{1}{2}\overline{u_i u_i} \qquad / 4.7$$

The isotropic viscous dissipation rate ε is (Arpaci and Larsen, 1984)

$$\varepsilon = \mu\overline{\left(\frac{\partial u_i}{\partial x_j}\right)^2} \qquad / 4.8$$

Local values of k and ε are obtained solving the continuity equations

The equation used to model k is of the form (Rees et al., 2001):

$$\frac{\partial(\rho k)}{\partial t}+\frac{\partial(\rho\overline{u}_j k)}{\partial x_j}-\frac{\partial}{\partial x_j}\left(\left(\mu+\frac{\mu_t}{\sigma_k}\right)\frac{\partial k}{\partial x_j}\right)=P_k+G-\rho\varepsilon \qquad / 4.9$$

where P_k is the production due to strain and is given by

$$P_k = \mu_t\left(\frac{\partial\overline{u}_i}{\partial x_j}+\frac{\partial\overline{u}_j}{\partial x_i}\right)\frac{\partial\overline{u}_i}{\partial x_j} \qquad / 4.10$$

And G is the production due to buoyancy forces and is given by

$$G = \frac{\mu_t}{\sigma_t}\beta g_i\frac{\partial\overline{T}}{\partial x_i} \qquad / 4.11$$

For high Reynolds number the epsilon ε equation are

$$\rho\frac{\partial(\varepsilon)}{\partial t}+\rho\frac{\partial(\overline{u}_j\varepsilon)}{\partial x_j}-\frac{\partial}{\partial x_j}\left(\left(\mu+\frac{\mu_t}{\sigma_\varepsilon}\right)\frac{\partial\varepsilon}{\partial x_j}\right)=C_1\frac{\varepsilon}{k}P_k-C_2\rho\frac{\varepsilon^2}{k} \qquad / 4.12$$

where

$$\mu_t = \frac{C_\mu \rho k^2}{\varepsilon} \qquad / 4.13$$

The constants C_μ, C_1, C_2, σ_ε and σ_k have the values 0.09, 1.44, 1.92, 1.0 and 1.3 respectively.

The turbulent Prandtl number σ_t in

/ 4.11 is introducing the effect of stratification dependent on buoyancy (Nielsen et al., 1979) for horizontal flows

$$\sigma_t = 0.67 \frac{1 + 0.83f + 0.112f^2 + (0.267 + 0.242f)B}{1 + 0.417f + 0.093B} \qquad / 4.14$$

where

$$f = \left(\frac{k^{\frac{3}{2}}}{\varepsilon}\right)\left(\frac{C_\mu^{\frac{3}{4}}}{\kappa d}\right) \qquad / 4.15$$

and B is the parameter characteristic of the buoyancy effects defined as

$$B = -\beta g \frac{k^2}{\varepsilon^2} \frac{\partial T}{\partial x_i} \qquad / 4.16$$

where κ is the von Kárámán constant (κ=0.41), d equal to the distance to the nearest boundary accounts for the vicinity to the nearest wall.

4.2 Radiation

Radiation in the diffuse ceiling ventilated room is affected of both radiation from solid surfaces and radiation from diffuse material. In HVAC systems radiation is a relatively important energy transfer mechanism because low temperature differences are considered in these systems. Radiation is a energy transport process that requires no transport medium. For gasses or transparent solids the transport emission is a volumetric process, but between two non transparent objects radiation is most often assumed a surface process. Hence the radiation energy transport is independent on the

conservation formulation and is only dependent on the temperature and properties of surfaces in the domain.

The nature of radiation may be viewed as either the propagation of particles called photons or in terms of electromagnetic waves. In any case radiation properties is termed in line with standard wave description of wavelength λ and frequency υ. The monochromatic radiant emission of radiation varies with the wavelength, the term spectral is used to refer to this relation. Thermal radiation is in the spectrum between 0.1-100 μm. Radiation from a surface is emitted in all possible directions and this directionality describes the nature of radiation. Each surface emits a total hemispherical emissive power E(T) (W/m^2) defined as the rate at which radiation is emitted per unit area at all possible wavelengths in all possible directions.

The dimensionless material specific parameter, total hemispherical emissivity ε(T), is defined as the ratio of radiation emitted by a given surface to the radiation emitted by a blackbody at the same temperature (Incropera and De Witt, 1990)

$$\varepsilon(T) = \frac{E(T)}{E_b(T)} \qquad / 4.17$$

where the total emissive radiative power from a blackbody is given by

$$E_b(T) = \sigma T^4 \qquad / 4.18$$

where the Stefan-Boltzmann constant is σ=5.670e-8 $Wm^{-2}K^{-4}$.

Into the porous media radiation is not a surface phenomenon but a volumetric phenomenon. Spectral radiation in a semitransparent liquid is a function of the absorption coefficient $\kappa_{\lambda,a}$ (1/m), scattering coefficient $\kappa_{\lambda,s}$ (1/m) and the thickness of the medium. If a monochromatic beam of spectral radiative intensity I_λ ($Wm^{-2}s^{-1}r^{-1}$) is incident on the medium thickness L, the path length dx and absorption coefficient $\kappa_{\lambda,a}$ the absorbed energy is

$$dI_\lambda(x) = -\kappa_{\lambda,a} I_\lambda(x) dx \qquad / 4.19$$

Integrated over the entire medium layer Beer's law of exponential decay is evolved

$$\frac{I_{\lambda,L}}{I_{\lambda,0}} = e^{-\kappa_{\lambda.a} L} \qquad / 4.20$$

Where the transmissivity τ_λ and absorptivity α_λ is defined accordingly

$$\alpha_\lambda = 1 - \tau_\lambda = 1 - e^{-\kappa_{\lambda,a} L} \qquad / 4.21$$

The scattering energy is defined analogous

$$dI_\lambda(x) = -\kappa_{\lambda,s} I_\lambda(x) dx \qquad / 4.22$$

The spectral radiative intensity is the radiation energy in the direction θ per unit time, per unit projected area, per unit solid angle and per interval dλ around λ. Other material properties of porous material that are related to radiation is the scattering albedo defined as

$$\omega_a = \frac{\kappa_{\lambda,s}}{\kappa_{\lambda,s} + \kappa_{\lambda,a}} \qquad / 4.23$$

The radiation dependent parameter of porous materials is the radiative extinction coefficient κ [1/m] defined by (Barra et al., 2003) for mean pore diameters d>0.6mm as

$$\kappa = \frac{3}{d}(1 - \varepsilon) \qquad / 4.24$$

where ε is the porosity of the material

/ 3.3 and d is the mean pore diameter [mm].

Several authors have examined the effect of radiation on the flow characteristic in porous material. (Raptis, 1998) numerically examined the natural convection flow in a vertical porous plate exposed to radiation from one side and with a forced flow horizontally through the porous material. He found that the vertical upward velocity

component decreased when the porous material was exposed to cooling. That is the energy that is transferred to the solids of the porous material from radiation affects its buoyancy driven flow. Chen et al.,(2005) numerically investigated the flow and radiative conditions in a duct flow with a porous core in the center of a cooling tube. It was found that the heat flux trough the tube wall was increased 1.1-2.7 times with the application of a porous insert, physically because of the transformation from pure convective heat transfer to both radiative and convective heat transfer.

The radiative heat flux on the boundary layer of the porous surface of the diffuse material is simulated with the Rosseland diffusion approximation (Bakier, 2001; Kahn, 2005; Raptis, 1998). If the radiative heat flux in the x and z direction (parallel to the porous material surface) is assumed negligible then the energy equation at the porous boundary is from / 3.5:

$$\frac{\partial(\rho u_i T)}{\partial x_i} = \frac{\partial}{\partial x_i}\left[\frac{k}{C_p}\frac{\partial T}{\partial x_i}\right] - \frac{1}{\rho C_p}\frac{\partial q_R}{\partial y} \qquad / 4.25$$

Where the Rosseland parameter is

$$q_R = \frac{4\sigma}{3\kappa_{\lambda s}}\frac{\partial T^4}{\partial y} \qquad / 4.26$$

4.3 Convection in porous material

Natural convection in a system that involve a fluid reservoir and a porous medium saturated with the same fluid is of great practical interest. The ability to model the system matematically has undergone much attention (Beckermann et al., 1987; Beckermann et al., 1988; Lemos and Silva, 2005; Mohammadein et al., 1998; Neale and Nader, 1974; Sathe et al., 1988). Mathematically the problem involves the coupling of the momentum equations for the fluid region (the Navier –Stokes equation) / 3.2 with the equation for the porous region (Darcy's law) though an

appropriate set of matching conditions at the fluid/porous interface. Darcy's law explains the effect of pressure drop of a viscous flow in a porous medium. For an isotropic media Darcy's law is written:

$$-\frac{\partial p}{\partial x_i} = \left(\frac{\mu}{\kappa_i}\right) u_i \qquad / 4.27$$

Where κ_i is the direction dependent permeability [m^2] of the porous medium and μ is the dynamic viscosity [$kgs^{-1}m^{-1}$].

The permeability κ_i is the measure of the flow conductance of the matrix.

When a viscous fluid flows past the surface of a porous saturated medium the effects of viscous shear in the unobstructed fluid will penetrate beneath the permeable surface to form a boundary layer region in the porous medium Figure 2.2. Hence the usual non-slip boundary condition of solid surfaces can not be applied on porous media. The Darcy equation is not compatible with the existence of a boundary layer region in the porous medium because no macroscopic shear term is associated with this equation. Brickmann extended the Darcy equation with the macroscopic shear term to the form (Neale and Nader, 1974)

$$\frac{\partial p}{\partial x_i} = -\left(\frac{\mu}{\kappa_i}\right)u_i + \tilde{\mu}\frac{\partial}{\partial x_i}\left(\frac{u_i}{\partial x_i}\right) \qquad / 4.28$$

Where $\tilde{\mu}$ is the effective porous dynamic viscosity, which depends on the fluid viscosity as well as the structural properties of the porous medium, can be derived from the empirical structural parameter α:

$$\alpha = \sqrt{\frac{\tilde{\mu}}{\mu}} \qquad / 4.29$$

that is determined experimentally through

/ 4.28 (Kaviany, 1995).

The extension of the boundary layer into the porous medium was examined by Beckermann (1988) and Sathe (1988) who used a non-Darcian model in boundary layer natural convection flows with the Forchheimer-Brickmann extension in the momentum equation in the porous media:

$$0 = -\frac{\partial p}{\partial x_i} + \frac{\partial}{\partial x_i}\left(\mu_{eff}\frac{\partial u_i}{\partial x_i}\right) + \rho g_i \beta(T_0 - T) + \left(\frac{\mu}{\kappa_i} + \frac{\rho C}{\kappa_i^{1/2}}|u_i|\right)u_i \qquad / 4.30$$

where C is the empirical inertia coefficient. Lemos and Silva (2005) and Braga and Lemos (2004) applied a k-ε turbulence model on / 4.30.

Connecting the solid and fluid through the convective heat transfer term in the energy equations produces the coupled differential equations for the gas and solid phase respectively(Talukdar et al., 2004):

$$\varepsilon\rho_g\left(\frac{\partial T_g}{\partial t} + \frac{\partial(u_i T_g)}{\partial x_i}\right) + \frac{1}{C_{p,g}}(1-\varepsilon)Ah(T_g - T_s) = \varepsilon\frac{\partial}{\partial x_i}\left[\frac{k_g}{C_p}\frac{\partial T_g}{\partial x_i}\right]_T \qquad / 4.31$$

$$(1-\varepsilon)\rho_s\left(\frac{\partial T_s}{\partial t}\right) + \frac{1}{C_{p,s}}(1-\varepsilon)Ah(T_g - T_s) = (1-\varepsilon)\frac{\partial}{\partial x_i}\left[\frac{k_s}{C_p}\frac{\partial T_s}{\partial x_i}\right] - \nabla q_R \qquad / 4.32$$

where A is the surface area per unit volume of solid, q_R is the radiative heat flux, h it the heat transfer coefficient and ε is the porosity. The porosity is defined as

$$\varepsilon = \frac{V_g}{V_s + V_g} \qquad / 4.33$$

where V_g is the void volume occupied by gas and V_s is the solid volume occupied by the porous matrix.

On a microscopic level the solid material of the porous media has conductive properties corresponding to a nonporous material. Decreasing the solid conductivity k [W/mK] will reduce the conduction heat transfer, the heat recirculation through the solid is reduced.

The volumetric heat transfer coefficient h_v [-] is a function of pore diameter and geometry(Younis and Viskanta, 1993). The volumetric heat transfer coefficient is determined experimentally by measuring the air temperature history and solving the energy equations for the two phase system. Pore diameter affects the volumetric heat transfer coefficient through the surface area to volume ratio A [1/m]. A smaller pore diameter means greater surface area pr. volume and a higher volumetric heat transfer coefficient (Fu et al., 1998). In general voids in the porous media are nonuniform in size and distribution throughout the porous matrix. Hence a statistical average of the distribution of pore diameter is applied presented as the average pore diameter.

4.4 Conclusions

In the preceeding paragraphs a semi deterministic approach to solving the heat and mass transfer relations has been outlined. The multitude of empirical parameters in the differential equations is a limitation to accessibility of solving the equation system. Some of the parameters include:

Empirical structural parameter α

Empirical inertia coefficient C

Surface area pr unit volume A

Porosity ε

Scattering coefficient $\kappa_{\lambda,s}$

These parameters are not found in the product specification reference of most diffuse materials except maybe ceramic materials intended for porous burner technologies. To achieve these material parameters are an interesting study which can be examined in the above mentioned references. If the material parameters were specified the solution would still be dependent on a mean value approach except if a DNS solution is pursued. The DNS solution method is outside this project resources and an mean value solution does not satisfy the spatial and dynamical conditions that is important elements of the convective heat exchanging process in the diffuse material, chapter.2.3. In the following a stochastic model of the thermal conditions of the diffuse material under livestock environmental condition is persued.

5 Experiments

Two types of experiments has been performed a full scale experiment and a model scale experiment.

The purpose of the full scale experiment was to examine the thermal conditions and air velocity in the room.

The purpose of the model scale experiment was to examine the heat exchanging function of the diffuse inlet under prescribed conditions.

The experiments were performed in the Air Physics lab on the Danish Institute of Agricultural Science (DIAS) in Bygholm, Horsens..

5.1 Model scale room

Like most experimental praxis the ability to conduct experiments in a model scale by applying the principle of similarity opens perspectives of both reduction of resource

consumption when conducting the experiment. The 3 conditions of applying the similarity principle is (Nielsen, 1999):

1. Identical dimensionless sets of boundary conditions in room and model
2. Identical sets of dimensionless numbers in the governing equation for the room and model.
3. The assumed physical constants should only have a small variation within the applied thermal conditions.

Those conditions pose some questions upon application in the diffuse ceiling inlet room. The requirements of identical dimensionless boundary conditions are met when the model is geometrical similar to the full scale room in all details. But the requirements of similarity of geometrical conditions, can be replaced by a requirement of similarity of the flow in the model, in simplified geometrical conditions in the model. But to simplify the inlet conditions of the diffuse ceiling ventilated room, requires that the change in dimensionless boundary conditions of the diffuse inlet are examined, to find the correlation between the flow in the room and the thermal properties of the diffuser. The hypothesis of the experiment is that the heat exchanging function of the boundary condition of the diffuse material is dependent on flow and radiative conditions in the room. Hence when applying the first condition, the model inlet is not likely replaced by a simplified diffuser, because the hypothesis stating that the microscopic properties of the diffuse inlet determines the heat exchanging capacity of the diffuse inlet (Kaviany, 1995; Younis and Viskanta, 1993). And the heat exchanging capacity is decisive to the thermal conditions in the room. Before choosing identical sets of dimensionless numbers its important to examine the appropriate use of dimensionless numbers and their applicability in the present problem. In the present case the diffuse ceiling ventilated room can be considered a

free convection room without ventilation (because the inlet flow momentum is negligible compared to the buoyancy driven flow momentum). An appropriate choise of dimensionless number could be the Grasshoff number because it is independent on the inlet velocity:

$$Gr = \frac{\beta g \rho_0^2 h^3 (T_R - T_0)}{\mu_0^2} \qquad / 5.1$$

Relating the Grasshoff number to the experimental room and assuming that T_R is the surface temperature of the heated surface (the pigs) and the reference temperature T_0 is the outlet temperature of the room, the Grasshoff number is identical and independent of ambient conditions under normal operating conditions in a pig housing facility.

Conclusively, observing a model room for examining thermal environment of a diffuse inlet ventilated room, is restricted by the ability to reproduce a thermal boundary condition with a simplified inlet and diffuser material, although the condition of identical dimensionless numbers are satisfied.

5.2 Full scale room

The climatic conditions were examined in a full scale room Figure 2.1 the Air Physics Laboratory on Danish Institute of Agricultural Science, Bygholm, Denmark, by measuring the turbulence intensity, airflow velocity and thermal conditions in the occupational zone at different air exchange rates and space parcelling. The results of the experiments were compared to the results of CFD simulations.

5.2.1 Full scale room with heating facilities

An experiment has been conducted to examine the temperature conditions in a diffuse ceiling ventilated room with heating facilities, pen partition equipment and pig heat

simulators in different positions (Jacobsen et al., 2004), **paper 3**. The purpose was to examine:

- the correlation between temperature measurements in the occupational zone close to the floor and temperature measured in a central position and
- to investigate the deviations between measured and simulated temperature profiles close to the floor and ceiling.

Pen partitions are located as 8 equal size pens positioned 4 in a row at each side of a central inspection alley of full room length so that the vertical plane through the centre of the central alley is a symmetry plane of the room Figure 5.1. The pig heat simulators were located symmetrically around the central alley in the full room length as a horizontal panel on the floor in two positions, close to the central aisle and close to the room outer wall envelope. Temperature conditions were measured in pen #2, Figure 5.1, in horizontal profiles at the occupational zone near floor location and close to the diffuse ceiling inlet in the central plane of a pen. Room temperature was measured at a central location equivalent to the location of most climate control sensors. Simulations were performed with boundary conditions similar to the experimental room.

Results

Regarding the temperature conditions at the measuring location close to the diffuse ceiling inlet, at the setup with pig simulators close to the central alley, comparison of the measurement and the simulations, demonstrate the presence of a significant difference between measurements and simulations. The deviance was up to 5 K and only 6.7% of the simulations have results within the 90% confidence interval (CI) of the measurements. The measured temperature close to the diffuse ceiling is higher than the simulated temperature in 90% of the measuring positions. For the simulations

close to the floor the picture is different. 67% of the simulated values are within 90% CI of the measurements. When the pig simulators were located close to the aisle the deviance between the measurements at the central room temperature location and the floor position is below 1.1K and 80% of the temperature measurement locations the deviance was below 0.2K.

In the setup with pig simulators close to the wall an inexplicable temperature drop of almost 4K is measured at the location close to the wall. The temperature difference between measurements and simulations at the measuring location close to the diffuse ceiling inlet, was up to 3.6 K and none of the simulations have results within the 90% CI of the measurements. The measured temperature close to the diffuse ceiling is higher than the simulated temperature in all of the measuring positions. For the simulations close to the floor 13% of the simulated values are within 90% CI of the measurements. When the pig simulators were located close to the wall the deviance between the measurements at the central room temperature location and the floor position was up to 1.9K and 13% of the temperature measurement locations the deviance was below 0.2K.

Examining the airflow velocity simulations the situation with pig heat simulators close to the wall have one circulating movement on each side of the aisle driven by the convection from the heating facilities that are both located in close to the wall. This does not stimulate a fully mixed air distribution in the room and there were a temperature stratification and temperature distribution gradients were large in the measuring plane close to the floor. The simulation with the pig simulators located close to the aisle had a good mixing convection conditions due to several circulating movements in the room.

Conclusions

The results indicate that the applied simulation boundary conditions of diffuse ceiling inlet were not equivalent to the actual conditions. The simulation results deviate more from the measurement results than what can be explained with random measurement errors at the location close to the ceiling. Apparently the temperature close to the ceiling and presumably the temperature at the ceiling inlet boundary were significantly higher than the inlet temperature upstream of the diffuse inlet applied in the simulation.

The predictions of occupational zone temperature with a central location measurement were dependent on the position of the pig simulators. If the pig heat simulators were located close to the wall the simulation prediction is dissatisfactory from a control point of view. If the heat simulators were situated close to the aisle the temperature simulation prediction were very reasonable.

5.2.2 Full scale room setpoint strategies

In **paper 4** (Jacobsen et al., 2006a) a full scale experimental room Figure 2.1 with diffuse ceiling inlet the thermal conditions at floor level was examined at 3 different inlet temperatures and inlet velocities was used and the room with and without pen partitions equivalent to **paper 3** (Jacobsen et al., 2004). Pig heating simulators Figure 2.1 was located close to the wall at full room length. The thermal gradients and the airflow velocity in the occupational zone close to the floor were examined at steady state conditions. The purpose of the experiment was to:

- examine the effect of different inlet temperature, inlet velocity and pen partitions on the climatic conditions in the occupational zone
- compare the experimental results with simulation results of the same boundary conditions.

The temperature in the occupational zone was measured in a horizontal profile perpendicular to the wall close to the floor in the central axis of pen enclosure #3 Figure 5.1.

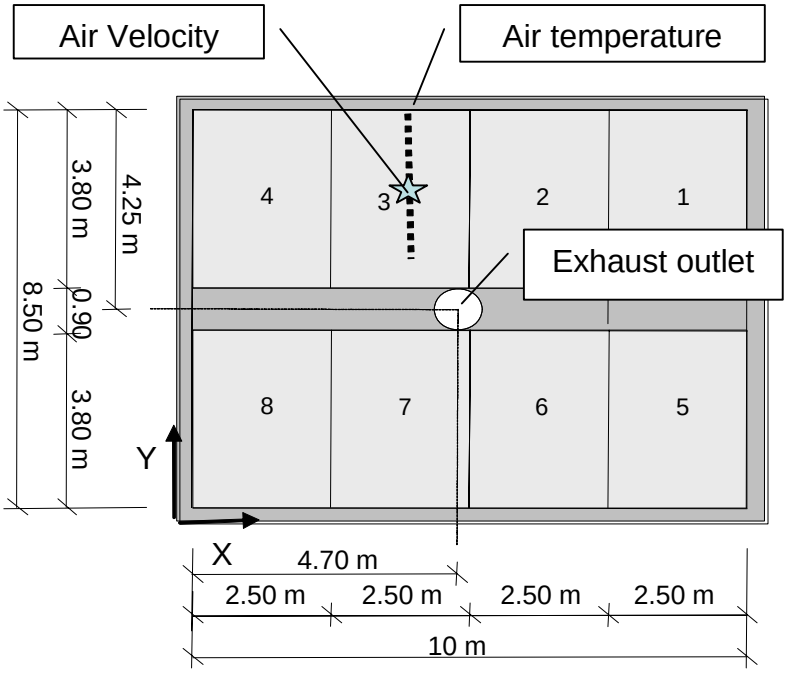

Figure 5.1: Experimental room showing pen partitions and measuring location in pen #3. The air velocity was measured close to the floor in the middle of the same pen.

Inlet and outlet temperatures and airflow rate were measured. The experimental design gives (3*2) 6 different combinations (trials) of the independent variables, air exchange rate and pen partitions, Table 5.1. A two factor variance analysis was used to analyse the experimental and simulation results. In the measurements, it was found that there is not a significant difference in temperature in the occupational zone for the 6 different combinations. The only exception was at the measurement location close to the wall (0.25m from the wall) where there was a significant difference between the measurements with or without pen partitions.

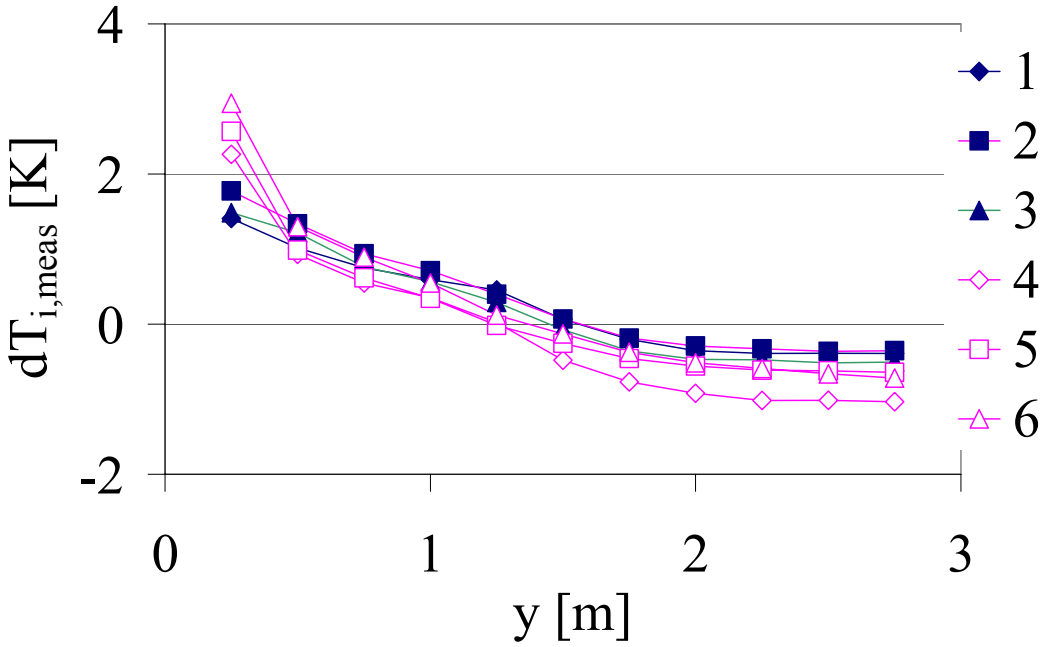

Figure 5.2:Measured temperature difference dTi,meas as a function of horizontal profile observation location y distance from the wall.at different setup trials (1-6). Vertical measuring location 0.2m above the floor. (Jacobsen et al., 2006a)

With the two factor test it is tested if there is a significant difference in the temperature profile or velocity with or without pen partitions and at the different air exchange rates, at both the measuring and simulation results. The test was performed using a linear model with two factors for both the measurements and simulation and different combinations of the independent variables: with and without pen partitions, and three levels of air exchange rates, and two different data sources: simulation or measurement with one repetition.

The analysis results in **paper 4** show that it can be assumed that there is an effect on *air temperature* of pen partition but there is no effect of air exchange rate on $dT_{i,meas}=T_{i,meas}-T_{out,meas}$ in the measurement results, Figure 5.2. There is no effect on the simulated values $dT_{i,meas}$ from either exchange rate or pen partition. Comparing the measurements with the simulations in the configuration without pen partition, trial 1-3, there is no statistical difference between the results of the measurement and

simulation on the temperature. For the configuration with pen partition, trial 4-6, there are significant difference between measurement and simulation in the chosen location. Performing a two factor variance test like the above the significant difference of *air velocity* with or without pen partitions and at the different air exchange rates at both the measured and simulation results can be tested. The test show,(**paper 4**) there is no effect of air exchange rate or pen partition on the measured air velocity. In the simulation results there is a significant effect on velocity from pen partition but no effect of air exchange rate. Without pen partitions, there is a significant difference between the measuring and simulation result. However, in the configuration with pen partition, the difference between measurement/simulation is not significant.

The simulation and measurement reach significantly different results of temperature without pen partitions, and velocity in the setup with pen partitions.

It is a significant result that there is no effect of inlet temperature or inlet velocity on the temperature in the occupational zone particularly because the inlet velocity is increased a factor 3 from a air exchange rate of 4.9-17.91/h, the inlet temperature is increased approximately 17K. The measured thermal conditions in the occupational zone were independent on inlet velocity and temperature. The air velocity in the occupational zone was independent on inlet temperature, inlet velocity and pen partition. The mean air velocity and variance of each trial (30 min. mean values of 1 Hz measuring frequency) is shown in Table 5.1. The trials without pen partitions demonstrate mean velocity values not significantly different from the velocity measured in the trials with pen partition, but the variance of the velocity is significantly different with and without pen partitioning. Comparing Figure 5.3 with Figure 5.4 the differences in variance in trial 2 and 5 respectively is visible. Particularly the velocity in the y-direction has a significantly larger variance in trial 2

than in trial 5. The comparability of the different trials is tested with the chi-test for compatibility to the Gauss distributions. A low P-value (P<0.05, 95% probability) of the chi-test show that there is not significant divergence from the Gauss distribution. The chi-test show that there is not a significant evidence that the velocity distribution in the trials should not be a Gauss-distribution, Table 5.1, and it can be assumed that the data follows a Gauss-distribution. The difference in variance is hence significant from a statistical point of view. There is a tendency towards a better adaptation to the Gauss-distribution for the trials without pen partition than for the trials with pen partition. The normal distribution of the velocity frequency is shown in Figure 5.5.

Table 5.1: Mean air velocity, variance and standard deviation of 30 min. measuring span with 1 hz measuring frequency. Chi-test to the Gauss distribution.

Trial		1	2	3	4	5	6
Air exchange rate	1/h	4.9	9.8	17.9	4.9	9.8	17.9
Pen partition wall height	m	0	0	0	0.6	0.6	0.6
Mean	m/s	0.16	0.21	0.17	0.10	0.23	0.22
Variance	m/s	0.0034	0.0024	0.0034	0.0016	0.0014	0.0013
SD	m/s	0.058	0.049	0.058	0.041	0.038	0.036
P-value chi-test		1.1.E-07	1.7.E-10	7.9.E-12	8.0.E-03	1.5.E-02	4.9.E-04

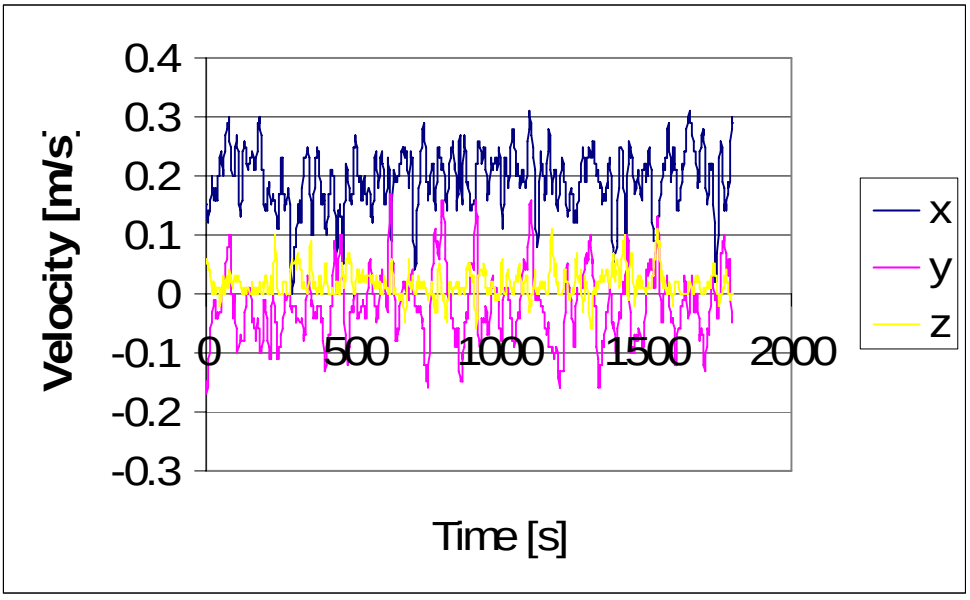

Figure 5.3: Trial 2 measured air flow velocity in cartesian components z,y,z, direction in a 1800s measuring period. z-direction vertical.

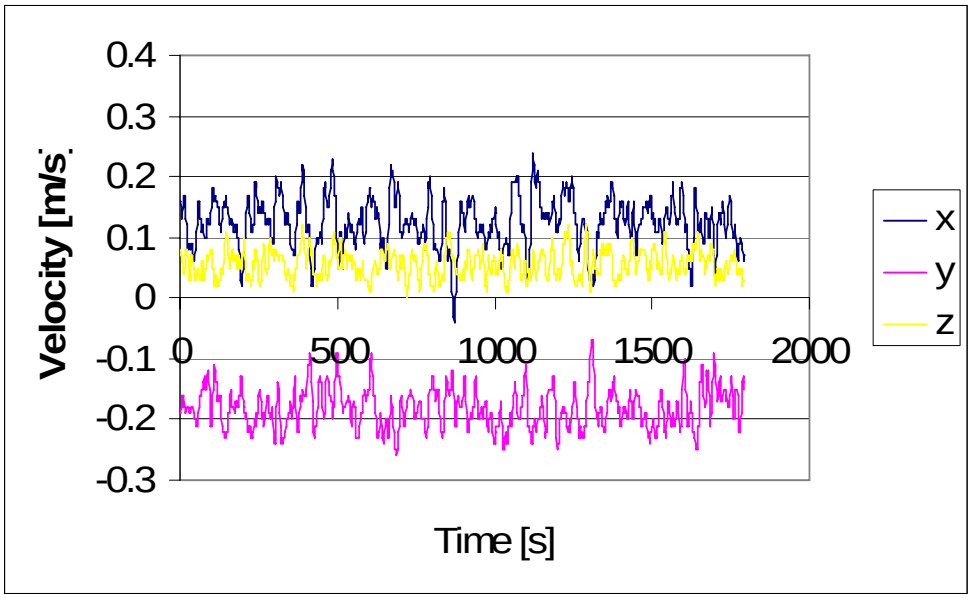

Figure 5.4: Trial 5 measured air flow velocity in cartesian components z,y,z, direction in a 1800s measuring period. z-direction vertical.

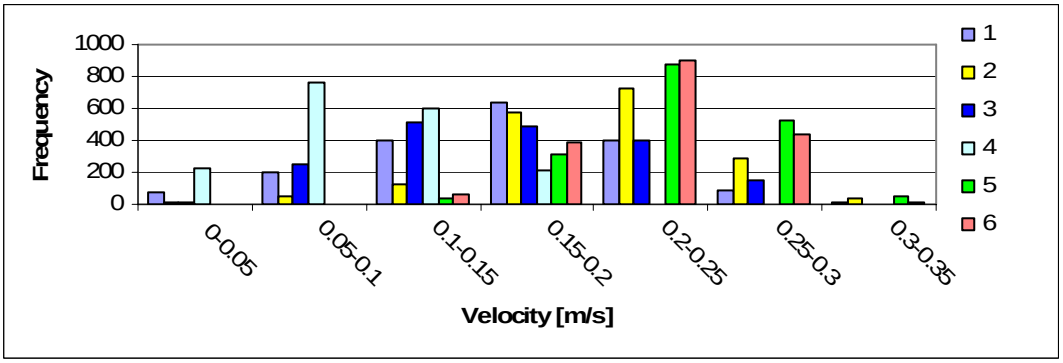

Figure 5.5: Normal distribution of measured resulting velocity of 6 different experimental trials.

From the velocity measurements Figure 5.3 and Figure 5.4 there is not a obvious periodic variance visible. If there is a periodic variance this could indicate unsteady conditions in the room. Fast Fourier Transformation (FFT)(2006) analysis and the derived power spectrum Figure 5.6 reveals periodic variation of 0.05-0.002Hz or periods of 20-500s. The periodic variation is the same in the setup with and without pen partitions. There is a tendency towards that the majority and the most frequent of the periodic variations are of 0.05-0.01Hz, or 20-100s.

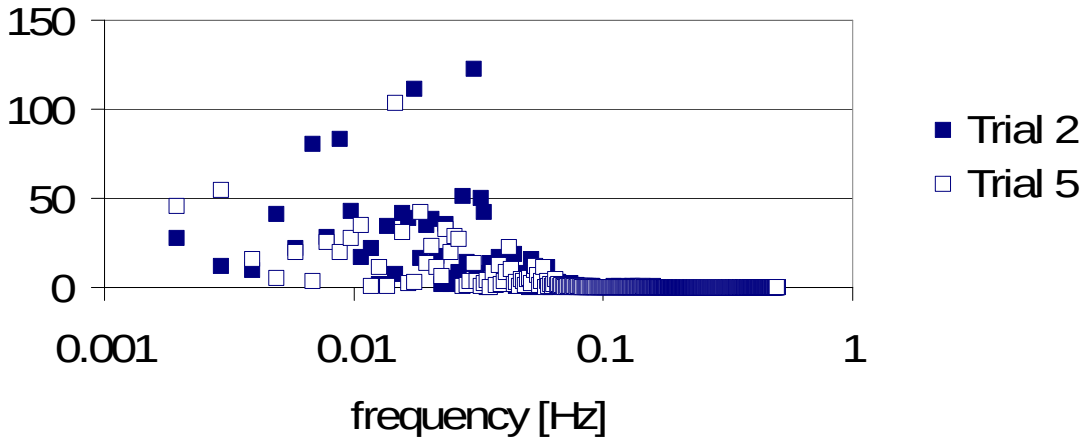

Figure 5.6: Frequency content chart of the Fourier transformated velocity distribution of the resulting velocity of trial 2 and 5. The primary axis is the period frequency and the secondary aksis is the number of incidence.

Simulating the air flow distribution in trail 2 and 5 under unsteady conditions the result does not indicate that there is a discrepancy between the solution of the steady and unsteady flow conditions. The frequency of periodic variation that can be observed in the simulations is bigger than the measuring frequency. Possibly there is unsteady boundary conditions that initiate the periodic variation in the measurements that is not accounted for in the simulation.

From the measurements of the velocity the turbulence intensity can be calculated.

The turbulence intensity is of interest to the convective heat transport. For the convective heat flux in different trials to be comparable, the turbulence intensity, the air temperature and the air velocity close to the heated surface should be constant in all trials.

On the basis of measured air temperature and velocity the turbulence intensity was calculated from:

$$Tu = \frac{SD}{\bar{u}} \qquad / 5.2$$

where SD is the standard deviation defined as:

$$SD = \sqrt{\frac{1}{n-1}\sum_{i=1}^{n}(u_i - \bar{u})^2} \qquad / 5.3$$

Here the mean velocity is defined as:

$$\bar{u} = \frac{1}{n}\sum_{i=1}^{n} u_i \qquad / 5.4$$

where n is the number of measurements.

The air velocity was measured in the Cartesian components u_x, u_y, u_z (m/s). The resulting air velocity in each observation can be expressed as:

$$u_i = \sqrt{u_{x,i}^2 + u_{y,i}^2 + u_{z,i}^2} \qquad / 5.5$$

Where i=1-n and n is the number of measurements.

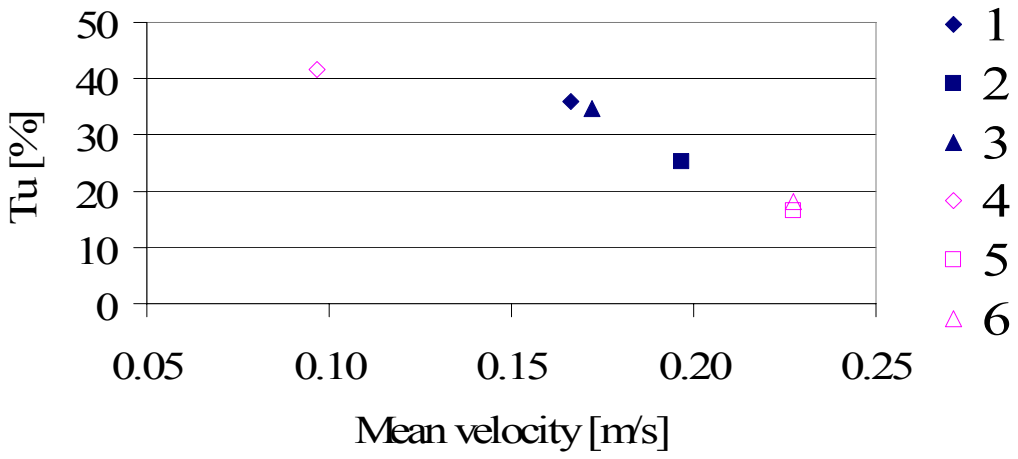

Figure 5.7: Turbulence intensity T_u as a function of mean velocity $\bar{u}$ in location (x,y,z)=(3.75,6.5,0.2)m of trials 1-6.

A increase in turbulence intensity at decreasing velocity is observed Figure 5.7. According to EN ISO 7730(1997) Figure 5.8 the environmental comfort is not jeopardized at this relation between air flow velocity and turbulence intensity particularly not when the thermal conditions in the occupational zone is independent of inlet air temperature and velocity conditions.

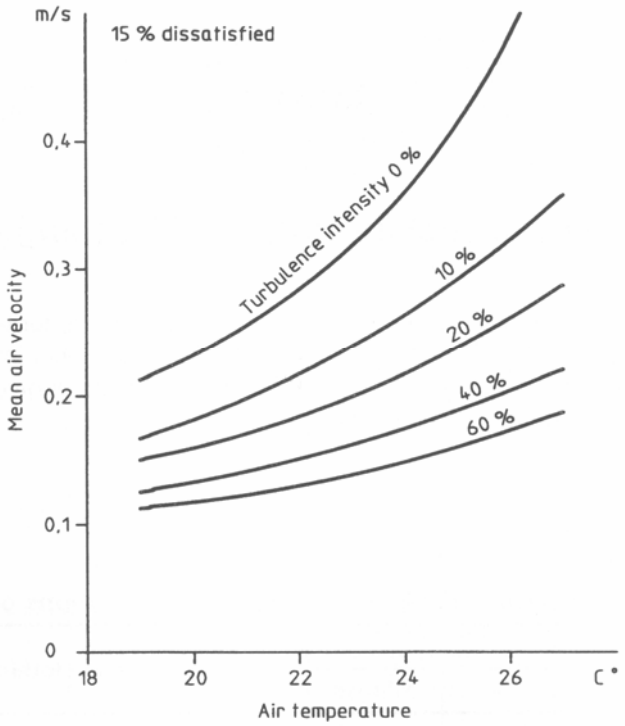

Figure 5.8: Mean air velocity as a function of air temperature and turbulence intensity at 15% dissatisfied (PPD) (EN ISO 7730, 1997)

The simulations were performed with boundary conditions similar to the experimental room. The boundary condition at the diffuse inlet was a simple velocity inlet with a inlet temperature equivalent to the experimental setup. The flow system in the diffuse ventilated room is clearly driven by buoyancy forces. By comparing the simulations to the experimental data, showed that there was a significant difference between the measured and simulated temperature, at the location close to the wall in the setup with pen partitions. Except for the location close to the wall, the difference between the measured and simulated temperatures in each measuring location in the entire horizontal profile have a almost constant deviation in all trials except trial 2. Examining the velocity and temperature contours of a simulation with pen partitions with the equivalent simulation without pen partitions, show that there is significant difference in the mixing convection conditions of the room with and without pen partitions. The room without pen partitions show a 3D flow character where the flow

in the room with pen partitions has thermal and airflow velocity symmetry plane located as the room setup symmetry plane. The formation of 3D flow conditions in a room with symmetric boundary conditions has been examined by Bjerg et al. (1999) and Zhang et al.(2000) and is discussed and illustrated with an example in appendix 2. The simulation accuracy on trial 2 has been tested according to the recommendations in Sørensen et al.(2003) and appendix 1. Changes in grid resolution and differencing scheme order gave no effect on the general picture of a 3D flow solution. The solution was not stable after 6000s iteration time.

There was a significant difference between measured and simulated velocity in the setup without pen partitions. The maximum simulated velocity was a factor 60 times higher than the inlet velocity through the diffuse inlet ceiling.

Conclusions

The air flow system is driven by convective forces and not the inlet momentum which is very weak in this system.

The simulations show that a 3D asymmetric flow systems in the room can be changed to a symmetric flow system with the introduction of impervious pen partitions.

Measurement and simulation apparently give significantly different results of velocity in the configuration without pen partition in the central location. The steady and unsteady simulations results indicate that 3D conditions prevail in the room without pen partitions but that the 3D situation is steady. The measurements are performed in one location only. Because the flow system is 3D other measurement locations would possibly show various discrepancy from the simulation results.

The measured temperature gradients in the occupational zone at the floor in the near wall location are significantly dependent on pen partition configuration but

independent on air exchange rate and inlet temperature. The pen partitions clearly have an effect on the convective conditions in the room and from a climate control viewpoint the pen partitions improve the predictability and reduce the spatial variance of the climate in the room.

In the configuration with pen partitions in the near wall location the temperatures of the measurements are numerically significantly different from the temperatures of the simulations.

The measured air velocity in the occupational zone is independent on the pen partition, air exchange rate and inlet temperature. The measured air velocity in the occupational zone is comparable to air velocities in slot ventilated housing facilities.

5.3 Tunnel model

An experiment has been conducted to examine the heat exchanging function of the diffuse inlet material, **paper 5**,(Jacobsen et al., 2006b). The purpose of the experiment is to

- examine the convection and radiation influence of the preconditioning of the air through a diffuse ventilation inlet and to
- determine the thermal boundary conditions of a diffuse ventilated inlet.

Both the effect of the *radiative and convective heat transfer* and a *boundary layer mixing convection* is to be examined. The boundary layer mixing convection is a consequence of the room air flow. From the simulations and measurements in the preceeding experiments, **paper 3** and **paper 4**, the room air flow is assumed to have a flow perpendicular to the flow direction of the fresh air inlet through the diffuse material. The results will be applicable as boundary conditions in a CFD simulation of the diffuse ventilated room

Materials and methods

Initially the flow conditions in two different available flow tunnels, an expansion flow tunnel and a uniform crossection area tunnel, is examined with regard to producing uniform flow gradients perpendicular to the downstream boundary surface of the diffuse material. The expansion tunnel system is examined in appendix 2 and significant air velocity gradients is found in a plane perpendicular to the potential inlet of the diffuse inlet. The velocity profile in the uniform cross section tunnel Figure 5.9 is examined under isothermal conditions. The experimental setup consists of two flow tunnels with flow direction perpendicular to each other.

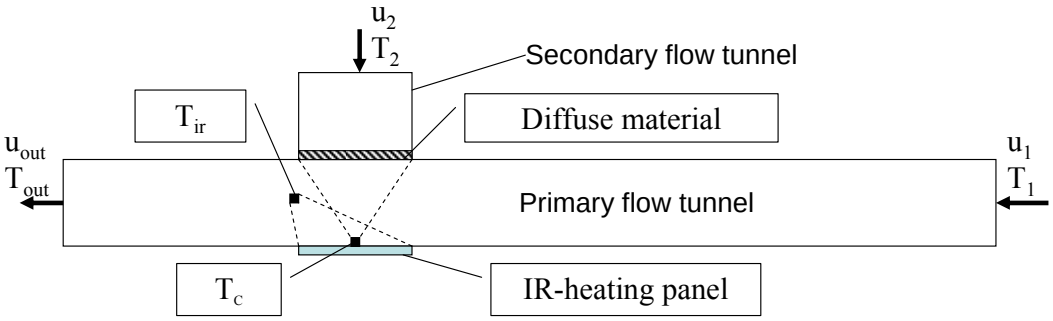

Figure 5.9: Cross section of the experimental tunnel, ■ indicating infrared sensor measuring instrument location, T_{ir} and T_c. Measuring area indicated with dotted lines.

A primary flow tunnel where the flow conditions close to the downstream boundary surface of the diffuse material in diffuse ventilated room is reproduced. And a secondary flow tunnel where the inlet conditions through the diffuse ceiling is reproduced. The horizontal interface between the two tunnel systems is at the downstream surface of the diffuse inlet material. On the opposite wall to the downstream surface of the diffuse material in the primary tunnel, a infrared heating panel is located. The flow volume and air temperature in each tunnel is regulated individually. Measurements of the flow volume and air temperature in each tunnel and surface temperature of the diffuse material and infrared heating panel is performed at

steady state conditions at chosen setpoint span relevant to the corresponding climatic conditions in a diffuse ventilated pighousing facility.

Results

It must be assumed that if there is no convective and radiative heat exchange in the diffuse material then the surface temperature of the downstream temperature of the diffuse material must be the equivalent to the upstream surface temperature. The temperature of the air in the primary tunnel were higher than the air in the secondary tunnel in the measurements. The temperature of the downstream surface the downstream surface temperature of the diffuse material was between 1-12 K higher than the upstream air temperature.

The effect of the different parameters, on the observed preheating of the diffuse material downstream surface (the surface facing the occupational room), is examined. It is observed that the downstream surface temperature of the diffuse material is lower than temperature of the infrared heating panel and higher than the primary tunnel air. Conclusively the downstream surface of the diffuse material is heated by the radiative energy input. A temperature increase up to 7 K is observed that can substantially be accredited to the infrared radiation heating, **paper 5,**.

A linear model has been developed that expresses the surface temperature of the downstream surface as a function of flow velocity and air temperature in each tunnel and surface temperature of the diffuse and infrared heating panel. It is assumed that the airflow velocity can be expressed as the ratio of airflow volume to tunnel cross section area. Linearity assumption is assessed in all energy transport. In radiation the energy transfer is a function of the fourth power of the temperature in kelvin [K], but at high values of temperature the logarithmic function of energy transfer by radiation can be approximated a linear function.

Assumingly that the variables are normally distributed and independent the linear model of the surface temperature T_c are

Model A: $T_c = \beta_0 + \beta_1 u_1 + \beta_2 u_2 + \beta_3 T_1 + \beta_4 T_2 + \beta_5 T_{ir}$

where T_c is the downstream surface temperature of the diffuse inlet, u_1 is the mean flow velocity in the primary tunnel, u_2 is the mean flow velocity in the secondary tunnel, T_1 is the air temperature in the primary tunnel and T_2 is the air temperature in the secondary tunnel.

The coefficients estimate for the linear model are shown in Table 5.2.

Table 5.2: Coefficient estimate and 95% confidence intervalf (CI) for estimates model A, dependent variable T_c,upper, n=991, T_1>T_2.

Coefficient	β_1	β_2	β_3	β_4	β_5	*s.s.*	*m.s.*
Estimate Model A	-1.9137	-272.81	0.40232	0.46737	0.14000	706	0.72
CI95% upper	-2.570	-285.1	0.3905	0.4537	0.1333		
CI95% lower	-1.258	-260.5	0.4142	0.4810	0.1467		

Examining the residuals of the dependent and independent variables reveal that the model give a good fit with the data. A sensitivity analysis reveals that the model prediction uncertainty increases at the periphery of the data span. Extrapolating the model is hence not recommendable.

Conclusion

The exchange of energy and the preconditioning of inlet air in the diffuse material is found to be dependent on both convective and radiative conditions in the occupational room.

A linear model of the downstream surface of the diffuse material is developed. The model can not be extrapolated outside the data range.

5.4 Conclusions

The conclusions of the experimental work can be divided in two sections. One, concerning the environmental comfort conditions in the animal occupational zone and one, concerning the inlet boundary conditions of the surface of the diffuse ceiling.

Animal occupational zone

The temperature conditions in the occupational zone are independent of inlet velocity and inlet temperature in the diffuse inlet ventilated room. Pen partitions have a significant influence on the temperature conditions close to the housing envelope wall and the formation of 3D flow systems in the room.

The simulations show that the air flow movements in the room are strongly buoyancy driven and the airflow velocity in the room are significantly higher than the boundary condition inlet velocity.

Inlet boundary conditions

The comparison of the experiments and the simulations of a full scale room conclusion is that a significantly elevated temperature in the region close to the diffuse ceiling is observed in the experiments compared to the simulation. The simulation was performed with simple velocity boundary conditions at the diffuse ceiling.

The boundary conditions of a diffuse inlet were examined in a windtunnel and a linear model of the boundary surface temperature as a function of the independent variables was developed.

6 General discussion and conclusion

In terms of the sensible temperature the diffuse inlet ceiling has been found to provide the animals in the occupational zone with thermal environment independent of the inlet conditions. The simulations of the diffuse ceiling ventilated room show that simple inlet boundary conditions give a significant deviation from the measured temperature conditions in location close to the diffuse ceiling inlet. The measured temperature was significantly higher than the simulated temperature. Measurements in a wind tunnel system show that the downstream inlet temperature out of the porous material was significantly higher than the upstream inlet temperature, the conclusion was that the porous material has both convective and radiation dependent heat exchanging properties. The convective heat exchange imply a convective boundary layer extending into the porous material hence a non-slip boundary surface condition on the downstream surface of the porous material can not be assumed. A non-slip boundary condition on the downstream surface could be assumed if the porous material was ideally isotropic and the fluid incompressible. Then there would be no penetration depth of boundary layer into the diffuse material and the preheating of inlet air would only depend on the radiation from other surfaces. It must be assumed that the pressure and momentum, and possibly the turbulence conditions, in the air flow at the boundary surface, displace the inlet flow to form an effective non-slip boundary condition inside the porous material. The location of the effective non-slip boundary surface is dependent on the flow conditions in the room but also on the

material deviance from ideal isotropic conditions. This means that there will be both spatial and temporal variance of effective non-slip boundary location. Simulating this system with mean value assumption of material parameters is not negotiable because this would be equivalent to assuming ideal isotropic conditions. A possible way to solve the problem is using a DNS method.

A model for this purpose has been developed in this project. It is important to note that the application of the boundary condition model in a CFD simulation of a diffuse ventilated room is not compatible with the simulation of thermal radiation in the same domain and the model can not be extrapolated.

6.1 Questions for further research

Many new questions rise on the fundaments of the conclusions derived form the present research.

3D conditions has been found in rooms that are symmetric. Simulations show that the formation of 3D conditions are dependent on the initial conditions but the solution are steady. In a room where the boundary conditions change with the mobility of the animals it is likely that the conditions will be unsteady. The transition time from different steady conditions, dependent on the location of the animals, would be a interesting study in order to develop a predictive environment regulation system.

The physics of the porous material could be subject to further examination.

Is it possible to determine the physical properties of the porous material to develop a deterministic model of the boundary surface temperature? How is it possible to determine the material properties that give the transient flow conditions and presumably the spatial variation in boundary layer thickness inside the porous material?

Nomenclature

Latin letters	
$\bar{t}_r$	Mean radiant temperature [°C]
φ	General variable
Γ	Effective diffusive coefficient
q'_R	Radiative heat transfer pr. unit length [W/m]
$\tilde{\mu}$	Effective porous dynamic viscosity
A	Constant
A	Area [m^2]
A	Surface area per unit volume of solid [1/m]
C	Emperical inertia coefficient
C	Coefficient of discharge
C_1	Constant=1.44
C_2	Constant=1.92
CI 95%	Confidence interval 95%
C_p	Isobaric specific heat [$Jkg^{-1}K^{-1}$]
C_μ	Constant=0.09
D	Mean pore diameter [mm]
dh	Enthalpy difference [J/kg]
dT	Temperature difference [K]
E(T)	Hemispherical emissive power [W/m^2]
$E_b(T)$	Total emissive power from blackbody [W/m^2]

G	Production due to buoyancy forces
g_i	Gravitational acceleration component [m/s^2]
Gr	Grasshoff number
h	Convection heat transfer coefficient [$Wm^{-2}K^{-1}$]
h_v	Volumetric heat transfer coefficient [-]
I_λ	Spectral radiation intensity [$Wm^{-2}s^{-1}r^{-1}$]
k	Turbulent kinetic energy
k	Thermal conductivity [$Wm^{-1}K^{-1}$]
L	Medium thickness [m]
N	Air exchange rate [h^{-1}]
P	Pen partition
p	Pressure [N/m^2] [Pa]
P_k	Production due to strain
Q	Energy[J]
q	Heat transfer rate [W]
Q_C	Energy loss through convection [J]
Q_D	Energy loss through conduction [J]
Q_{Ere}	Latent and dry respiration energy loss [J]
Q_{Esw}	Energy loss through transpiration and evaporation [J]
Q_H	Internal heat production [J]
q_R	Radiative heat flux
Q_R	Radiative energy loss [J]
S_m	Momentum source/sink
S_T	Thermal source/sink
St	Net source term

T	Temperature [K]
t	Time [s]
T_0	Reference temperature [K]
t_a	Air temperature [°C]
t_o	Operative temperature [°C]
T_u	Turbulence intensity
u	Velocity [m/s]
u_{ar}	Relative air velocity [m/s]
V	Volume [m^3]
V_g	Volume occupied by gas in porous medium [m^3]
V_s	Volume occupied by solid in porous medium [m^3]
α	Empirical structural parameter
α	Thermal diffusivity [m^2/s]
α_λ	Radiative absorptivity
β	Isobaric thermal expansion coefficient [1/K]
δ_{ij}	Kronecker delta, $i=j \rightarrow \delta_{ij}=1$, $i \neq j \rightarrow \delta_{ij}=0$
Δp	Pressure difference [Pa]
ε	Isotropic viscous dissipation rate
ε	Porosity [-]
$\varepsilon(T)$	Emissivity []
ε_1	Expansibility factor
θ	Direction
κ	Von Kárámán constant =0.41
κ	Radiative extinction coefficient [1/m]
κ_i	Direction dependent permeability [m^2]

$\kappa_{\lambda,a}$	Absorption coefficient [1/m]
$\kappa_{\lambda,s}$	Scattering coefficient [1/m]
Λ	Wavelength [m]
μ	Dynamic viscosity [$kgs^{-1}m^{-1}$]
μ_{eff}	Effective dynamic viscosity [$kgs^{-1}m^{-1}$]
μ_t	Turbulent dynamic viscosity [$kgs^{-1}m^{-1}$]
ρ	Density [kg/m^3]
σ	Stefan-Boltzmann constant: 5.670e-8 $Wm^{-2}K^{-4}$
σ_k	Constant=1.3
σ_t	Turbulent Prandtl number
σ_ε	Constant=1.0
τ_λ	Radiative transmissivity
υ	Frequency of radiation [1/s]
ω_a	Scattering albedo

Special symbols

$\overline{\varphi}$	Time average variable
φ'	Fluctuating, deviation from average variable
$\lvert\varphi\rvert$	Absolute value variable
φ^+	Dimensionless variable
φ_g	Variable gas
φ_0	Variable reference

Subscripts

0	Reference
a	Air
g	Gas
i	i-th coordinate direction
i	Observation
l	Laminar
meas	measurement
out	outlet
s	Solid
sim	simulation
t	Turbulent
x	x direction component
y	y direction component
z	z direction component

Abbreviations

CFD	Computational Fluid Dynamics
CI	Confidense Interval
DCV	Diffuse Ceiling Ventilation
DNS	Direct Numerical Simulation
DVS	Displacement Ventilation System
FFT	Fast Fourier Transformation

HVAC	Heating, Ventilating, Air Conditioning
MVS	Mixing Ventilation System
NS	Navier Stoke
PMV	Predicted Mean Vote
PPD	Predicted Percentage of Dissatisfied Individuals
RANS	Reynolds time Averaging Navier Stokes

Reference List

Reference List

FFTW. http://www.fttw.org . 2006.
Ref Type: Electronic Citation

Aarnink, A. J. A. and M. J. M. Wagemans. 1997. Ammonia volatilization and dust concentration as affected by ventilation systems for fattening pigs. *Transactions of the ASAE* 40:1161-1170.

Ardehali, M. M., N. G. Panah, and T. F. Smith. 2004. Proof of concept modeling of energy transfer mechanisms for radiant conditioning panels. *Energy Conversion and Management* 45:2005-2017.

Arpaci, V. S. and P. S. Larsen. 1984. *Convestion heat transfer*. Prentice-Hall, Inc..

Bakier, A. Y. 2001. Thermal radiation effect on mixed convection from vertical surfaces in saturated porous media. *International Communications on Heat and Mass Transfer* 28:119-126.

Barra, A. J., G. Diepvans, J. L. Ellzey, and M. R. Henneke. 2003. Numerical study of the effects of material properties on flame stabilization in a porous burner. *Combustion and Flame* 134:369-379.

Beckermann, C., R. Viskanta, and S. Ramadhyani. 1987. Natural convection flow and heat transfer between a fluid layer and a porous layer inside a rectangular enclosure. *Journal of Heat Transfer* 109:363-370.

Beckermann, C., R. Viskanta, and S. Ramadhyani. 1988. Natural convection in vertical enclosures containing simultaneously fluid and porous layers. *Journal of Fluid Mechanics* 186:257-284.

Benzinger, T. H. 1978. The physiological basis for thermal comfort. *Proc. of the 1th Int. Indoor Climate Symp. Copenhagen, Denmark*441-476.

Bjerg, B., S. Morsing, K. Svidt, and G. Q. Zhang. 1999. Three-dimensional airflow in a livestock test room with two-dimensional boundary conditions. *Journal of Agricultural Engineering Research* 3:267-274.

Bjerg, B., K. Svidt, G. Q. Zhang, and S. Morsing. 2000. The effects of pen partitions and thermal pig simulators on airflow in a livestock test room. *Journal of Agricultural Engineering Research* 77:317-326.

Braga, E. J. and d. M. J. S. Lemos. 2004. Turbulent natural convection in a porous square cavity computed with a macroscopic k-e model. *International Journal of Heat and Mass Transfer* 47:5639-5650.

Chen, Q. 1990. Comfort and energy consumption analysis in buildings with radiant panels. *Energy and Buildings* 14.

Chen, X. and W. Sutton. 2005. Enhancement of heat transfer: Combined convection and radiation in the entrance region of circular ducts with porous inserts. *International Journal of Heat and Mass Transfer* In Press.

EN ISO 7730. EN ISO 7730: Moderate thermal environments-Determination of PMV and PPD indicies and specification of the conditions for thermal comfort. 1997.
Ref Type: Report

Fanger, P. O. 1970. *Thermal comfort; analysis and applications in environmental engineering*. McGraw-Hill.

Farge, B. d. l. 1972. L'ambiance des batiments d'elevage. Un index de comfort? *Bulletin I. T. P.* 5.

Fu, X., R. Viskanta, and J. P. Gore. 1998. Measurement and correlation of volumetric heat transfer coefficients of cellular ceramics. *Experimental Thermal and Fluid Science* 17:285-293.

Gan, G. 2000. Effective depth of fresh air distribution in rooms with single-sided natural ventilation. *Energy and Buildings* 31:65-73.

Holmberg, S., F. Molin, and J. Myhren. 2004. Space heating at low temperature difference between heating unit and ambient air. *Proceedings of 9'th Int. Conf. of Air distribution in rooms, Roomvent 2004, Univercity of Coimbra, Portugal*162-163.

Incropera, F. P. and D. P. De Witt. 1990. *Introduction to heat transfer*. John Wiley & Sons.

Jacobsen, L., P. V. Nielsen, and S. Morsing. 2004. Prediction of indoor airflow patterns in livestock buildings ventilated through a diffuse ceiling. *Proceedings of 9'th Int. Conf. of Air distribution in rooms, Roomvent 2004, Univercity of Coimbra, Portugal* 9.

Jacobsen, L., P. V. Nielsen, and S. Morsing. 2006a. Low momentum air supply through diffuse ceiling in livestock buildings. *Agricultural Engineering International: CIGR Journal of Scientific Research and Development*.

Jacobsen, L., P. V. Nielsen, S. Morsing, and G. Q. Zhang. 2006b. Boundary condition of porous ventilated ceiling exposed to convection and thermal radiation. *Agricultural Engineering International: CIGR Journal of Scientific Research and Development*.

Jiang, Z., Q. Cheng, and A. Moser. 1992. Indoor airflow with cooling panel and radiative/convective heat source. *ASHRAE Transactions.* 1:33-42.

Kahn, S. K. 2005. Heat transfer in a viscoelastic fluid flow over a streching surface with heat source/sink, suction/blowing and radiation. *International Journal of Heat and Mass Transfer* In press.

Kaviany, M. 1995. *Principles of heat transfer in porous media*. Springer-Verlag, New York.

Kim, T., S. Kato, S. Murakami, and J. Rho. 2005. Study on indoor thermal environment of office space controlled by cooling panel system using field measurement and the numerical simulation. *Building and Environment* 40:301-310.

Launder, B. E. and D. B. Spalding. 1974. The numerical computation of turbulent flows. *Computer Methods in Applied Mechanics and Energy* **3**:296-289.

Lemos, M. J. S. and R. S. Silva. 2005. Turbulent flow over a layer of a highly permable medium simulated with a diffusion-jump model for the interface. *International Journal of Heat and Mass Transfer*.

Mohammadein, A. A., M. A. Mansour, S. M. Abd el Gaied, and R. S. R. Gorla. 1998. Radiative effect on natural convection flows in porous media. *Transport in Porous media* 32:263-283.

Morsing, S., S. Pedersen, J. S. Strøm, and L. Jacobsen. 2005. Energy consumption and air quality in growing-finishing pig houses for three climate regions using cigr 2002 heat production equations. *Agricultural Engineering International: CIGR Journal of Scientific Research and Development* 7.

Morsing, S., J. S. Strøm, G. Q. Zhang, and L. Jacobsen. 2003. Prediction of indoor climate in pig houses. *Proc. 2nd Int. Swine Housing Conf. Rayleigh, USA ASAE publ. 701P1303*41-47.

Neale, G. and W. Nader. 1974. Practical significance of Brinkman's extension of Darcy's law: coupled parallel flows within a channel and a bounding porous medium. *Canadian Journal of Chemical Engineering* 52:475-478.

Nielsen, P. V. 1999. *Lecture notes on scale model experiments*. Department of building tecnology and structural engineering.

Nielsen, P. V., A. Restivo, and J. H. Whitelaw. 1979. Buoyancy-affected flows in ventilated rooms. *Numerical Heat Transfer* 2:115-127.

O'Shaughnessy, P. T., C. Achutan, and A. W. Karsten. 2002. Temporal variation of indoor air quality in an enclosed swine confinement building. *Transactions of the ASAE* 8:349-364.

Olsen, A. W., L. Dybkjær, and H. B. Simonsen. 2001. Behavior of growing pigs kept in pens with outdoor runs II. Temperature regulatory behavior, comfort behavior and dunging preferences. *Livestock production science* 69:265-278.

Pedersen, S. and K. Sällvik. Climatization of animal houses, Heat and moisture production at animal and house levels. Pedersen, S. and Sällvik, K. 4, -45. 2002. International Comission of Agricultural Engineering, section II, CIGR.
Ref Type: Report

Raptis, A. 1998. Radiation and free convection flow through a porous medium. *International Communications on Heat and Mass Transfer* 25:289-295.

Rees, S. J., J. J. McGuirk, and P. Haves. 2001. Numerical investigation of transient buoyant flow in a room with displacement ventilation and a chilled ceiling room. *International Journal of Heat and Mass Transfer* 44:3067-3080.

Sako, T., T. Mochida, K. Nagano, and K. Shimakura. 2002. Curved line of constant thermal sensation expressed using mean skin temperature and skin wettedness. *Proceedings of 8'th Int. Conf. of Air distribution in rooms, Roomvent 2004, Copenhagen, Denmark*313-316.

Sathe, S. B., W. Q. Lin, and T. W. Tong. 1988. Natural convection in enclosures containing an insulation with a permable fluid-porous interface. *International Journal of Heat and Fluid Flow* 9:389-395.

Sørensen, D. N. and P. V. Nielsen. 2003. Quality control of computational fluid dynamics in indoor environments. *Indoor Air* 13:2-17.

Strøm, J. S. and A. Feenstra. 1980. Heat loss from cattle, swine and poultry. *American Society of Agricultural Engineers, Summer Meeting.* 80-4021.

Talukdar, P., S. C. Mishra, D. Trimis, and F. Durst. 2004. Heat transfer characteristics of a porous radiant burner under the influence of a 2-D radiation field. *Journal of Quantitative Spectroscopy & Radiant Transfer* 84:527-537.

Wagenberg, A. V. and M. A. H. H. Smolders. 2002. Contaminant and heat removal effectiveness of three ventilation systems in a nursery room for pigs. *Transactions of the ASAE* 45:1985-1992.

Wilhelm, L. R. and D. B. McKinney. 2001. Environmental measurements in production swine facilities. *Transactions of the ASAE* 17:669-675.

Xin, H. 2005. Assesing swine thermal comfort by image analysis of postural behaviors. *Journal of animal science* 77:1-9.

Younis, L. B. and R. Viskanta. 1993. Experimental determination of the volumetric heat transfer coefficient between stream of air and ceramic foam. *International Journal of Heat and Mass Transfer* 36:1425-1434.

Zhang, G. Q., S. Morsing, B. Bjerg, K. Svidt, and J. S. Strøm. 2000. Test room for validation of airflow patterns estimated by computational fluid dynamics. *Journal of Agricultural Engineering Research* 74:141-148.

Zhang, G. Q., S. Morsing, J. S. Strøm, B. Bjerg, and K. Svidt. 2003. Velocity fields and CO2 distribution in the near floor regions of a room with pig-simulators and partition wall . *Proc. 2nd Int. Swine Housing Conf. Rayleigh, USA ASAE publ. 701P130*348-55.

PAPER NO.1:

S. Morsing, S. Pedersen, J. S. Strøm and L. Jacobsen: Energy Consumption and Air Quality in Growing-Finishing Pig Houses for Three Climate Regions Using CIGR 2002 Heat Production Equations.

Energy Consumption and Air Quality in Growing-Finishing Pig Houses for Three Climate Regions Using CIGR 2002 Heat Production Equations

S. Morsing, S. Pedersen, J. S. Strøm, & L. Jacobsen
Danish Institute of Agricultural Sciences, Research Centre Bygholm, DK-8700, Horsens, Denmark. E-mail: soeren.pedersen@agrsci.dk

ABSTRACT

Simulation of indoor climate, air quality and energy consumption for animal houses requires precise information on animal heat and moisture production at different housing conditions. In this article results are presented from an analysis of energy consumption for heating and ventilation of a dry and a wet growing-finishing pig house as well as on indoor climate and air quality in three climate regions in Finland, Denmark and Portugal. The analysis is based on the latest CIGR models of animal heat and moisture production on house level, not only taking the body weight, but also the feed intake into account.

Four temperature set-point levels were analyzed. As representative of a house with no bedding, an indoor start temperature set-point of 22°C was used for 30 kg growing-finishing pigs. After 7 days the set-point was decreased linearly until reaching the lower temperature set-point of 18°C at an end weight of 100 kg. The effect on energy consumption for heating and ventilation of houses with bedding or covered pens was investigated using three lower temperature set-point levels with start set-points of 20, 18 and 16°C with the corresponding end set-points of 16, 14 and 12°C.

In selecting set-point strategies for maximum relative humidity (RH), it is assumed according to CIGR recommendations, that higher RH is acceptable at lower temperatures. When normal air quality and low energy consumption is given first priority, the set-point sum of temperature (°C) and RH (%) is 90, e.g. for a 22-18°C temperature set-point level a RH set-point of 68-72 % is used. An alternative would be to use extra energy to achieve good air quality by selecting a set-point sum of 85.

The energy consumption for ventilation decreases nearly linearly with about 20 % when the start temperature for pigs of 30 kg decreases from 22 to 16°C. For fans with the energy efficiency 20 000 m^3 per kWh, the energy consumption for ventilation is between 6.6 for Finland and 8.7 kWh per produced pig for Portugal for start set-point temperature of 22°C. Compared to Finland the energy consumption for ventilation is approximately 6 % higher in Denmark and 32 % higher in Portugal, due to higher outdoor temperatures and hence increased ventilation need.

The energy consumption for heating under dry housing conditions is less than 1.5 kWh per produced pig in Denmark and Portugal at start temperatures up to 22°C, and less than 10 kWh per produced pig in Finland. The heat consumption under wet indoor housing conditions is higher and up to 8 kWh for Denmark and up to 23 kWh per produced pig for Finland at a start temperature of 22°C.

S. Morsing, S. Pedersen, J. S. Strøm and L. Jacobsen "Energy Consumption and Air Quality in Growing/Finishing Pig Houses for Three Climate Regions Using CIGR 2002 Heat Production Equations". Agricultural Engineering International: the CIGR Ejournal. Vol. VII. Manuscript BC 05 007. September, 2005.

Keywords: Pig housing, animal heat production, feed intake, ventilation rate, energy, simulation.

1. INTRODUCTION

Precise information is needed on animal heat and moisture production in simulations of indoor climate, air quality and energy consumption for growing-finishing pigs. Energy simulations were presented by Pedersen et al. (2005) for heating of a weaner house while this article is primarily dealing with the energy consumption for ventilation and heating of a growing-finishing pig house.

As discussed by Brown-Brandl *et al.* (2003), the animal latent and sensible heat production depend on several parameters like genetics, feed intake, feed composition, and housing conditions. For the period 1984-2001 they found an increase in the maintenance heat production of 19 %, due to increased lean tissue content and consequently less fat insulation.

Information on the partition of total heat on sensible and latent heat is needed at house level, taking evaporation of spilt water and water evaporated from feed and manure into account. The heat required for evaporation is taken from the sensible heat supplied by the animals. In the CIGR (2002) report, equations for heat production for growing-finishing pigs are given, not only taking the body weight, but also taking the feed intake into account.

Design rules for animal heat and moisture production have been available for decades, e.g. in Strøm (1978), ASHRAE (2001a and 2001b) and CIGR (1984, 1992, 1999 and 2002). Today, manual simulations are replaced by computer simulations, e.g. as described by Morsing & Strom (1992), Morsing et al. (1997), and Pedersen et al. (2004)

This article deals with the results from an analysis of indoor environment and energy consumption in a growing-finishing pig house using the computer program StaldVent version 5.0 (Morsing et al., 2003), in which the CIGR (2002) design equations are implemented. The program contains algorithms for the design of ventilation and heating systems based on performance data for ventilation equipment (Pedersen & Strom, 1995). The performance of the selected system is simulated over a three-year production period for all inn/all out production. The long simulation period is used to compensate for different starting time in the year. Local weather data generated by Meteonorm (2000) are used for the simulations.

Results are presented for dry and wet housing conditions in three climate regions in Europe. Four temperature set-point levels and two control strategies for indoor climate and air quality are analysed.

2. PRODUCTION, HOUSING CONDITIONS AND ANIMAL HEAT

In order to facilitate comparisons of performance, the same growing-finishing pig production, housing conditions, heating and ventilation system, and control strategies are assumed in all three climate regions.

2.1 Production

The simulations are based on a 200 pig all-in/all-out production. After three days between batches, the pigs were started at an average live weight of 30 kg. They reach the end weight of 100 kg after 84 days, assuming an average daily growth rate of 830 g, Figure 1. The relation between age and body weight is based on a smooth curve starting with a body weight of 1 kg for new-born piglet and body weights for growing-finishing pigs from 30 to 100 kg according to Danish recommendations.

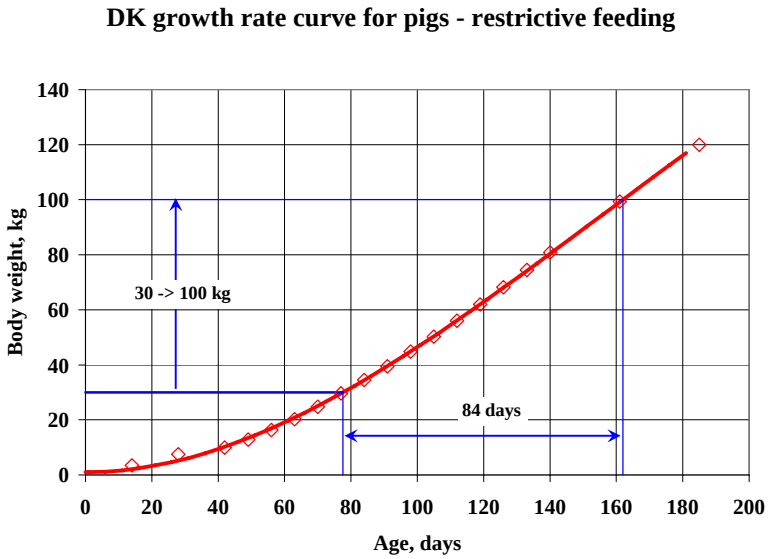

Figure 1. The time for the growing-finishing pigs to grow from 30 to 100 kg is 84 days, according to Danish recomendations for growing pigs.

The start temperature set-point was maintained for seven days before decreasing linearly to a 4 ^{o}C lower end set-point at 100 kg. The house was assumed to be empty and unheated for the three days between batches.

2.2 House

The insulated building was 10.0 m wide and 19.4 m long with 2.6 m high side walls. Assuming a 0.8 m wide inspection alley the total pen floor area was 178.5 m^2 equal to 0.89 m^2 pen floor area per pig. The ceiling was flat, and roof double sided sloped 25°.

2.3 Weather

The outdoor temperature and the relative humidity vary considerably from one region to another. Detailed information on an hourly basis is available world-wide, e.g. Meteonorm (2000). Figure 2 shows the outdoor temperatures accumulated over the year for the three following climatically

different regions in Europe: North inland (Kaajani, Finland), North coastal (Karup, Denmark) and South coastal (Porto, Portugal) according to Meteonorm.

Based on the accumulated outdoor temperatures the percentiles may be calculated and used for design of the ventilation and heating system. The 1% and 99% temperature percentiles, shown in Table 1, are used in this article, i.e. on average, the heating and ventilation capacity will be insufficient only 1% of the time, corresponding to 88 hours per year, assuming constant diurnal animal heat and moisture production.

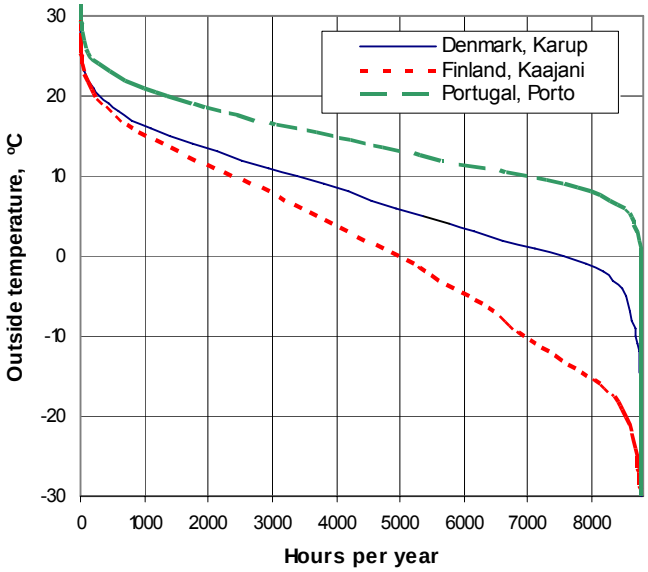

Figure 2. Outdoor temperatures in three European regions (Meteonorm, 2000)

Table 1. 1% and 99% temperature percentiles for the three selected regions

	Portugal (Porto) °C	Denmark (Karup) °C	Finland (Kaajani) °C
Outdoor temperatures exceeded 1% of time	26	23	23
Outdoor temperatures exceeded 99% of time	4	-9	-23
Annual average	14.2	7.5	2.3

2.4 Design Airflow Rate

The design airflow rate was calculated on the basis of the acceptable temperature difference between outside and inside, $\Delta t_{s\ design}$, given in Table 2. The resulting design airflow rate in Denmark and Finland was at $\Delta t_{s\ design} = 2.5$ °C 18 900 m^3/h and in Portugal at $\Delta t_{s\ design} = 2.0$ °C 23 700 m^3/h.

Table 2. Accepted temperature increases according to CIGR (1984) and Design Δt_s, used in this article.

Outside temperature, °C, exceeding 99% percentile CIGR (1984)	CIGR (1984) Δt_s °C	Design $\Delta t_{s\ design}$ °C	Location
18.0-20.9	4	3.5	
21.0-23.9	*3*	*2.5*	*Karup, Kaajani*
24.0-26.9	*2.5*	*2*	*Porto*
27.0-30.9	2	1.5	

2.5 Selected Ventilation System

A negative pressure ventilation system was designed based on the performance data for selected wall inlets and roof-top exhaust units. The operating point in the ventilation diagram for a system with18 inlets and 4 exhaust units was computed with StaldVent. As shown in Figure 3 the ventilation system was able to provide 23 500 m^3/h at -14.7 Pa, which is 24% more than the design target $\Delta t_{s\ design}$ = 2.5 °C for Finland and Denmark and only 1 % less than the target $\Delta t_{s\ design}$ = 2.0 °C for Portugal.

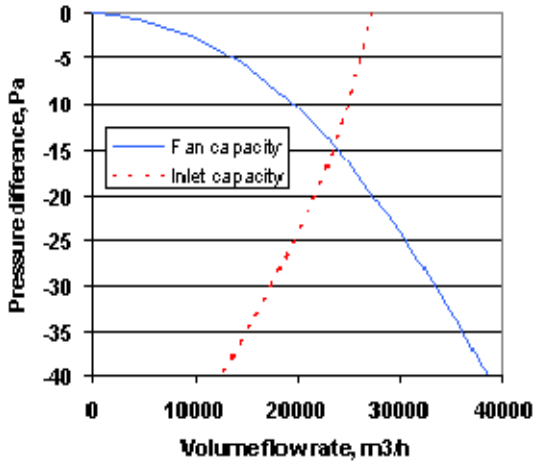

Figure 3. Ventilation diagram for a system consisting of 18 inlets and 4 exhaust units.

To keep temperature at the set–point value, the airflow rate can be controlled in different ways, e.g. using on/off fans, damper control, staged fans or frequency or voltage controlled fans in combination with damper control. The connection between air flow rate and energy consumption will depend on the chosen control strategy.

In this article the airflow rate is adjusted by fan speed, fan damper and inlet opening. At 100 % airflow rate with maximum fan speed and fully open damper and inlets the energy consumption for the four fans is 1175 W (100 %) decreasing linearly with airflow rate to 470 W (40 %) at no airflow rate as shown in Figure 4.

2.6 Design Heat Requirement

The design heat requirement was determined with 30 kg pigs in a room with a temperature set-point of 22°C. StaldVent was used to calculate the necessary heating capacity. The results were 15.350 W in Finland, and 5.600 W in Denmark. To make sure that enough heat was available to cover the requirement in all cases an over designed heating capacity of 20 kW used in the simulations.

2.7 Animal Total Heat Production

The total heat production at 20 °C for growing-finishing pigs was calculated on the basis of the CIGR (2002) equation for the total heat production due to maintenance and growth taking daily feed energy intake into account.

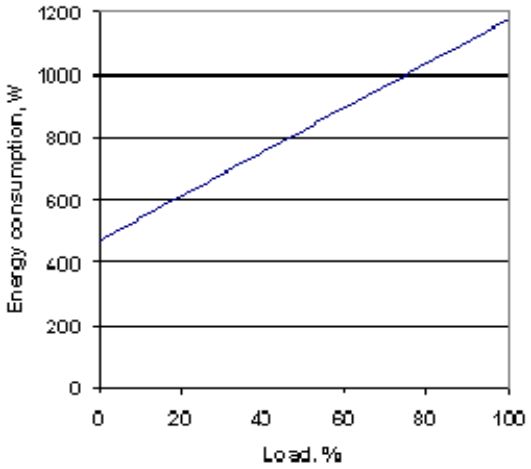

Figure 4. Energy consumption at different ventilation loads (100% = maximum fan capacity and fully open dampers and inlets)

The feed intake can be specified individually or as standard values. Table 3 shows the used n-values for restricted feeding based on Danish feeding recommendations assuming that 1 kg pig feed is equivalent to 12 900 kJ metabolizable energy. The maintenance was calculated in accordance with CIGR 2002.

Table 3. Feeding level for growing-finishing pigs expressed as n times maintenance

Body mass (m) Kg	Maintenance (n=1) MJ/day	Restricted feeding (n) (Danish recommendations)
30	5.64	3.30
40	6.99	3.31
50	8.27	3.26
60	9.48	3.19
70	10.64	3.09
80	11.76	2.98

90	12.85	2.75
100	13.91	2.54

Former recommendations for total heat production for pigs was based on a heat producing unit (HPU) that was defined as 1000 W total heat production at 20°C (Strøm, 1980). It was given as a function of live weight only and did not include the possibility to adjust for the daily feed energy intake.

Comparison between the old and the new values may be done by converting the specified feeding levels to total heat production according to the CIGR 2002 equation. The result is given in Figure 5 using the feed curves for Sweden (S-norm) and The Netherlands (NL700, NL750 and NL800) compared to the Danish recommendation (DK-restr) for growing-finishing pigs from 20 kg to 120 kg. The three curves for The Netherlands refer to 700, 750 and 800 g of average daily growth rate, and the DK-restr curve matches well with the NL750 curve. The DK-restr curve was selected as the representative for restricted feeding. It is seen that the old values for heat production as a function of body mass is close to the new DK-restr. values for pigs up to about 70 kg, but is not taking restrictive feeding for pigs above 70 kg into account.

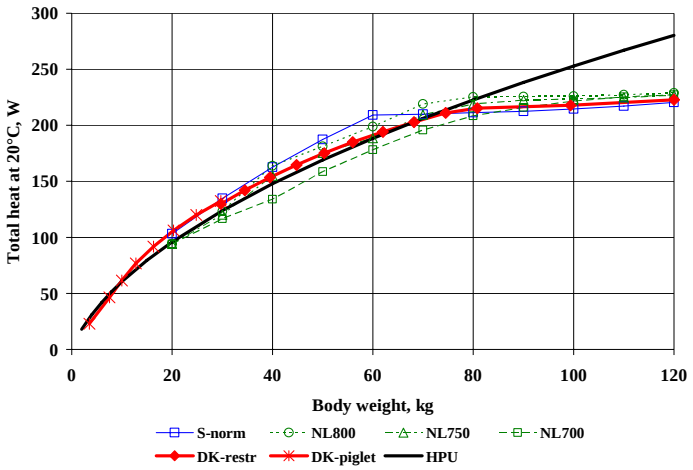

Figure 5. Total heat production for growing/finishing pigs according to heat producing units and the new CIGR 2002 recommendations.

2.8 Pigs' Sensible and Latent Heat

The distribution of pigs' total heat on sensible and latent heat is important for simulaton of both the indoor climate and the energy consumption. Figure 6 shows the distribution of total heat on sensible and latent heat for growing-finishing pigs based on results from Europe (Pedersen *et al.* 2005, CIGR 2002).

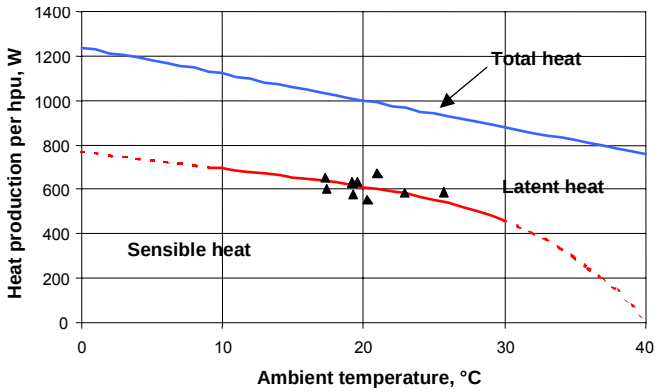

Figure 6. Total, sensible and latent heat production from fattening pigs on partly or fully slatted floor in Europe, CIGR (2002)

2.9 Set-Point Strategy

The basic set-point strategy for indoor temperature and RH specified by CIGR (1984) is used in this article (Figure 7). The set-point sum of temperature (°C) and RH (%) should be kept below 90 to avoid too high indoor RH. The strategy with set-point sum 90 will be referred to as normal air quality. The dotted curve indicates improved indoor climate with a 5% reduction in maximum, accepted RH. This strategy with set-point sum 85 is referred to as improved air quality because it results in increased ventilation and consequently reduced concentrations of carbon dioxide and other gases.

The lower, solid curve indicates the lower limit for the indoor RH in order to avoid too dry room air, which can occur during winter with increased minimum ventilation compensated with supplemental heat. This curve is not used in this article, however.

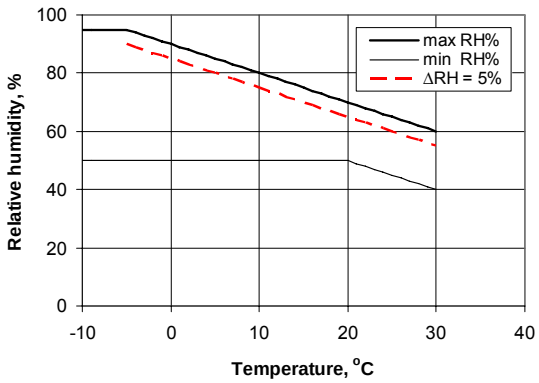

Figure 7. Recommended minimum and maximum RH as a function of room temperature. The dotted line indicates improved indoor climate by reducing the humidity set-point by 5 %.

2.10 Dry and Wet Housing Conditions

At house level some of the sensible heat from the animals may be used for evaporation of water from wet surfaces, feed, and manure. In this article it is assumed that all the sensitive heat production from the pigs is available for heating of ventilation air and covering transmission heat

losses in a dry house. This is roughly the case for houses with dry feeding systems and dry floor surfaces. For wet houses it is in this article assumed that 10% of the animals sensible heat production is used for evaporation of water, i.e. a sensible heat correction factor of 0.9.

2.11 Design Criteria

An overview of the design criteria is shown in Table 4. The Meteonorm reference year provided the hourly ambient temperature and RH throughout the year. In the simulations, the need for supplemental heat is calculated hour-by-hour and summarized on a yearly basis. To equalize for different production start times, the simulations were carried out over a three-year period. The results are referring to the average energy consumption per pig during this period.

Table 4 Design criteria

Constants		Unit	Values
Herd size			200
Live weight	Start End	Kg	30 100
Management			All-in/all-out
Building dimensions	Length Width Ceiling height	m	19.4 10.0 2.6
Ceiling slope		°	0
Heat transmission coefficients	Floor Wall Flat ceiling	$Wm^{-2}\,{}^{o}C^{-1}$	0.20 0.40 0.35
Variables			
Temperature set-points		^{o}C	22-18 20-16 18-14 16-12
Set-point sum	Normal air quality Improved air quality	C + RH ≤	90 85
Feeding principle			*Restricted*
Housing condition (Sensible heat used for evaporation)	Dry Wet	Sensible heat factor	1.00 0.90

In some periods of the year, the outside air is so humid that the RH cannot be kept below the set-point value by means of heating and ventilation. Heating is therefore not applied when the ventilation airflow rate exceeds 50 % of the maximum capacity.

3. RESULTS

3.1 Energy Requirement

The energy consumption for ventilation and supplemental heat is shown in Figure 8. Energy consumption for ventilation is shown as solid lines and the supplemental heating as dotted lines. It is seen that the effect of temperature set-point level on energy consumption for ventilation is

reltively small, while the requirement for supplemental heat is highly dependent on the temperature set-point levels.

3.1.1Ventilation

As expected the energy consumption for ventilation increases with increasing outside temperature. Compared to Finland the energy consumption for ventilation is 6 % higher in Denmark and 32 % higher in Portugal for a set-point temperature level of 22-18°C. In all cases the energy consumption decreased linearly with about 20 per cent for set-point temperatures level increasing from 16-12 to 22-18 °C.

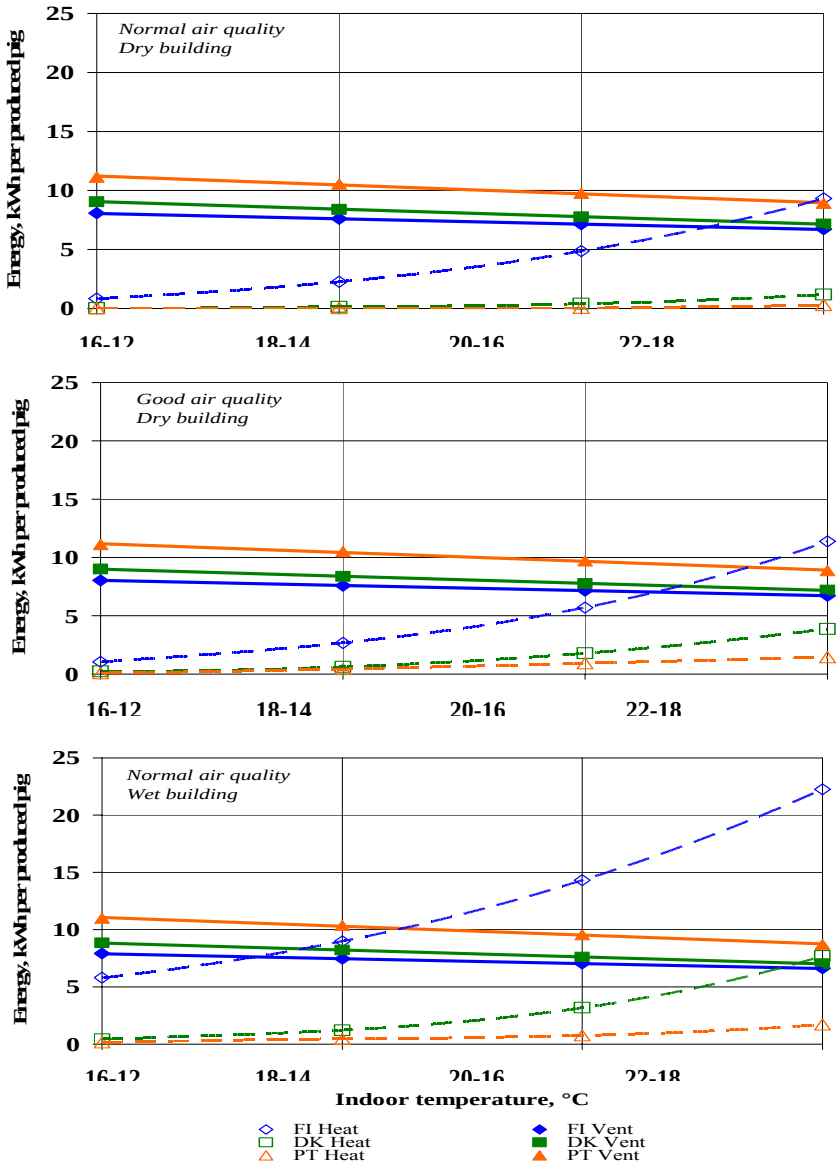

Figure 8. Energy consumption for ventilation and heating for three combinations of air quality set-points and building wetness in the three climatic zones.

With fan energy efficiency of 20 000 m^3 per kWh, the energy consumption for ventilation is between 6.6 kWh for Finland and 8.7 kWh per produced pig for Portugal for a set-point temperature level of 22-18^oC. Furthermore the figures show that the energy consumption for ventilation is nearly independent of the wetness condition of the animal house.

3.1.2 Supplemental Heating

The requirement for supplemental heat is much higher in Finland than in the two other climatic zones due to lower winter temperatures. The figure also shows that the supplemental heat requirement is much higher in a wet than a dry building. Due to the mild weather insignificant supplemental heat was required for Portugal in a dry building, using normal air quality set-point strategies, but in the other two regions some heat was needed particularly at high temperature set-point levels.

As seen in the upper diagram in Figure 8, the energy consumption for heating under normal air quality strategy and dry conditions is below 1 kWh per produced pig for Denmark and negligible for Portugal for the investigated temperature set-points. For Finland the energy consumption is approximately 10 kWh per produced pig and is of the same size as the energy consumption for ventilation at set-point temperature levels of 20-16 and 22-18°C.

In the middle diagram it is seen that the energy consumption for heating at improved air quality by using a set-point sum of 85 is only slightly higher than for a set-point sum of 90.

In the lower diagram is shown the consumption of supplemental heat under wet housing conditions. The heat consumption under wet conditions is up to 8 kWh for Denmark and up to 23 kWh per produced pig for Finland at a set-point temperature level of 22-18^oC.

3.1.3 Total Heat Consumption for Ventilation and Heating

In Table 5 is summarized the total energy consumption for ventilation and heating under dry respectively wet housing conditions for a set-point temperature level of 22-18^oC.

Table 5. Total energy consumption for ventilation and heating at start set-point temperature of 22 °C

Country (location) Yearly average outdoor temperature	Finland (Kaajani) 2 ^oC		Denmark (Karup) 8 ^oC		Portugal (Porto) 14 ^oC	
Housing condition	Dry	Wet	Dry	Wet	Dry	Wet
Supplemental heat	9,3	22.3	1.2	7.7	0.3	1.7
Ventilation	6.7	6.6	7.2	7.0	8.9	8.7
Total	16.0	28.9	8.4	14.7	9.2	10.4

The table shows that the total energy consumption for ventilation and heating is 16.0 kWh per produced pig in Finland, 8.4 kWh in Denmark and 9.2 kWh in Portugal under dry housing conditions. The lowest consumption occurs in Denmark and the highest in Finland. Especially in Finland the total energy consumption is very sensitive to housing conditions, where the total heat consumption is up to 28.9 kWh per produced pig.

3.2 Air Quality

The number of hours with room CO_2 concentrations exceeding the recommended 3000 ppm limit (CIGR 1984) is shown in figure 9. Carbon dioxide concentrations above 3000

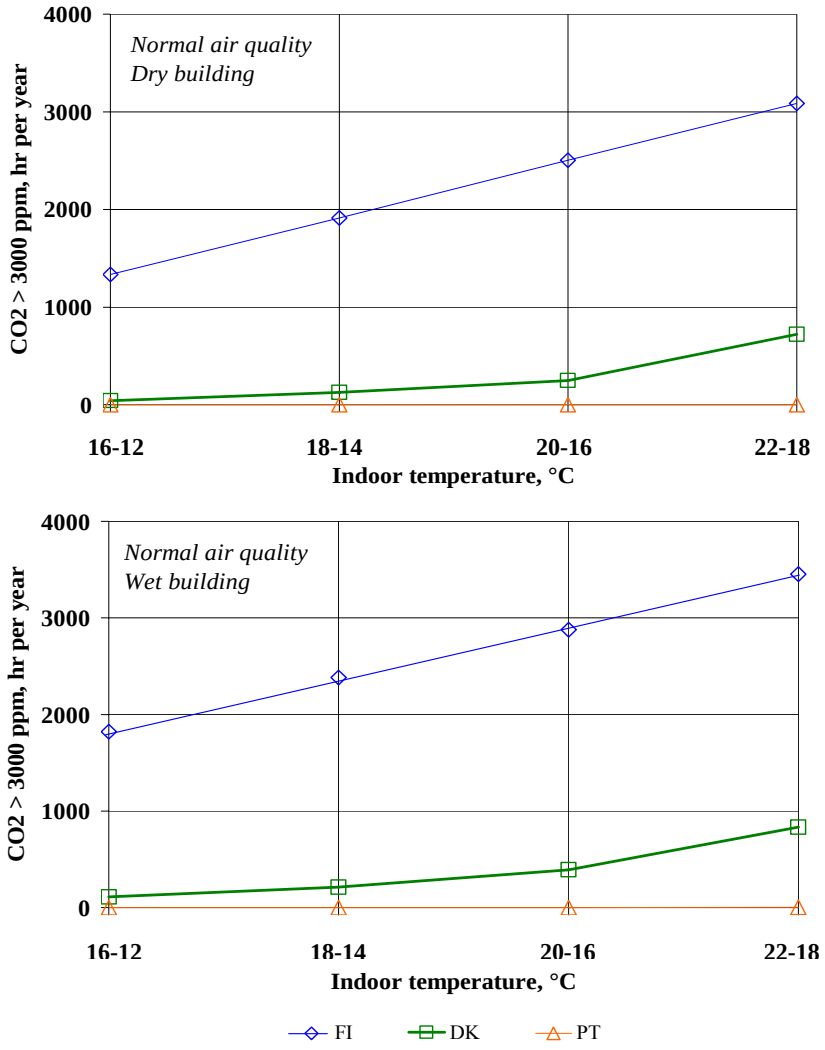

Figure 9. Hours with CO_2 > 3000 ppm for different air quality set-points and building humidity in the three climatic zones.

ppm are not critical in respect to the carbon dioxide concentrations in itself, but it is a good indicator for the indoor air quality in general. In practically all the simulated cases the air quality was acceptable in Portugal and problematic primarily in Finland.

Using the limit 3000 ppm CO_2 for acceptable air quality, unacceptable air quality occurred less than 5% of the time in Denmark, except for a temperature set-point level of 22-18°C that resulted in unacceptable conditions 10% of the time. In Finland unacceptable air quality was much more frequent, and increased linearly with set-point temperature. For the dry building it increased from 1300 hours per year at 16-12°C set-point temperature level to 3100 hours at 22-18°C. For the wet building the time with unacceptable air quality increased from 1800 to 3500 hours a year for the same temperature set-point levels.

4. DISCUSSION

In the simulations, care was taken to use realistic input assumptions, but a number of simplifications were made to be able to generalize.

4.1 Climate Zones

The three climate regions of Finland, Denmark and Portugal were selected to get specific weather data for costal climate in Southern Europe and coastal and inland climate in Northern Europe. According to Meteonorm the maximum outside temperature was fairly similar while it was primarily the number of hours with low temperature that differed. It should be noted that for inland areas in Southern Europe the summer temperatures are often considerably higher than for the coastal area selected.

4.2 Adaptation of Facility

In order to facilitate comparisons the same growing-finishing pig production, housing conditions, heating and ventilation system, and control strategies were assumed in all three climate regions. In praxis less insulation is normally used in Portugal and more insulation is used in Finland than assumed in the simulations. Regarding the maximum ventilation capacity it was close to the design target for Portugal but 24% more than the design target for Finland and Denmark.

4.3 Energy Efficiency of Fans

In order to get a system that was stable and wind resistant it was assumed that the fan dampers were adjusted proportionally to the fan voltage. In the simulations this system was characterized by energy consumption that decreased linearly from 100 % at maximum airflow rate to a minimum of 40 % at no airflow rate with fully closed fan damper and inlets. The energy consumption of a specific ventilation system can only be determined in simulations with specific performance and weather data.

The average energy efficiency in Denmark for 47 tested fans was 23 000 m^3/kWh at a pressure difference of 20 Pa (Pedersen and Strøm, 1995). Since then many of the fans in Denmark have

achieved energy efficiencies better than 30 000 m^3/kWh, corresponding to a lower energy consumption than estimated. In the simulations fans with an energy efficiency of 20 000 m^3 per kWh in the whole control range were used. The yearly energy consumption will change proportionally for fans with better or worse energy efficiency.

4.4Air Quality

The strategy with set-point sum 85 is referred to as improved air quality, because the lower maximum RH set-point results in increased ventilation and reduced concentrations of carbon dioxide and other gases. The use of carbon dioxide sensor for minimum ventilation control would be more suitable for this purpose, but has so far been considered too expensive for practical use.

The number of hours with room CO_2 concentrations exceeding the recommended 3000 ppm limit (CIGR 1984) is specified for the simulated situations. Carbon dioxide concentrations above 3000 ppm are not critical with respect to the carbon dioxide concentrations in itself, but it is considered a good indicator for the indoor air quality in general. For humans, the upper limit for CO_2 is e.g. often set to 5000 ppm.

4.5 Bedding

Previously, it was common in Europe to use bedding in pig pens with solid floors. In recent decades, the tendency has been towards using slatted floors and to avoid the bedding, owing to problems involved with manure handling. However, the present opinion in Europe, in accordance with EU directives, tends to be that rooting materials are necessary. As such, it is likely that pig pens with bedding will again become common. The use of bedding has a great influence on the optimal temperature in pig houses. Bedding will thus allow a 4°C lower set-point temperature at the same production level, compared to no bedding. This again, will influence the energy consumption for supplemental heat.

Today some types of pig pens have a cover over the laying are to make a warmer micro climate than in the house. Therefore the simulations are carried out in the range from high indoor temperature set-point level of 22-18^{o}C, corresponding to pens without bedding, down to 16-12^{o}C, referring to pens with bedding, in combination with covered laying area.

4.6 Housing Conditions

Most experimental data on animal heat and moisture production originate from measurements in climatic chambers, where conditions deviate from conventional production conditions. It is important that guidelines for climatization of animal houses are adapted to modern production systems including water evaporated from feed, floors, spilt drinking water and the diurnal rhythm in respect to light and feeding routines. Until the ‘eighties, laboratory scale results were used directly as guidelines in practice.

In CIGR (1984), some provisory correction factors were introduced, expressing that under very dry conditions with dry floors and feed with low water content, the results from laboratory meas-

urements could be applied directly. Under wet conditions with wet floors and feed, a correction factor of 0.9 for conversion of sensible heat should be used, i.e. 10% of the animal sensible heat is used for evaporation of water. A 10 % decrease in the sensible heat due to wet conditions may for instance lead to a considerable increase in energy consumption for supplemental heat.

An inland climatic zone with extremely high summer temperatures was not included in the simulations. The main reason for this is that little or no information is available on total heat production and the partition between sensible and latent heat particularly under practical conditions. More knowledge on animal heat and moisture production in hot climate can be expected in the coming years from a CIGR working group established in 2005 on "Animal Housing in Hot Climate".

5. CONCLUSION

In order to get reliable information on the energy consumption for ventilation and heating of animal houses, precise information is needed on housing conditions, yearly outdoor climate, animal heat and moisture production as well as control strategy for temperature and RH set-points. For typical production conditions, the following conclusions can be made:

- The energy consumption for ventilation for growing-finishing pigs is decreasing nearly linearly with about 20 per cent when the set-point temperature level increases from 16-12 to 22-18^{o}C.
- For a fan with energy efficiency 20 000 m^3 per kWh the energy consumption for ventilation is between 6.6 kWh for Finland and 8.7 kWh per produced pig in Portugal.
- The energy consumption for supplemental heat is very sensitive to the wetness of the housing conditions. For a wet house the energy consumption for heating may be more than doubled compared to a dry house.
- The heat consumption for supplemental heat increases progressive by increased set-point temperature level and is for a dry house up to 1.5 kWh per produced pig in Portugal, 7 kWh in Denmark and 11 kWh in Finland.
- A decrease of a few per cent in maximum indoor RH set-point may result in a small increase of the heat consumption requirement due to a higher ventilation rate.
- Simulation results on supplemental heat requirements cannot be transferred from one climatic region to the other, because of complicated interactions of different parameters.
- Estimations of the supplemental heat requirement under different climatic and production conditions can easily be made by means of a computer program on the basis of specific outdoor climate according to Meteonorm and CIGR 2002 equations for animal heat production.

6. REFERENCES

ASHRAE, 2001a, Handbook, Standard.. American Society of Heating, Refrigerating, and Air-conditioning Engineers: Atlanta, GA, USA.

ASHRAE, 2001b, Handbook, Fundamentals.. American Society of Heating, Refrigerating, and Air-conditioning Engineers: Atlanta, GA, USA.

Brown-Brandl, T.M., Nienaber, J.A., Xin, H. & Gates, R.S. 2003., A Literature Review of Swine Heat and Moisture Production. Proceedings of the 2nd International Conference on Swine Housing II, October 2003: 31-40.

CIGR, 1984. Climatization of Animal Houses. Report of working group. Scottish Farm Building Investigation Unit. Craibstone, Aberdeen, Scotland.

CIGR, 1992 Climatization of Animal Houses. Second working group report. Faculty of Agricultural Sciences, State University of Ghent, Belgium.

CIGR, 1999. CIGR Handbook of Agricultural Engineering, Volume II. Animal Production & Aquacultural Engineering. Published by American Society of Agricultural Engineers.

CIGR, 2002 Climatization of Animal Houses; Working Group Report on: Heat and Moisture Production at Animal and House Level. Published by DIAS, Denmark.

WWW.agrsci.dk/jbt/spe. ISBN 87-88976-60-2.

Meteonorm, 2000. Version 4, Meteotest, Fabrikstrasse 14, CH-3012 Bern, Switzerland.

Morsing, S. & Strøm, J.S. 1992. Using test data for ventilation units for computerized system selection. International Winter Meeting. Nashville, Tennessee. ASAE Paper No. 92-4534. St. Joseph, Mich. USA.

Morsing, S., Strom, J.S. & Jacobson, L.D. 1997. StaldVent – A Decision Support Tool for Designing Animal Ventilation Systems. Proceedings from the Fifth International Livestock Environment Symposium. ASAE publication 01-97. (2): 843-850.

Morsing, S., Strom, J.S., Zhang,G.Q. & Jacobsen, L., 2003. Prediction of Indoor Climate in Pig Houses. Proceedings of the 2nd International Conference on Swine Housing II, October 2003, 41-47.

Pedersen, S. and Strøm, J.S.,1995. Performance Testing of Complete Ventilation Units, ASAE, Applied Engineering in Agriculture, Vol. 11(1):131-136., 1995

Pedersen, S., Morsing, S., Strøm J.S. & Jacobsen L. 2004. Simulation of Indoor Climate in Animal Houses using CIGR 2002 Heat Production Equations. International symposium of the CIGR Section II in Évora, Portugal, May 2004.

Pedersen, S., Morsing, S. and Strøm, J.S. 2005. Simulation of Heat Requirement and Air Quality in Weaner Houses for Three Climate Regions Using CIGR 2002 Heat Production Equations. Agricultural Engineering International: the CIGR Ejournal. Manuscript BC 05 001. Vol VII June 2005

Strøm J.S., 1978. Heat loss from cattle, swine and poultry as basis for design of environmental control systems in livestock buildings (in Danish). SBI-Landbrugsbyggeri 55, Danish Building Research Institute, Denmark. CIGR Evora, January 2005, version 1.

Strøm, J.S., 1980. Farm building design and animal heat loss. Building Research and Practice, Vol. 8(2):28-37

PAPER NO.2:

Jacobsen, L., Morsing, S., Nielsen, P. V., and Strøm, J. S.: Boundary Condition of Diffuser Ceiling Inlet Exposed to Convection and Thermal Radiation under Nonisothermal Conditions.

Boundary Condition of Diffuser Ceiling Inlet Exposed to Convection and Thermal Radiation under Nonisothermal Conditions

Jacobsen, L.[1], Morsing, S.[1], Nielsen, P.V.[2], and Strøm, J.S.[1]

[1]Danish Institute of Agricultural Sciences, Department of Agricultural Engineering, Schüttesvej 17,

DK-8700 Horsens, Denmark. Tel.: 8999 3082. Fax: +45 8999 3100. Email: lis.jacobsen@agrsci.dk, www.agrsci.dk

[2]Institute of Building Technology and Structural Engineering, Aalborg University, Sohngaardsholmsvej 57, DK-9000 Aalborg. Denmark. Tel.: +45 9635 8080. Fax: +45 9814 8243. Email: pvn@civil.auc.dk

Abstract

The air flow and thermal characteristic for diffusor air inlets covering the whole ceiling of a room has been discussed. The boundary condition of a diffuser air inlet consisting of porous material of mineral wool bats in the entire ceiling of a room is simulated in an windtunnel. The independent variables were inlet air temperature and velocity through the diffuse inlet, temperature and velocity of the room air in the occupational zone and thermal radiation from the occupational zone. The dependent variable was the surface temperature of the diffuse material facing the occupational zone. A linear model of downstream surface temperature of the diffuse material is generated from the observations.

Introduction

Special ventilation systems where the ceiling construction is used as inlets are used in different application. One is ventilation in surgery facilities (Brohus et al., 2004; Chen et al., 1992). Another is in some livestock building (Aarnink and Wagemans, 1997; Strøm et al., 1993; Wagenberg and Smolders, 2002) and occupational rooms(Johannis, 1968). Different construction configurations are used, the one of concern in the present is a porous ceiling consisting of thick mat of porous fine fibers of isotropic material covering the downstream surface of the inlet.

Airflow through the porous ceiling in livestock buildings are normally generated with an exhaust fan creating a negative pressure in the occupational room. Fresh ventilation air, usually unheated air, is sucked down through the porous material that covers major parts of or all of the ceiling. The setpoint of regulating the airflow through the room is set to a constant temperature interval on the outlet- or room-temperature throughout the year. The airflow in the occupational zone is highly buoyancy driven (Bjerg et al., 2000; Hoff et al., 1992). The buoyancy driven airflow pattern in the occupational room is dependent on the location of the heating sources but generally have a recirculating character (Jacobsen et al., 2004) that is evident in different other types of buoyancy driven types of ventilation systems (Heber and Boon, 1993; Nielsen et al., 1979; Randall and Battams, 1979). Hence there is a boundary layer flow parallel to the downstream surface of the diffuse ceiling.

The optimal function of the porous ceiling inlet is to:

- Generate a uniform ventilation flux through the entire porous area at any given time. Creating a low momentum even distributed fresh air supply in the occupational zone.
- Prevent the occurrence of condensation or downdraft of cold ventilation air into the occupation zone.
- Prevent negative radiation effects from ceiling inlet surfaces on the thermal environment in the occupational zone.

In preceding experiments in a heated porous ventilated experimental room the surface temperature has been measured with thermovision and the measured temperature on the downstream surface material is found to be higher compared to the surface temperature on the upstream surface. The exact physical nature of the heating or preconditioning process in the porous material is not known and can consist of both a *radiative and convective heat transfer* and a *boundary layer mixing convection* between the incoming fresh air and heated air inside the diffuse ventilated room. In the porous ceiling room the ventilation flow is a combination of forced flow and natural convection buoyancy driven flow (Jacobsen et al., 2005). Natural convection flows controls the air movement in the occupational zone and forced flow control the flow in the inlet through the diffuse material and outlet in the exhaust channel. In the porous material boundary layer mixing convection heating is possible if the dynamic pressure (momentum) of the room airflow displaces the fresh air flow from above the ceiling. In the majority of the room the direction of the room airflow will be perpendicular to the ceiling lower surface facing the inside of the room, (Jacobsen et al., 2004) thus creating a boundary-layer and a flow-gradient that may extent into the porous ceiling material. In such case the displacement

can only occur in a local or microscopic scale or in a transient state over the entire surface because the dominating flow direction is forced flow given by the mechanical ventilation in the outlet.

Preconditioning of inlet air through radiative heating of the porous material surface and air/solid convection transfer to the air is not in contradiction to the prescribed flow in the porous material. The radiative energy is an effective heat transfer process at low temperature differences. The radiation from surfaces or objects in the room radiates to the surface of the porous ceiling. The solid in the porous ceiling either, transmits, absorbs or reflect the radiation. If the material is opaque transmission is zero, in the infrared specter, as present in a occupational room, most materials are opaque. The radiative heat absorbed by the solid increase the temperature of the solid. When cold air pass the warmer solid material, the solid works as a convection heat exchanger and heats up the inlet air. Holmberg et al.(2004) showed that the ratio of radiation to convection heat transfer from a radiator at isothermal room temperature (293K) was 0.61 at a surface temperature of 308K but 0.35 at 338K. The explanation is that the convective energy transfer is a linear function of the temperature difference between surface and fluid but the radiative heat transfer is a function of the temperature difference between the 4. power of the temperature on the surfaces (Incropera and De Witt, 1990). A decrease in temperature difference between the surfaces of a room increases the relative radiative heat contribution between the surfaces of the room. Hence at low temperature difference in the room the radiation contribution to the heat transfer processes becomes the governing heat transport process.

Because the traditional non-slip wall boundary conditions or a non radiative inlet boundary condition are not applicable for the porous inlet in a non-isothermal system, a more adequate description of the boundary conditions of the diffuse inlet is needed. Assuming that the inlet velocity is homogenous over the inlet, the surface temperature of the downstream surface facing the occupational room is the unknown parameter that determines the boundary conditions. A different approach to the formulation of a boundary condition must be applied because exact numerical simulation of the details of a material build up by thick mats of fine fibers will require a resolution of the system that is beyond any supercomputers capacity of solution within a foreseeable time. The box method or momentum method as shown by Nielsen(1992) and Srebric and Chen(2002), can be used to prescribe boundary conditions at an artificial boundary. In buoyancy driven flows, as the present case, the flow takes character of buoyancy driven flow close to the boundary surface, conditions that favor the use of the momentum method(Srebric and Chen, 2001). The boundary conditions used in the momentum method boundary surfaces must be determined analytical from either measurements or detailed (abbreviated) numerical studies.

As above mentioned the heat transfer system is complex and composed of transport properties of both convection and radiation. It is not possible to separate the different energy transport processes convection, conduction and radiation because of the physical coupling but still the partitioning of heat transfer between convection and radiation is critically important. E.g. assuming there is no air circulation in the occupational room, the boundary layer temperature of the downstream surface of the diffuse material is dependent on the inlet airflow velocity and air temperature through the diffuse material

and the surface temperature in the room radiating heat energy to the diffuse surface. If there is a recirculation horizontal air movement parallel to the diffuse ceiling downstream surface, the surface temperature will also be dependent on the air velocity and air temperature of the occupational room.

Surface temperatures of porous materials have been the study of many researchers engaged in development of porous burner technology, regenerative heat exchangers, chemical process technology and electronic equipment.

For numerical modeling the volumetric heat transfer coefficient parameter describe the coupling of heat transfer between conduction and convection heat transfer between solid matrix and gas for different porous materials. Knowing the volumetric heat transfer coefficient the downstream surface temperature on a regenerative heat exchanger can be calculated. Fu (1998) and Younis and Viskanta (1993) showed experimentally that the volumetric heat transfer coefficient is dependent on the mean pore diameter and that the convective heat transfer coefficient is a strong function of local velocity and the flow passage in the porous material.. Materials with different pore diameter was described using a Reynolds- vs. Nusselt number correlation. The authors did not examine the effect of radiation and a boundary layer parallel to the downstream surface.

The convective and and radiative material properties of a porous material exposed to radiation, quantitatively determine the energy flux transferred from the material to the air. The material properties: optical debth, porosity and scattering albedo, determining the radiative performance was examined by Kulkarni and Peck (1996), Sathe et al (1990) and Tong and Li (1995). The authors did not consider the effect of a secondary flow boundary layer parallel to the surface on the downstream surface of the burner.

Boundary layer flow parallel but outside a porous material has been examined by several authors (Jen and Yan, 2005; Nield and Kuznetsov, 2005). The interesting study of the extent and velocity gradient of the boundary layer into the porous material dependent on the material parameters has not been covered by these authors. The interface and boundary layer between a fluid flow and a saturated porous media has been studied by Alazmi and Vafai (2001), Neale and Nader (1974) Ochos-Tapia and Whithaker (1997) but not with a secondary flow through the porous medium. The flow conditions in the interface was dependent on the material parameters porosity and permeability. The boundary layer problem with thermal radiation on the surface of a permeable sheet with viscoelastic fluid flow through the sheet has been studied by Kahn (2005). The sheet was thin and the boundary layer inside the sheet was assumed infinitive small.

A through search in the literature did not reveal published work on the thermal surface conditions of the combination of flow through a porous media with radiation and convection flow parallel to the downstream surface. The literature search revealed a multitude of material parameters to be determined experimentally to solve the model equations and predict the surface temperature of the inlet surface of the diffuse ceiling inlet. A more global approach is persued in the following.

Problem formulation

This experiment will examine the convection and radiation influence of the preconditioning of the air through a diffuse ventilation inlet and to determine the boundary conditions of a diffuse ventilated inlet. Both the effect of the *radiative and convective heat transfer* and a *boundary layer mixing convection* is to be examined. The

boundary layer mixing convection is a consequence of the room air flow, where the room air flow is assumed to have a flow perpendicular to the flow direction of the fresh air inlet through the diffuse material. The results will be applicable as boundary conditions in the box or momentum method in a numerical model of the diffuse ventilated room

Material and methods

Facilities, instrumentation and data acquisition

Tunnel system: The primary flow tunnel (suffix 1), a rectangular flow tunnel of inside flow dimensions 0.5×0.5m (0.25m^2 cross section area) and inlet section of 4.8m, was connected to the secondary flow tunnel (suffix 2), a perpendicular inlet section of inside section area of 0.5×0.5m, such that the two flow systems had interface in the downstream boundary surface of the diffuse inlet material that was situated in the bottom section of the secondary flow tunnel system, Figure 1. Opposite to the diffuse material in the bottom of the primary flow tunnel a infrared heating section was placed, consisting of a matt black painted 2 mm thick aluminum sheet of 0.5×0.5m with a light bulb heating source underneath with reflectors to establish a uniform temperature of the sheet.

Materials: The diffuse material was a 0.1m thick Isover Diffus® mineral wool (Danish Institute of Agricultural Science, 2001) of 0.5×0.5m (surface area of 0.25m^2). The diffuse material was placed on a horizontal grill of Ø1mm stretched out nylon wires each 40 mm apart.

Flow system: The flow velocity of the two tunnel systems were individually controlled and flow rate was measured with ISO orifice plates. The room humidity and barometric reading was measured at midday each day. In the primary flow tunnel, turbulent

conditions were aimed at by placing turbulence screens in the inlet (Lengweiler, 2000). The inlet temperature in the secondary inlet were adjustable and the primary inlet was room temperature and heating fan placed 2 m from the tunnel inlet. The room humidity and barometric reading was measured at midday each day.

Measuring system: The sensitive temperature T_1, T_2 and T_{out} were measured with thermocouples type T and the surface temperature T_c and T_{ir} with infrared thermometers type EL21A and EL101A in the positions shown in Figure 1. Measurements were registered each minute as a mean value of 12 scans. All measurements were taken at equilibrium and steady conditions.

Methods: The variable parameters were temperature difference between primary and secondary inlet, inlet velocity in both tunnel systems and infrared radiation.

The parameter variation was kept close to the conditions in a housing facility for weaning pigs where the room temperature were maintained between 291-298K and the air exchange was in the interval 2-20 h-1, assuming the room height is 2.6m consequently the volume flow rate in the secondary tunnel was kept at $\dot{V}_2 = 0 - 13 m^3 / h$. The airflow velocities perpendicular to the boundary surface of the diffuse material were measured in a fullscale experimental room to wind velocity between 0-0.2 m/s which was equivalent to a volume flow rate in the primary flow tunnel of approximately $\dot{V}_1 = 0 - 200 m^3 / h$. The inlet temperature in the primary tunnel section was between $T_1 = 291 - 306 K$ and in the secondary tunnel $T_2 = 288 - 297 K$. Isothermal conditions between the primary flow tunnel and the room temperature were aimed at to minimize energy loss to the surroundings. The concurrent temperature difference between inlet and outlet was between 0-15K and this was somewhat less then what can be expected in a realistic

situation in Denmark where the temperature difference was more than 15K 3200 hours of the year (indoor temperature 293K). The surface temperature of the infrared heating section was between $T_{ir} = 289 - 317K$.

Table 1: Experimental design parameter variation maximum and minimum values of the independent variables and aspired variance increment.

Variable	T_1	T_2	T_{ir}	u_1	u_2
	[K]	[K]	[K]	[m/s]	[m/s]
max	306	297	317	0.22	0.014
			308	0.175	0.010
			305	0.125	0.007
			294	0.075	0.005
min	291	288	289	0	0

Theory

Two variants of the surface temperature model is generated, one with and one without intercept. Physically there should be no intercept in the model, but in the present case the intercept can be a indication of the systematic errors in the model. Subscript 1 is the model without intercept and subscript 2 is the model with intercept. Assuming that the variables are normally distributed and independent the linear model of the surface temperature T_c are

Model A: $T_c = \beta_0 + \beta_1 u_1 + \beta_2 u_2 + \beta_3 T_1 + \beta_4 T_2 + \beta_5 T_{ir}$

/1

Where T_c is the downstream surface temperature of the diffuse inlet, u_1 is the mean flow velocity in the primary tunnel, u_2 is the mean flow velocity in the secondary tunnel, T_1 is the air temperature in the primary tunnel and T_2 is the air temperature in the secondary tunnel.

The models has been tested with the F-test:

$$F(y) = \frac{[s.s.(2) - s.s.(1)]/[d.f.(2) - d.f.(1)]}{s.ss(1)/d.f.(1)}$$

/2

Where s.s.(1) and s.s.(2) is the sum of squares of error from the model with or without intercept respectively. d.f.(1) and d.f.(2) are the equivalent degrees of freedom. s.s.(1)/d.f.(1) is equivalent to the mean square, m.s. of error. The F-test is used to evaluate if an intercept would improve the model and to evaluate whether variables are significant in the model.

Results

The precondition of inlet air can be caused by:

- Mixing in the boundary layer on the downstream surface of the diffuse material
- Radiation from heated surfaces to the diffuse material and successively convection heat transfer air/solid, of air through the diffusive material. The air/solid convection can be driven by flow from both the primary and secondary tunnel.
- Convective air/air mixing in the diffuse material from diffusion of airflows from the primary tunnel into the diffuse material, The diffusion is dependent on the airflow momentum of the primary and secondary tunnel, the airflow momentums counteract each other. It must be assumed that this effect is dominant when the airflow velocity of the secondary tunnel is low and the air flow velocity of the primary tunnel is high.

There is no convective heat transfer in the diffuse material if $u_1=0$ and $u_2=0$. When $u_1=0$ and $u_2>0$ there is no flow momentum of the air in the primary tunnel and the diffusion of air into the diffuse material is limited and there is limited air/air convective mixing in the diffuse material but there can be some air/solid convection between air from the secondary tunnel and the radiation heated diffuse material if $q_{ir}>0$. When $u_1>0$ and $u_2=0$ there can be some air/solid convection between the diffuse material and air from the primary tunnel if $q_{ir}>0$. When $u_1>0$ and $u_2>0$ there is a opposite direction momentum flow that will counteract air/air mixing and the air/solid convection of primary tunnel air into the diffuse material.

If there is no radiative heat transfer and a non-slip boundary condition is assumed at the downstream surface of the diffuse material, the mixing is in the boundary layer outside the diffuse material, the diffuse material should not experience any form of heating or cooling and the surface temperature T_c should be equal to the inlet temperature T_2. Plotting T_c-T_2 vs. the temperature difference T_1-T_2 in the primary and secondary tunnel. Figure 2 there is good indication that the mixing in all of the observations is either boundary layer or radiation dependent because the surface temperature T_c is always higher than the inlet temperature of the secondary tunnel T_2. If there is no radiative heat transfer q_{rad} then T_c-T_1<0 if T_{ir}>T_1>T_2 and if there is radiation heat transfer then T_c-T_1>0 if T_{ir}>T_1>T_2 and q_{rad}>0. From Figure 3 it is seen that at low temperature difference between T_1 and T_2 the radiation effect is indisputable. When T_c-T_1>0 there is a positive net energy input from the diffuse ceiling and when the T_c-T_1<0 there is a negative net energy output. The negative energy input is most pronounced at high values of T_1-T_2 and at flow conditions where u_1>0, u_2>0 and u_1=0 Figure 3. Normalizing T_c-T_1 and T_1-T_2 with the variable of radiation heat transfer T_{ir}-T_c the delineation of T_c-T_1 and T_1-T_2 becomes dimensionless and normalized with the effect of radiation. The values of u_1=0, u_2=0 is only dependent on changes in thermal radiation and (T_c-T_1)/(T_{ir}-T_c) is a constant except at values where T_1-T_2→0 where the random uncertainty of the measurement is increasing the observation variance. Comparing Figure 3 and Figure 4, as expected, the observation, where radiation and possibly air/solid convection has a major influence,u_1=0, u_2=0 and u_1>0,u_2=0,T_c-T_1>0, has decreased more (moved closer to (0,0)) compared to the observation where air/air mixing convection is dominating u_1=0, u_2>0 and u_1>0, u_2>0, T_c-T_1<0. The vertical spreading of the observation T_c-T_1<0 in Figure 3

has increased proportionally compared toFigure 4. The spreading of the observation $u_1>0$, $u_2>0$, can be due to different ratio of u_1 and u_2..

The coefficients estimate for the linear model are shown in **Fejl! Henvisningskilde ikke fundet.**Table 2.

Table 2: Coefficient estimate and 95% confidence intervalf (CI) for estimates model A, dependent variable T_c,upper, n=991, $T_1>T_2$.

Coefficient	β_1	β_2	β_3	β_4	β_5	*s.s.*	*m.s.*
Estimate Model A	-1.9137	-272.81	0.40232	0.46737	0.14000	706	0.72
CI95% upper	-2.570	-285.1	0.3905	0.4537	0.1333		
CI95% lower	-1.258	-260.5	0.4142	0.4810	0.1467		

The F-test show that for model A, the model without intercept reflects the majority of data better than the model with intercept. The models have been tested for insignificant variables in the model with the F-test. The test show that all the variables are significant to the model. The plot of residuals of the dependent variable Tc in model A Figure 5 show that the variance is constant in the measuring interval. The plot of the residuals of the independent variables T_1, T_2, T_{ir}, u_1 and u_2 Figure 6 Figure 7 Figure 8 Figure 9 and Figure 10 respectively also show a constant variance in the measuring interval with a

marginal increase in variance at high values and T_{ir} and low values of u_2. The sum of squares are 706 and the mean square is 0.72.

Sensitivity analysis

A sensitivity analysis is performed to compare the results of the model relative to the independent parameters. In the model A T_c is the dependent parameter, $T_c=f(u_1, u_2, T_1,T_2;T_{ir})$. The absolute accuracy of measuring T_c is 0.1 K. In the sensitivity analysis combination 1-4 is isotherms hence the ceiling surface temperature T_c should be the same as the surrounding temperature. This condition is obtained with 0.1-2.6K accuracy in the model. In the non isothermal combination 5-10 the model is within the possible temperature range in all combinations.

Table 3: Sensitivity analysis of the model A estimating T_c..

Combination	u_1	u_2	T_1	T_2	T_{ir}	Tc,
	m/s	m/s	K	K	K	K
1	0.00	0.010	293.0	293.0	293.0	293.1
2	0.22	0.010	293.0	293.0	293.0	292.7
3	0.10	0.000	293.0	293.0	293.0	295.6
4	0.10	0.014	293.0	293.0	293.0	291.7
5	0.10	0.010	306.0	293.0	293.0	298.1
6	0.10	0.010	291.0	293.0	293.0	292.1
7	0.10	0.010	293.0	297.0	293.0	294.8
8	0.10	0.010	293.0	288.0	293.0	290.6

9	0.10	0.010	293.0	293.0	317.0	296.3
10	0.10	0.010	293.0	293.0	289.0	292.4

Determining the dependency of T_c of other variables, eg. dT_c/du_1, is found differentiating model A relative to the independent variable . The partial derivative terms are constants for all the different independent variables. The partial derivative du_1/dT_c and du_2/dT_c are negative and the derivative dT_1/dT_c, dT_2/dT_c and dT_{ir}/dT_c is positive

Model test

The model are tested against measuring data in a room geometry with a diffuse inlet, data reported in Jacobsen et al.(2004). The room dimensions are w×h×l=8.5×3.0×10m and the diffuse inlet covers the room ceiling 0.3 m below the room ceiling creating a inlet plenum above the diffuse ceiling. To prevent short circuit flow some of the ceiling is covered with impermeable material reducing the ceiling inlet area to 61.3m^2. 8 pen partitions of 0.6m impervious walls of each 3.8×2.5m alongside a central aisle of 0.9×10m are placed in the room. The room has adiabatic walls but are not isothermal, pig simulators emitting heat energy, Q_{pig}, is placed at the floor along the side walls of the room confinement. Room heating with a finned pipe Q_{finn} is provided along the side wall in both sides of the room Figure 11.The air temperature are measured with 15 equidistant thermocouples in the location (x,y,z)=(5.0-8.5,0.2,6.25)m and (x,y,z)=(5.0-8.5, 2.52,6.25)m. A reference temperature is measured in the location (x,y,z)=(6.6, 1.2, 6.25)m. The measurements are compared to simulations in 2D assuming a symmetry plane in the measuring location. Th simulation is performed with different boundary conditions:

Simulation with 42.4% of the ceiling as a inlet.

1. Simulation with model surface temperature. Inlet temperature T_c calculated from the model assuming the variables are: u_1=0.02m/s, T_1=305K, u_2=0.003m/s, T_2=277K, T_{ir}=310K. T_c=294K.
2. Simulation according to initial conditions (reference simulation).
3. Simulation with the ceiling divided into fins of both inlet and solid ceiling. Inlet area is reduced to 37.6% of the ceiling area.

4. Simulation with the ceiling divided into fins of both inlet and solid ceiling. Inlet area is 37.6% of the ceiling surface area. View-factor radiation model applied on all surfaces except the finned pipe heaters, all radiating surfaces emissivity 0.9. In order to compare the flow velocity conditions in the roon with and without radiation the heat emitting from the pig simulators is increased to Q_{pig}=328.4W/m^2 assuming that the convective and radiative energy contribution is emitting each 50% of the heat energy from this surface. The finned pipe heater emits primarily convective energy. Because the convective contribution is the same in the simulations without radiation it is possible to compare the flow systems in a simulation with and without radiation. Because the temperature distributions is relative to the reference temperature it is possible to compare the temperature distribution.

5. Simulation as in 4. but without increased heat flux from the pig simulators, Q_{pig}=164.2W/m^2.
6. .Simulation as in 1. but with temperature boundary conditions of pig simulators and finned pipe heaters. When the model inlet is introduced in the simulation the increased inlet temperature represents a heating energy source that in reality is

transmitted by radiation and convection to the ceiling from the other heating sources in the room. The temperature increase in the inlet with the model is 17.7K and in the full scale room this energy source is equivalent to 58% of the energy input into the room by pig simulators and finned pipe heaters. To keep the energy balance in the room either the energy flux from the energy sources must be reduced or the heat flux is transformed into a temperature boundary condition. Not knowing with which ratio the flux of the heating sources should be decreased, (this is dependent on how much heat is transmitted from each of the heating sources to the ceiling), the temperature boundary condition of the pig simulators; T_{pig}=305K; and the finned pipe heaters; T_{finn}=340K; is used. The surface area of the finne pipe heaters is increased from 0.08m^2 to 0.32m^2 to achieve a outlet temperature equivalent to trial 2.

Initial conditions. Parameters used in the simulation except else wise mentioned:

- Fluid: Air STP (standard pressure temperature)
- Turbulence model: Standard K-E model

Boundary values:

- Gravitational force: Boussinesq
- Inlet: Temperature Tin = 277ºK, Volume flow 600m^3/h. Ceiling inlet area 61.33 m^2. In 2 D simulation inlet area is 57.6% of the ceiling area.
- Outlet: Boundary condition = pressure, pressure coeff. = 1000, Velocity = computed.
- Wall: flux = 0 Wm^{-2}, except at heated wall boundary. Heating sources: Q_{pig}= = 164.2 Wm^{-2},
  Q_{ribb} = =148.7 Wm^{-1}.

Terms in mass transport equations:

- Convection: 1.st order
- Conduction: Harmonic 1st or non linear 2nd order?
- Time step variation: Automatic
- $t_{iteration}$ = =5000 s
- Solver control: Solver = incomplete factorization, number of iterations = 20, relaxation factor = 1, convergence tolerance = 0.001.
- Grid: Cartesian

- Radiation: None

The results of the simulation are shown in Figure 12, Figure 13 and Figure 14. The temperature difference is the difference between local temperature and outlet temperature. The outlet temperature are shown in Table 4.

In Figure 12, the location at the inlet (y=2.6), the difference between the outlet temperature and the ceiling temperature is maximum 5K. The maximum temperature difference is close to the wall where the ceiling is heated by convection of heated air. Without radiation (trial 3) the temperature gradients at the ceiling is large compared to the simulations without radiation (4. and 5.) The simulation s 1. and 2. is not significantly different. The temperature gradients in 1. and 2. is significantly larger than in 6.

In Figure 13, the location close to the floor, y=0.2m, the temperature gradients of 1.,2.,3. and 5. is not significantly different. The maximum temperature difference between local temperature and outlet temperature is 7K (4.), 6. has a very uniform temperature profile at the near floor location. The measurements has a similar temperature distribution as the simulations 1.-5.

In Figure 14 the location close to the floor, y=0m, the temperature gradients of 1.,2.,3. and 5. is not significantly different. The maximum temperature difference between local temperature and outlet temperature is 8K (trial 4.). 6. reflects the temperature boundary condition.

Table 4: Simulated and measured mean outlet temperature and mean ceiling temperature at z=2.6m and floor temperature at z=0m at 6 differnent simulation trials.

Simulation	1	2	3	4	5	6
Mean Outlet temperature [K]	318	301	301	311	300	299
Mean ceiling temperature [K]	319	301	302	314	302	299

Mean floor temperature [K]	319	301	302	314	302	301
Operative temperature [K]						

Th mean temperature of the outlet ceiling and floor are shown in Table 4. The refererence simulation is trial 2. The outlet temperature is significantly elevated in trial 1. and 4. compared to the reference simulation because energy is added through the model inlet and elevated level of flux input respectively. The values of ceiling temperature does not reflect the actual inlet temperature that in 2. is 277K. The mean temperature difference between floor and ceiling is less than 2K.

Discussion

The experimental system consisting of two tunnels and a intermediate diffuse material is used to examine the effects of both convection and radiation on the outlet temperature from a diffuse inlet. The tunnel system is not perfect for this purpose in the sense that many boundary effects influence the measurement. There is boundary effects from the vertical walls, ideally the tunnel should be of infinite width and the diffuse material should cover the entire tunnel upper surface. This could be done with using two concentric circular tunnels instead, with inlet in the center, intermediate the diffuse material and a outer tunnel simulating occupational room. But the results from this model would be sensitive to effects of buoyancy and pressure drop in the tunnel. Hence the boundary effects has been tested and sought minimized in different ways, the thermal stratification in the primary tunnel could influence the measuring of temperature. The vertical stratification in the primary tunnel has been measured under different flow velocities and is found to be less than 1K. The effect of inhomogeneous boundary layer on the wall has been sought minimized with a turbulence generating screen. The turbulence screen positively reduce the

thermal stratification. The temperatures are measured immediately before and after the tunnel intersection (within 0.5m) this to minimize the effect of heat conduction to the surroundings. The thermal conduction should not be of major importance to the result, hence the outlet temperature of the primary tunnel is newer more than 13K over the room temperature in the surrounding room. The measurements are validated with the energy balance model and the model has good correlation with the observations. Thus it can be assumed that there is minimal conduction loss in the measuring section. The variables q''_{ir} and q''_{conv} apparently is not significant in the model. Retain q''_{ir} and q''_{conv} in the model does not improve the correlation compared to the model without q''_{ir} and q''_{conv}.

The experiments show that the diffuse material works as a heat exchanger, the air flowing from the diffuse material downstream has a higher temperature than the upstream air. The heat exchange that takes part in the diffuse material is found to be both convective and radiative dependent. It is found that in some observations $T_c>T_1$ if $T_{ir}>T_1>T_2$ thus there is either a radiative or convective heat transfer between the infrared heating section and the downstream surface of the diffuse material. To make the conclusion that there is a radiative heat transfer $q_{ir}>0$, it must be assumed that the convective heat transfer q_{conv} does not interact with the downstream surface of the diffuse material. $T_c>T_1$ is found at $u_1>0$ hence there is a parallel flow to the heated surface of the infrared heating section in the tunnel and there is little probability that the thermal boundary layer from the infrared heating surfaces extend into the diffuse material.

The generating of a model of the downstream surface temperature of the diffuse material is a difficult task because the heat exchanging processes is complicated at a microscopic level. A linear model with Tc as the dependent variable is derived. The model showed good fit with the observations. The residual analyseis shov that the variance is constant in the measuring interval of both the dependent and independent variables. The marginal increase in variance at low values of u2 and high values of Tirdoes not justify a rejection of the linear model but indicate that a

extrapolation of the model would be connected with increased estimation uncertainty. Deriving values of T_c in a sensitivity analysis of the independent variables within the measuring interval give god acceptable results of T_c. Combination 3 is a isothermal condition at the lower range of u_2, values of T_c deviates from the isothermal condition with 1.4K. This may be effected by the marginal increase in variance and hereby increased estimation uncertainty in the lower range of the measuring interval. The partial derivative of the independent variables in the model are constants, indicating that the changes are independent on the other variables. Knowing that $T_1>T_2$ the negative constants of du_1/dT_c indicates that a increase in air velocity in the primary tunnel u_1, or if the subject was a realistic HVAC system, the air velocity at the ceiling surface of the room, will reduce the downstream surface temperature of the porous ceiling inlet T_c. Interpreting this effect physically indicate that the mixing convection in the boundary layer is reduced if the air velocity in the primary tunnel increases. But if the conditions are isothermal this effect can not explain the reduction of the porous surface temperature T_c. Hence the model may be of some value to estimate boundary conditions of the porous inlet but the model is not applicable in deriving the physical correlations between the independent variables.

Simulations

Calculating the operative temperature from the results of the simulations could give a misleading impression of the thermal conditions in the room. If the room was equipped with a inlet diffuser constructed of permeable high polished stainless steel sheet, then the radiative temperature of the ceiling surface would be close to the inlet air temperature. In the real room the resulting operative temperature would be significantly lower than the sensitive temperature, but this would not be reproduced in the simulations as is indicated by the results of trial 2.

Conclusion

If the ambient conditions are colder than the room conditions the diffuse inlet works as a heat exchanger and increases the temperature of the ambient air inside the diffuse matrix.

The exchange of energy and the preconditioning of inlet air in the diffuse material is found to be dependent on both convective and radiative conditions in occupational room (downstream conditions).

The generation of a model of the surface temperature is proposed assumed a linear dependency between the independent variables. The linear model can not be extrapolated.

The linear model does not explain the physical processes of convection and radiation heat transfer in the diffuse material, but the model is applicable in determining the downstream surface temperature of the diffuse material and hence the inlet temperature of the air.

Reference List

Aarnink, A. J. A. and M. J. M. Wagemans. 1997. Ammonia volatilization and dust concentration as affected by ventilation systems for fattening pigs. *Transactions of the ASAE* 40:1161-1170.

Alazmi, B. and K. Vafai. 2001. Analysis of fluid flow and heat transfer interfacial conditions between a porous medium and a fluid layer. *International Journal of Heat and Mass Transfer* 44:1735-1749.

Bjerg, B., K. Svidt, G. Q. Zhang, and S. Morsing. 2000. The effects of pen partitions and thermal pig simulators on airflow in a livestock test room. *Journal of Agricultural Engineering Research* 77:317-326.

Brohus, H., K. D. Balling, and D. Jeppesen. 2004. Local exhaust efficiency in an operation room ventilated by horizontal unidirectional airflow. *Proceedings of 9'th Int. Conf. of Air distribution in rooms, Roomvent 2004, Univercity of Coimbra, Portugal*216-217.

Chen, Q., Z. Jiang, and A. Moser. 1992. Control of airborne particle concentration and draught risk in an operation room. *Indoor Air* 2:154-167.

Danish Institute of Agricultural Science. Isover Diffusrulle til diffus ventilation. 936, 1-4. 2001. Research Center Bygholm.
Ref Type: Report

Fu, X., R. Viskanta, and J. P. Gore. 1998. Measurement and correlation of volumetric heaqt transfer coefficients of cellular ceramics. *Experimental Thermal and Fluid Science* 17:285-293.

Heber, A. J. and C. R. Boon. 1993. Air velocity characteristics in an experimental livestock building with nonisothermal jet ventilation. *ASHRAE Transactions.* 99:1139-1151.

Hoff, S. J., K. A. Janni, and L. D. Jacobson. 1992. Three-dimensional buoyant turbulent flows in a scaled model, slot-ventilated, livestock confinement facility. *Transactions of the ASAE* 35:671-686.

Holmberg, S., F. Molin, and J. Myhren. 2004. Space heating at low temperature difference between heating unit and ambient air. *Proceedings of 9'th Int. Conf. of Air distribution in rooms, Roomvent 2004, Univercity of Coimbra, Portugal*162-163.

Incropera, F. P. and D. P. De Witt. 1990. *Introduction to heat transfer*. John Wiley & Sons.

Jacobsen, L., P. V. Nielsen, and S. Morsing. 2004. Prediction of indoor airflow patterns in livestock buildings ventilated through a diffuse ceiling. *Proceedings of 9'th Int. Conf. of Air distribution in rooms, Roomvent 2004, Univercity of Coimbra, Portugal* 9.

Jacobsen, L., P. V. Nielsen, and S. Morsing. 2005. Low momentum air supply through diffuse ceiling in livestock buildings. *Transactions of the ASAE*.

Jen, T.-C. and T. Z. Yan. 2005. Developing fluid flow and heat transfer in a channel partially filled with porous medium. *International Journal of Heat and Mass Transfer* 48:3995-4009.

Johannis, G. 1968. Strömungs- und Temperaturverhaltnisse in Räumen mit Lüftungsdecken. *Zeitschrift für angewanse hygiene und gesundheitatechnik in stadt und land* 98:193-224.

Kahn, S. K. 2005. Heat transfer in a viscoelastic fluid flow over a streching surface with heat source/sink, suction/blowing and radiation. *International Journal of Heat and Mass Transfer* In press.

Kulkarni, M. R. and R. E. Peck. 1996. Analysis of a bilayerd porous radiant burner. *Numerical Heat Transfer* 30:219-232.

Lengweiler, P. 2000. Modelling deposition and resuspension of particles on and from surfaces. Swiss federal institute of technology, Zürich.

Neale, G. and W. Nader. 1974. Practical significance of Brinkman's extension of Darcy's law: coupled parallel flows within a channel and a bounding porous medium. *Canadian Journal of Chemical Engineering* 52:475-478.

Nield, D. A. and A. V. Kuznetsov. 2005. Thermally developing forced convection in a channel occupied by a porous medium saturated by a non-Newtonial fluid. *International Journal of Heat and Mass Transfer* 48:1214-1.

Nielsen, P. V. 1992. Description of supply openings in numerical models for room air distribution. *ASHRAE Transactions.* 98:963-970.

Nielsen, P. V., A. Restivo, and J. H. Whitelaw. 1979. Buoyancy-affected flows in ventilated rooms. *Numerical Heat Transfer* 2:115-127.

Ochoa-Tapia, J. A. and S. Whitaker. 1997. Heat transfer at the boundary between a porous medium and a homogenious fluid. *International Journal of Heat and Mass Transfer* 40:2707.

Randall, J. M. and V. A. Battams. 1979. Stability criteria for airflow patterns in livestock buildings. *Journal of Agricultural Engineering Research* 24:361-374.

Sathe, S. B., R. E. Peck, and T. W. Tong. 1990. A numerical analysis of heat transfer and combustion in porous radiant burners. *International Journal of Heat and Mass Transfer* 33:1331-1338.

Srebric, J. and Q. Chen. 2001. A method of test to obtain diffuser data dor CFD modeling of room air flow. *ASHRAE Transactions.* 107.

Srebric, J. and Q. Chen. 2002. Simplified numerical models for complex air supply diffusers. *ASHRAE HVAC&R Research Journal* 8.

Strøm, J. S., G. Q. Zhang, and S. Morsing. 1993. Supply temperatures for ceiling inlets taking air from an attic with un-insulated roof. *Proc. 4'th int. Symp. of Livestock Environment, Coventry, England, ASAE pub. 03-93*421-438.

Tong, T. W. and W. Li. 1995. Enchancement of thermal emission from porous radiant burners. *Journal of Quantitative Spectroscopy & Radiant Transfer* 53:235-248.

Wagenberg, A. V. and M. A. H. H. Smolders. 2002. Contaminant and heat removal effectiveness of three ventilation systems in a nursery room for pigs. *Transactions of the ASAE* 45:1985-1992.

Younis, L. B. and R. Viskanta. 1993. Experimental determination of the volumetric heat transfer coefficient between stream of air and ceramic foam. *International Journal of Heat and Mass Transfer* 36:1425-1434.

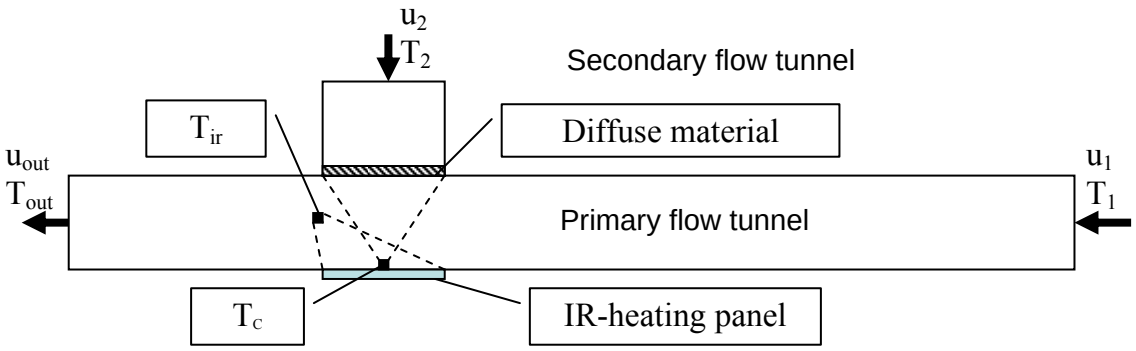

Figure 1. Cross section of the experimental tunnel, ■ indicating measuring instrument position. T_{ir} and T_c were infrared sensors, their measuring area are indicated with dotted lines

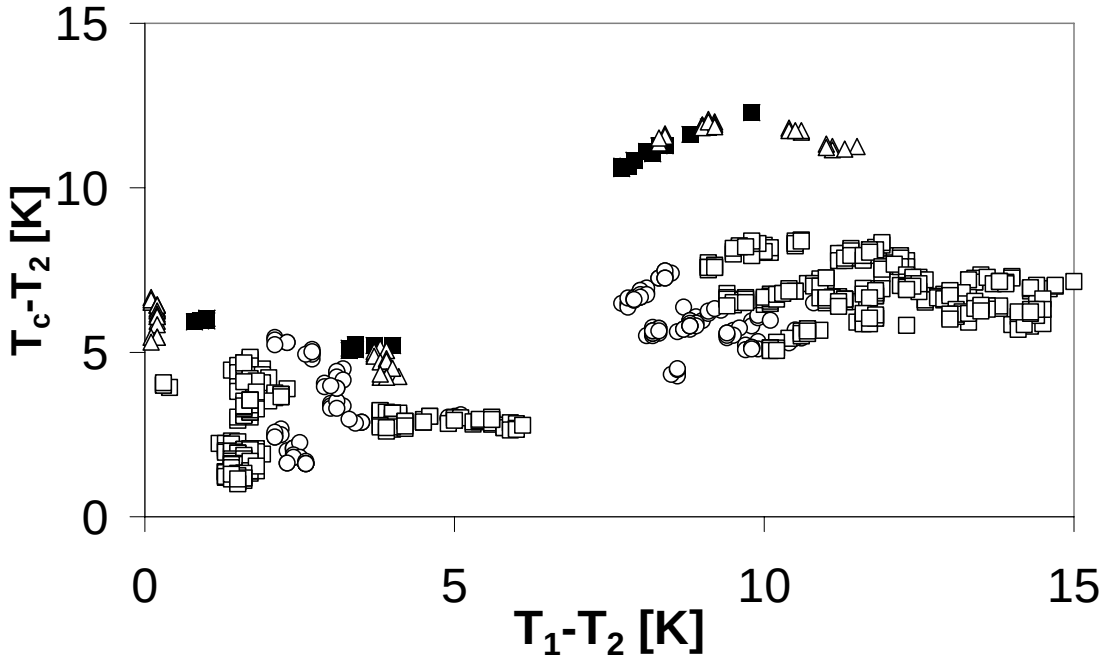

Figure 2:Temperature difference between surface temperature of diffuse ceiling and T_c. as a function of the air temperature difference between tunnel 1 and tunnel 2 T_1-T_2>0, q_{rad}>0,□:u_1>0,u_2>0, ○:u_1=0, u_2>0, Δ:u_2=0,u_1>0, ■:u_1=0,u_2=0

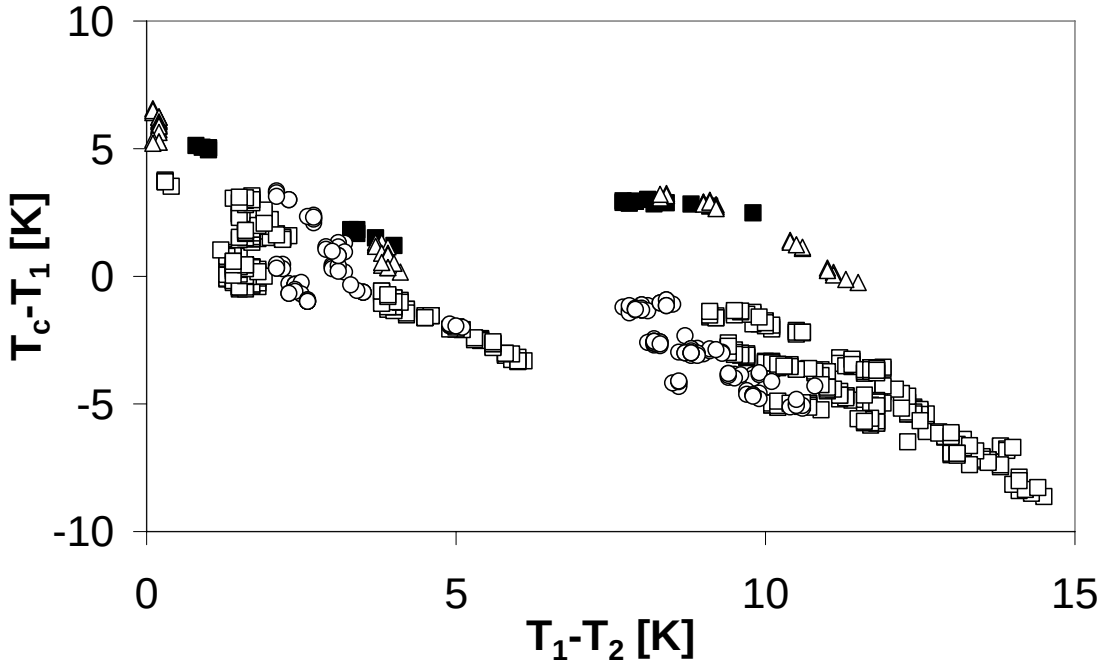

Figure 3:Difference between air temperature of tunnel 1 and dovnstream surface temperature of diffuse material as a function of difference between air temperature of tunnel 1 and 2

T_{ir}>T_1>T_2,□:u_1>0,u_2>0, ○:u_1=0, u_2>0, Δ:u_1>0, u_2=0, ■:u_1=0,u_2=0.

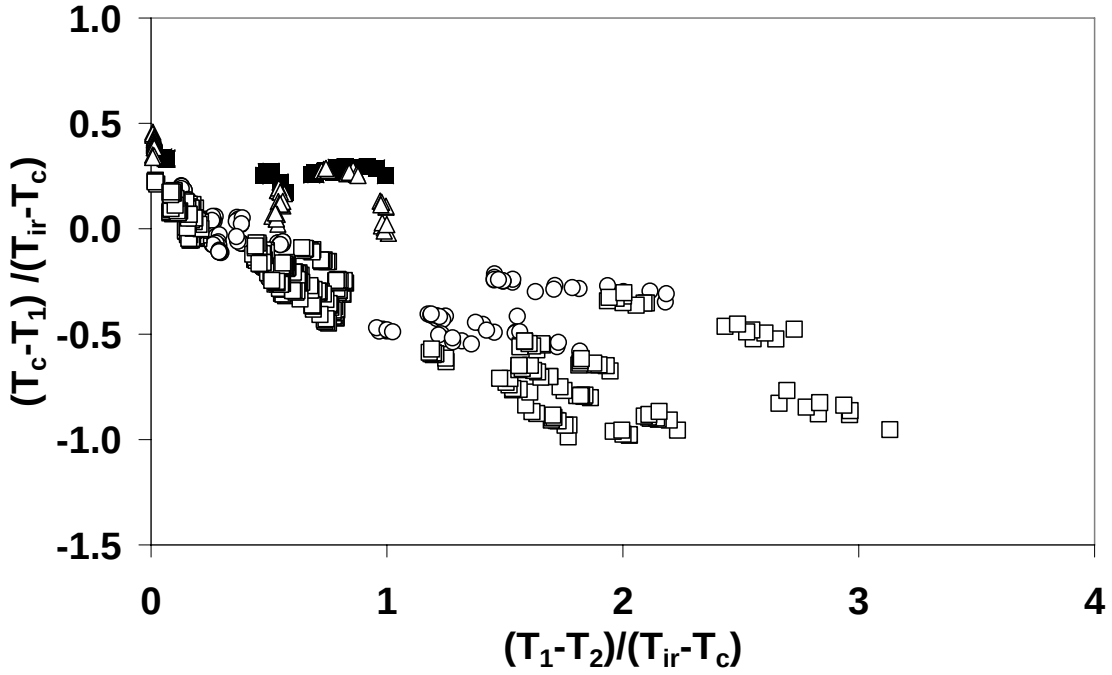

Figure 4: Non dimensional surface temperature difference as a function of the air temperature difference betveen tunnael 1 and 2. $T_{ir}>T_1>T_2>0$,□:$u_1>0$,$u_2>0$, ○:$u_1=0$, $u_2>0$, Δ:$u_1>0$, $u_2=0$, ■:$u_1=0$,$u_2=0$.

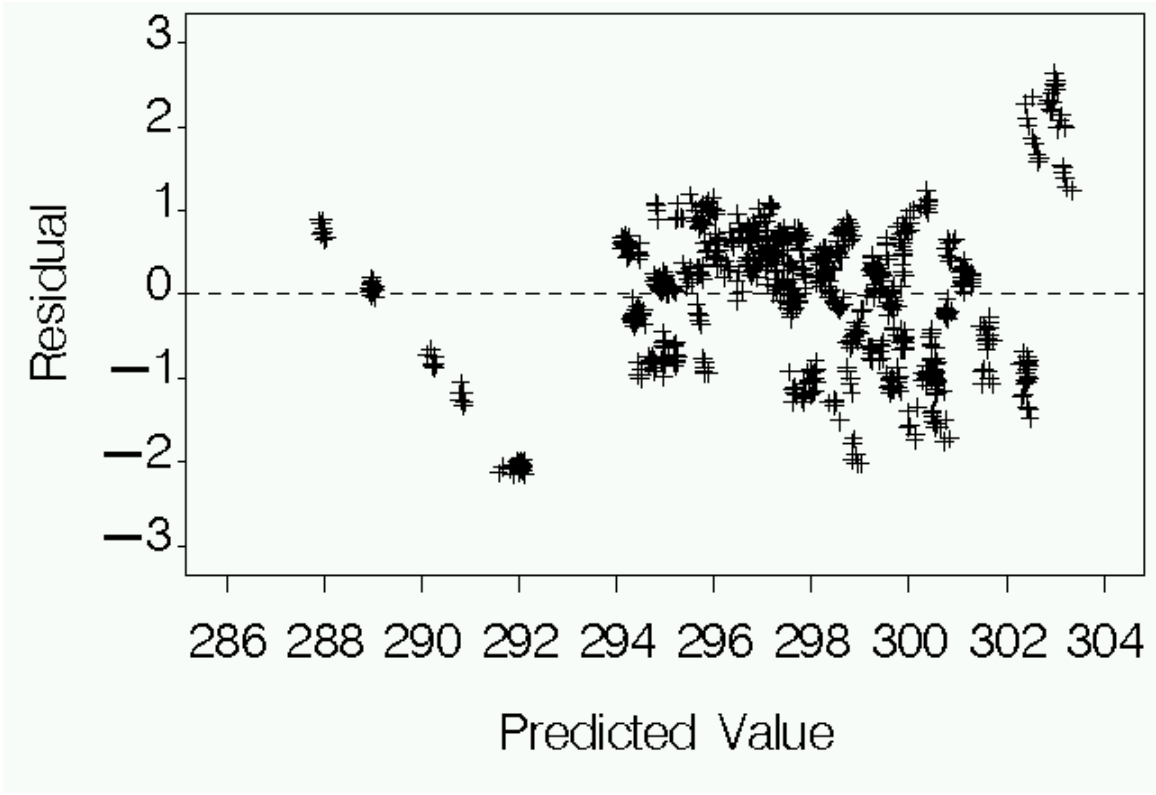

Figure 5: Residual plot Model A predicted value T_c.

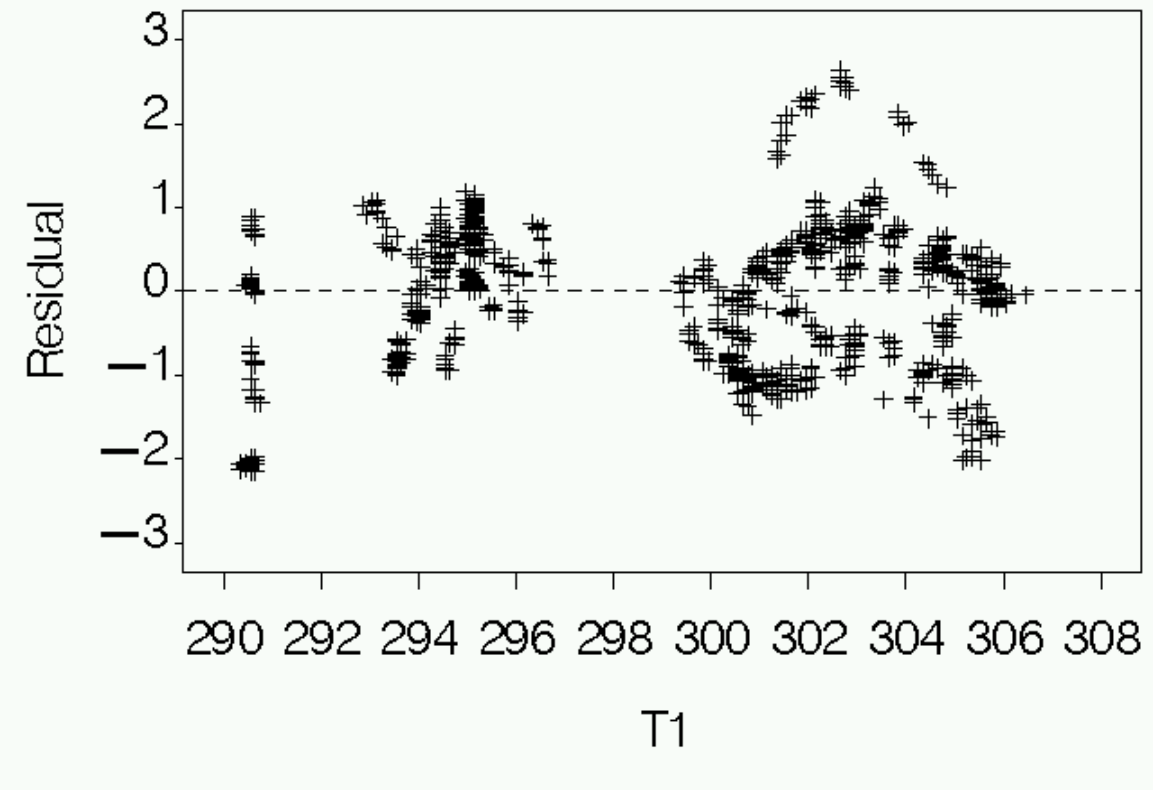

Figure 6:Residual plot Model A. Scatterplot of the residuals as a function of the independent variable T1

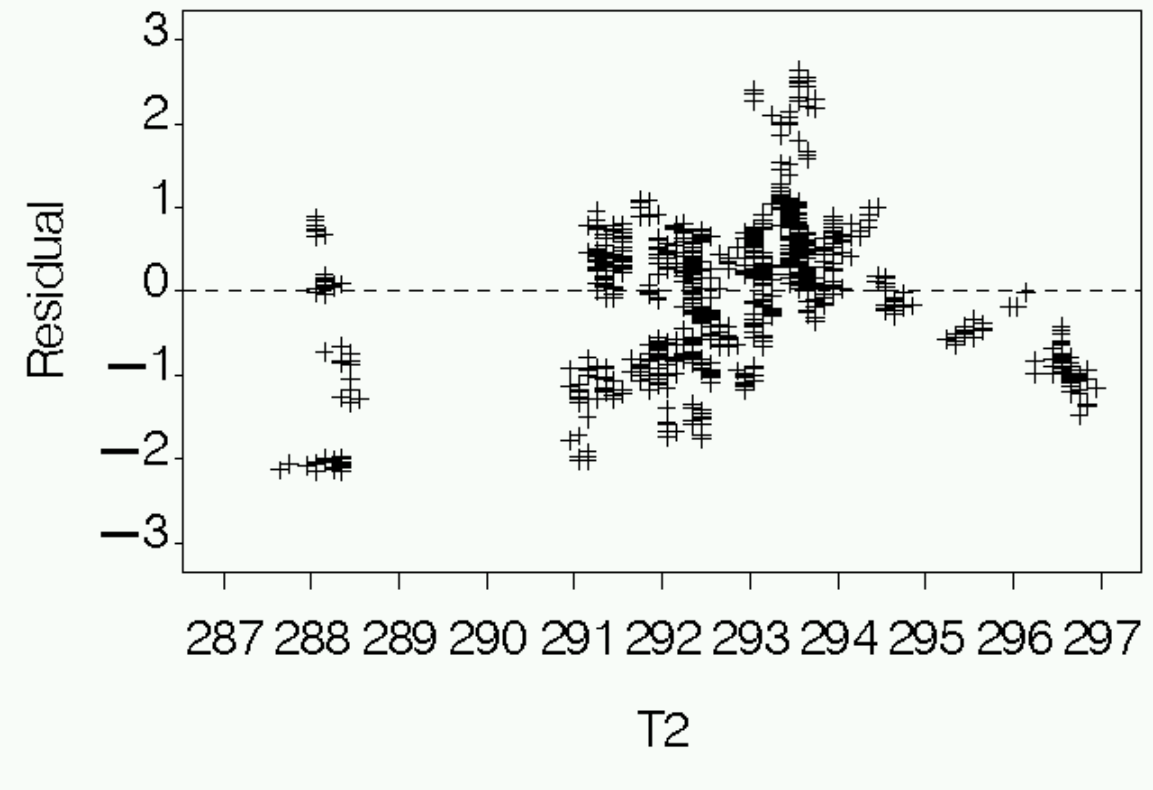

Figure 7:Residual plot Model A. Scatterplot of the residuals as a function of the independent variable T2

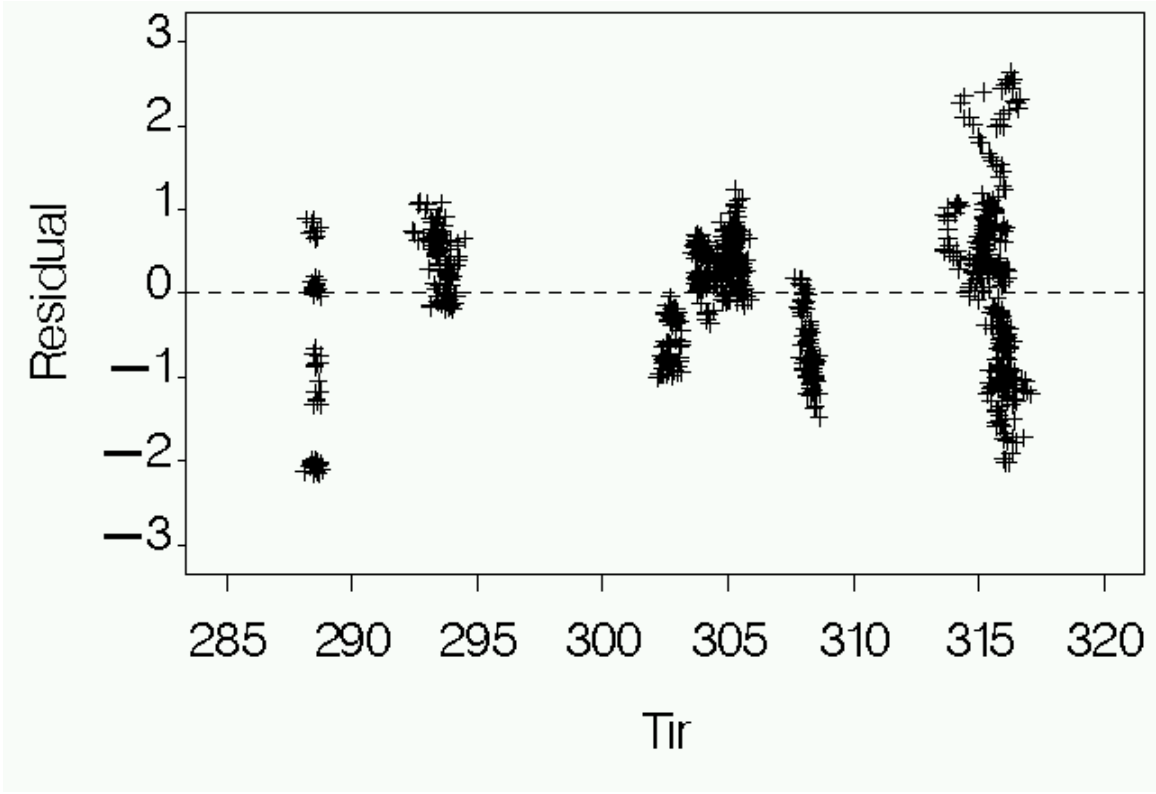

Figure 8:Residual plot Model A. Scatterplot of the residuals as a function of the independent variable Tir

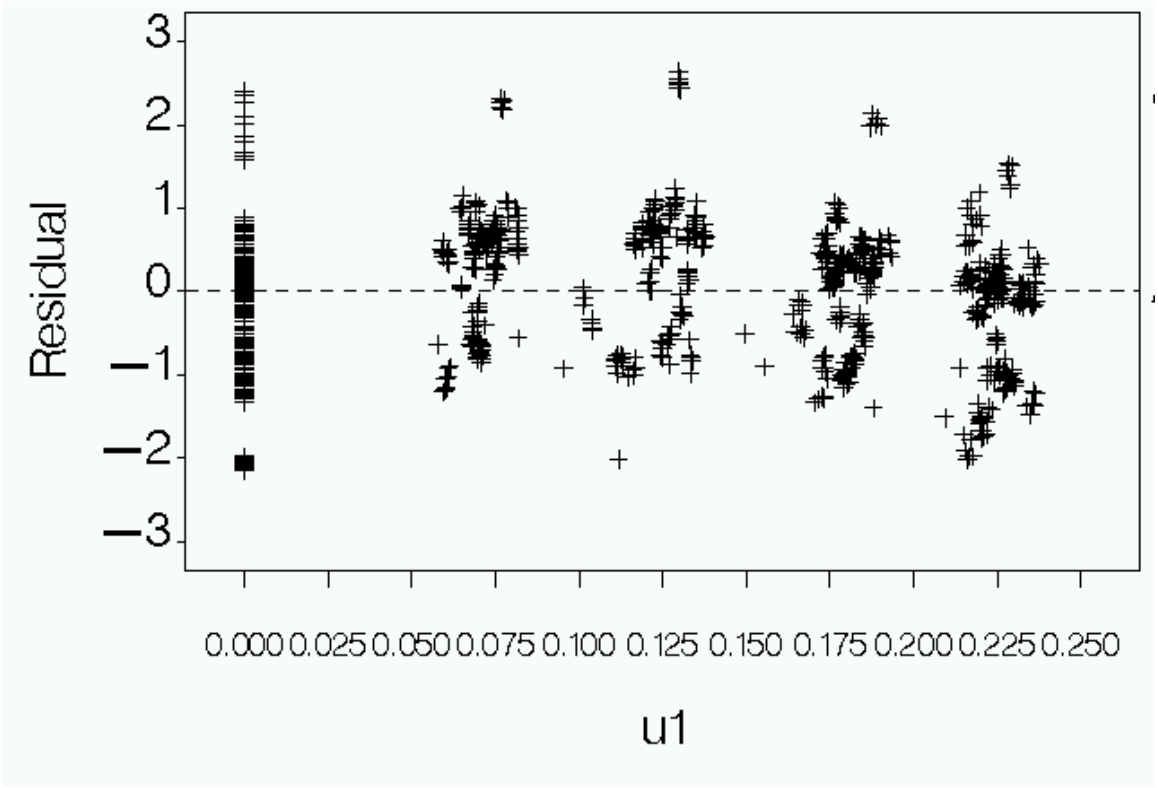

Figure 9:Residual plot Model A. Scatterplot of the residuals as a function of the independent variable u1

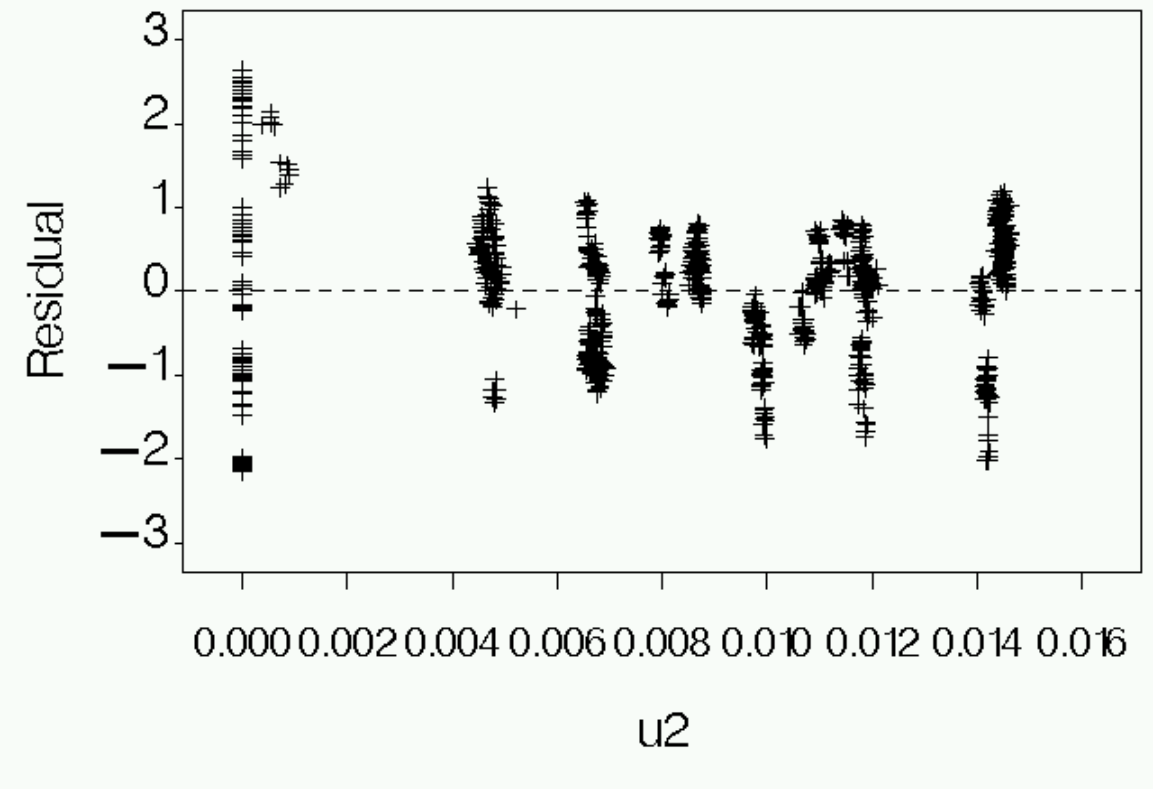

Figure 10:Residual plot Model A. Scatterplot of the residuals as a function of the independent variable u2

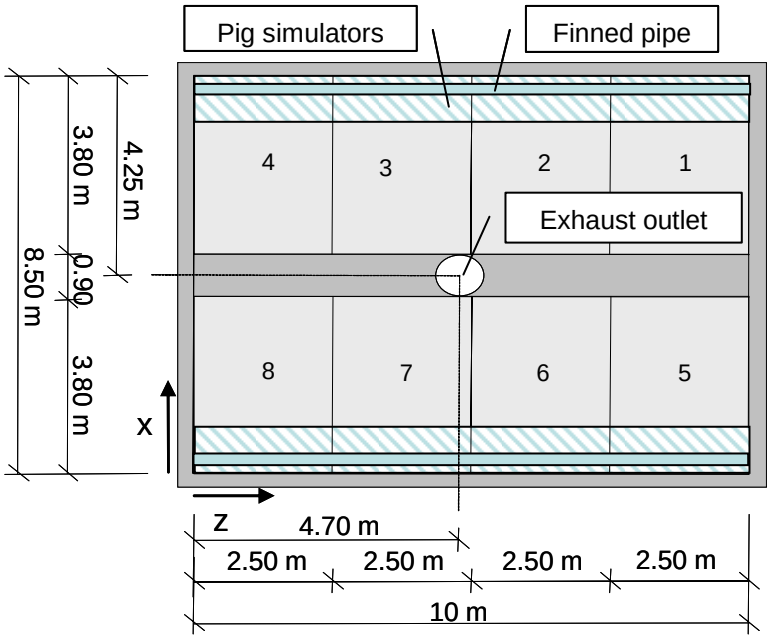

Figure 11: Experimental room showing room dimensions and pen partitions.

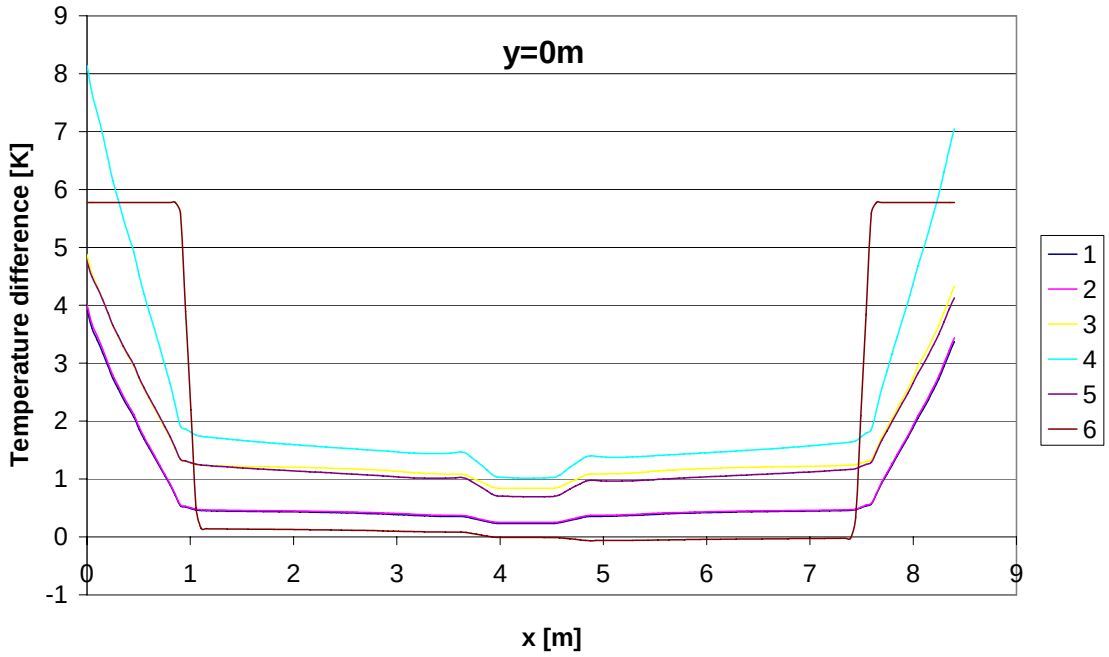

Figure 12: Simulated temperature difference between outlet temperature and local temperature in position (x,y,z)=(0-8.5,0,6.25) at 6 different simulation trials.

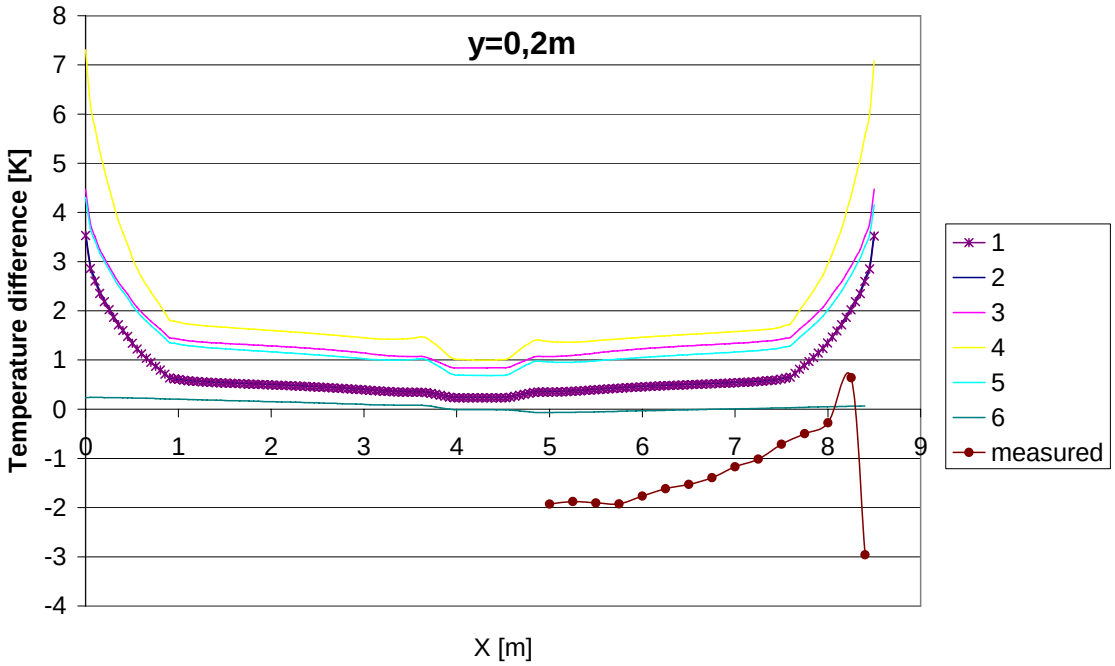

Figure 13 Simulated and measured temperature difference between outlet temperature and local temperature in position (x,y,z)=(0-8.5,2.6,6.25) at 6 different simulation trials and one measurement.

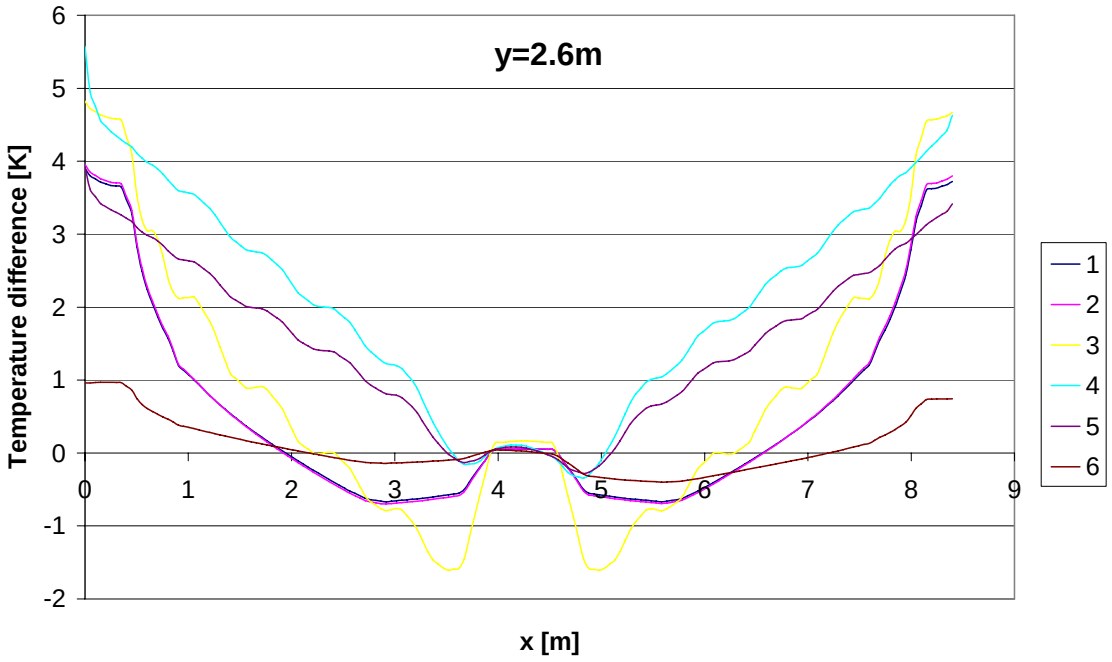

Figure 14 Simulated temperature difference between outlet temperature and local temperature in position (x,y,z)=(0-8.5,2.6,6.25) at 6 different simulation trials.

Nomenklature

$\dot{V}_1$	Volume flow rate in primary tunnel[m^3/h]
$\dot{V}_2$	Volume flow rate in secondary tunnel [m^3/h]
$\dot{V}_{out}$	Volume flow rate in outlet [m^3/h]
A1	Flow cross section area of primary tunnel [m^2]
A2	Flow cross section area of secondary tunnel [m^2]
Air	Area of infrared heating section [m^2]
Aout	Flow cross section area of outlet tunnel [m^2]

CI 95%	Confidence interval 95%
Cp,1	Air heat capacity primary tunnel [kJ/kgK]
Cp,2	Air heat capacity secondary tunnel [kJ/kgK]
Cp,out	Air heat capacity outlet tunnel [kJ/kgK]
f	Degrees of freedom
h	Convection heat transfer coefficient [W/m^2K]
n	Number of observations
q_1	Heat transfer rate primary tunnel[W]
q_2	Heat transfer rate secondary tunnel[W]
q_{conv}	Heat transfer rate convection[W]
q_{out}	Heat transfer rate outlet tunnel[W]
q_{rad}	Heat transfer rate radiation[W]
s.s	Error sum of squares
T_1	Air temperature in primary tunnel [K]
T_2	Air temperature in secondary tunnel [K]
T_c	Surface temperature of diffuse ceiling [K]
T_{ir}	Surface temperature of infrared heating section [K]
T_{out}	Air temperature in outlet [K]
u_1	Mean air velocity in primary tunnel [m/s]
u_2	Mean air velocity in secondary tunnel [m/s]
u_{out}	Mean air velocity in outlet [m/s]
α	coefficients
β	coefficients

ε	Emissivity []
ρ	Density [kg/m^3]
σ	Stefan-Boltzmann constant: 5.670e-8 W/m^2K^4
χ	coefficients

PAPER NO.3:

Jacobsen, L., Nielsen, P. V. and Morsing, S.: Prediction of Indoor Airflow Patterns in Livestock Buildings Ventilated through a Diffuse Ceiling. Roomvent 2004, 9th International Conference on Air Distribution in Rooms, Coimbra, 2004, Portugal.

PREDICTION OF INDOOR AIRFLOW PATTERNS IN LIVESTOCK BUILDINGS VENTILATED THROUGH A DIFFUSE CEILING

Jacobsen, L.[1], Nielsen, P.V.[2] and Morsing, S.[1]

[1]Danish Institute of Agricultural Sciences, Department of Agricultural Engineering, P.O. Box 536, DK-8700 Horsens, Denmark. Tel.: 7629 6082. Fax: +45 7629 6100. Email: lis.jacobsen@agrsci.dk, www.agrsci.dk
[2]Indoor Environmental Engineering, Aalborg University, Sohngaardsholmsvej 57, DK-9000 Aalborg. Tel.: +45 9635 8080. Fax: +45 9814 8243. Email: pvn@civil.auc.dk

Roomvent 2004, 9th International Conference on Air Distribution in Rooms, Coimbra, 2004.

PREDICTION OF INDOOR AIRFLOW PATTERNS IN LIVESTOCK BUILDINGS VENTILATED THROUGH A DIFFUSE CEILING

Jacobsen, L.[1], Nielsen, P.V.[2] and Morsing, S.[1]

[1]Danish Institute of Agricultural Sciences, Department of Agricultural Engineering, P.O. Box 536, DK-8700 Horsens, Denmark. Tel.: 7629 6082. Fax: +45 7629 6100. Email: lis.jacobsen@agrsci.dk, www.agrsci.dk
[2]Indoor Environmental Engineering, Aalborg University, Sohngaardsholmsvej 57, DK-9000 Aalborg. Tel.: +45 9635 8080. Fax: +45 9814 8243. Email: pvn@civil.auc.dk

***Summary**: The airflow conditions in an experimental pig housing unit are examined both experimentally and numerically (simulation) with particular focus on the airflow conditions in the occupational zone of the animals. Two heating setups are used, and the temperature is measured in a horizontal profile at the floor and at the ceiling. Good concordances between the measurements and the simulations are reached at the floor level. At the ceiling level, the conformity to the measuring results is unsatisfactory.*

***Keywords:** Diffuse ventilation, livestock buildings, CFD*
***Subject category**: Industrial and agricultural ventilation*

Introduction

The purpose of ventilation in livestock buildings is to provide the animals with uncontaminated air at a high level of thermal comfort at the lowest possible energy and investment costs.

In ISO 7730, the thermal quality is referred to as *the operative temperature*, which at air velocities below 0.2 ms^{-1} can be simplified to the mean of air and radiant temperatures. Traditionally, the control of thermal conditions in a pig house is controlled trough centrally placed sensors of air temperature and humidity. The animals' perception of the local climate may be far from optimal when the centrally measured climatic conditions in the house comply with the thermal setpoints of the control system. But from a productivity point of view, it is interesting for the farmers to acquire knowledge of the comfort and well-being of the animals.

The traditional climate control methods disregard the effects of air velocity and radiant temperature in the evaluating of the animals' experience of the thermal conditions. When combining behavioral studies and measurements of dynamic changes in air velocity and temperature, indicators of animal comfort can be established. Behavioral studies in which the effects of the thermal comfort of pigs in relation to the operative temperature are examined are not often published. Assuming that pigs' perception of thermal comfort is somewhat similar to that of humans, the definitions of thermal comfort expressed by Benzinger [1] can be adapted. The perception of thermal comfort, i.e. the condition when there are no impulses from the brain to regulate the environment by behavior, can be assumed to apply for both humans and pigs. This condition is achieved by satisfying the combination of the physical parameters: air velocity, air temperature, radiant temperature measured, as described in EN ISO 7726 [3] and EN ISO 7730 [4].

In diffuse ventilated rooms, buoyancy and radiation effects will control the flow patterns in the occupational zone. By heating the room, it becomes possible to change and control the airflow patterns in different areas of the occupational zone. The convection and the radiation heat from the animals can change the flow pattern and the air exchange in the occupational zone of the room.

In this examination, finned pipe heaters have been installed to keep the occupational zone well heated and ventilated and free of downdraft of cold air from the diffuse ceiling. The effect of the finned pipe heaters will be examined with animal simulators in two different positions.

By verifying the simulations with the measurements it becomes possible to determine the thermal comfort of the pigs in the confinement unit by use of simulation. Prediction of the thermal effect of a control action can prevent the occurrence of thermally uncomfortable events in pig houses.

Method

Experimental: The dimensions of the experimental room are: w × h × l = 8.5 × 3.0 × 10 m, fig. 1, with "diffusion" inlet, 0.1 m thick mineral wool (ISOVER diffusion) covering the entire room 0.3 m below the experimental room ceiling, creating a plenum above the diffuse ceiling. To prevent short circuit flow, the diffuse ceiling around the fan and the inlet is covered with non-diffusive foil over an area of 0.45 m from the wall and

0.9 m from the exhaust fan. The occupational zone measures 8.5 × 2.6 10 m. The occupational zone is divided into a central aisle (0.9 × 10 m), and with pen partitions each of the 8 pens floor measure 2.5 × 3.8 m, pen partitions are 0.6m high .

The air inlet to the plenum is situated at the plane (X, Y, Z) = (8.5, 2.7-2.6, 0-10 m), i.e. above the diffuse ceiling in one side of the room. The exhaust fan is situated at (X, Y, Z) = (4.25, 2.5, 4.7 m), Ø = 0.9 m. The heating sources in the room are the pig simulators and the finned pipe. The pig simulators are 0.9 m wide electric cable heating sources placed at the floor at full room length (10 m), and moreover, a 10 m convective heat source (1½" central heating finned pipe) is placed at each sidewall 1.3 m above the floor, and 0.05 m from the wall. The pig simulators are engaged at two different geometrical layouts; one where the pig simulators cover the floor adjacent to the wall, and one placed at the central aisle. The pig simulator heat sources emit 164.2 Wm^{-2},and the finned pipes emit approximately 148.7Wm^{-1} per running meter. The water flow inlet temperature in the finned pipes is kept at 341ºK, and the return temperature is 336ºK. The temperature is kept constant with a flow loop.

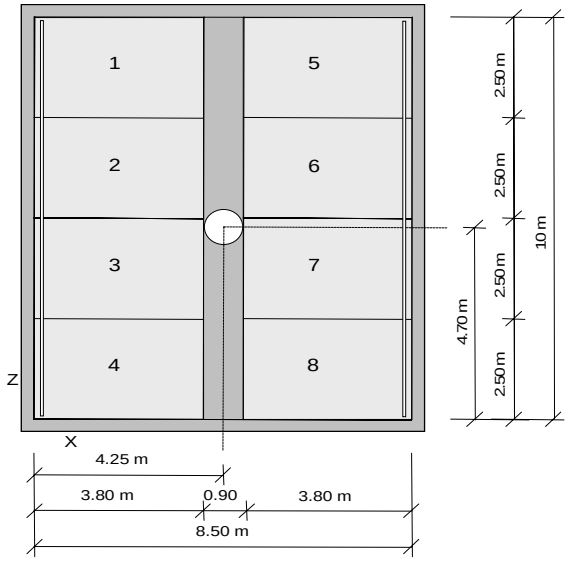

Fig. 1. Experimental room setup plane.

At a room temperature of 302ºK, a constant temperature difference of 25ºK between the inlet air temperature and the outlet air temperature is aimed at. Between each change in thermal load layout, adequate time is given for the equilibrium state in the room to develop and steady state conditions to evolve. The temperature profile is measured at the floor and at the ceiling in the central plane Y = 6.25 m at pen #2 (Fig 1). The temperature profile is measured with 15 thermocouples mounted on a horizontal rod each with a distance of 0.25 m, except for the wall adjacent thermocouple, which is placed 0.1 m from the wall. The horizontal temperature profile is measured at Y = 0.2 m and Y = 2.52 m above the floor. The room temperature is measured at the coordinates (X, Y, Z) = (1.9, 1.2, 6.25 m).

The 2D flow pattern has been visualized with smoke pulses from a heated smoke source (room temperature), a plane lighting source and a video monitor in the plane Y = 6.25 m in pen #2.

Simulation:
The purpose of the simulations is to verify the findings in the experimental investigation. Simulations are performed under 2D conditions with the STORMCFD2000 software.

The control equations for fluid dynamics, the Navier stokes equations, represent the conservation of mass, momentum and energy for a fluid continuum. The generic form of the transport equation can, for the general variable ϕ, representing quantity such as velocity, temperature T or concentration in any given control volume of the flow volume, be written as follows:

$$\underbrace{\frac{\partial \rho\phi}{\partial t}}_{T} + \underbrace{\frac{\partial(\rho u_i \phi)}{\partial x_i}}_{C} = \underbrace{\frac{\partial}{\partial x_i}\left[\Gamma_\phi \frac{\partial \phi}{\partial x_i}\right]}_{D} + \underbrace{S_\phi}_{S}$$

The sections represent the transient term T, the convective term C and the diffusive term D, where Γ_ϕ is the effective diffusion coefficient and the net source term S.

In the present case, the buoyancy force is included into the source term.

The geometry is similar to the experimental room in dimensions, but because the model has been reduced to 2D, the plenum inlet at both walls in X = 0 m and X = 8.5 m is above the diffuse ceiling in Y = 2.7-2.8 m (The diffuse ceiling has a thickness of 0.1 m). A reduction of the model from a 3D to a 2D model of the experimental room would be questionable, because the experimental room does not have the proper geometrical features to justify such a simplification. The room has an almost quadratic floor surface, and the exhaust fan is situated centrally in one point. 2D conditions would require a very long room and a linear exhaust fan. However, the experimental room has a symmetric plane vertically through the fan center, at which ideal 2D conditions

could be assumed, the outlet flow volume is very low and it is also well known that exhaust fan only has a small influence on the air flow in the room.

The grid is shown in Fig 2. The number of cells in 2D is 2870.

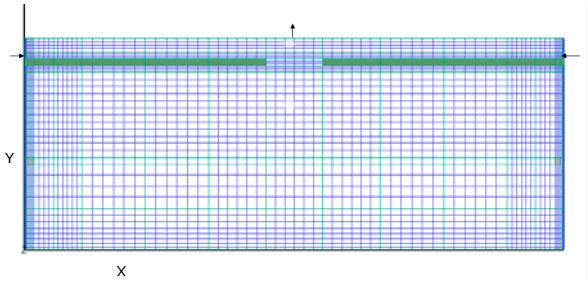

Fig.2. 2D mesh distribution of XY cross section

The permeability factor of the diffusion material has been verified in a specific model and compared to the results of a test report of the diffusion material: ISOVER diffusion [2]. The material shows a linear dependency between flow volume and pressure difference over the material. The porous media is isotropic, and the permeability factor is 5.1e-10 for 100 mm thick material. The permeability for the isotropic condition is calculated using Darcy's equation (vector notation)

$$-\nabla_i p = \left[\frac{\mu}{\kappa_i}\right] u_i$$

where p is pressure, μ is the dynamic viscosity, κ_i is the direction dependent permeability and u_i is the i^{th}-fluid velocity component.
Parameters used in the simulation:

- Fluid: Air STP (standard pressure temperature)
- Turbulence model: Standard K-E model

Boundary values:

- Gravitational force: Boussinesq
- Inlet: Temperature Tin = 277ºK, Velocity v_{in} = 0.083 ms^{-1}
- Outlet: Boundary condition = pressure, pressure coeff. = 1000, Velocity = computed.
- Wall: flux = 0 Wm^{-2},except at heated wall boundary. Heating sources: Q_{pig} = 164.2 Wm^{-2}, Hvor mange m^2
  Q_{ribb} = 148.7 Wm^{-1}.

Terms in mass transport equations:

- Convection: 1st order
- Conduction: Harmonic non linear 2nd order
- Time step variation: Automatic
- $t_{iteration}$ = 5000 s
- Solver control: Solver = incomplete factorization, number of iterations = 20, relaxation factor = 1, convergence tolerance = 0.001.
- Grid: Cartesian
- Radiation: None
- Iterations $4*10^5$-$8*10^5$

Results and discussion

The local deviance from the room temperature is the difference between the room temperature measured at the coordinates (X, Y, Z) = (1.9, 1.2, 6.25 m) and the locally measured temperature at the floor or at the ceiling. The value of the local deviance measurement gives an impression of the obstacles that will occur when the aim is to control the occupational zone temperature by measuring the temperature centrally. High numerical values of local deviances indicate that the temperature distribution in the occupational zone is far from well designed. In the occupational zone close to the floor, the local deviance from the room temperature is below 2K, except for the close wall measurement at the wall heating position. The flow pattern shows air velocities that are no higher than 0.1ms^{-1} in the occupational zone or at the ceiling. By comparing the measured local deviance temperature with the corresponding simulated values, it will be possible to evaluate the importance of different parameters in relation to simulation reproducibility of the temperature profile.

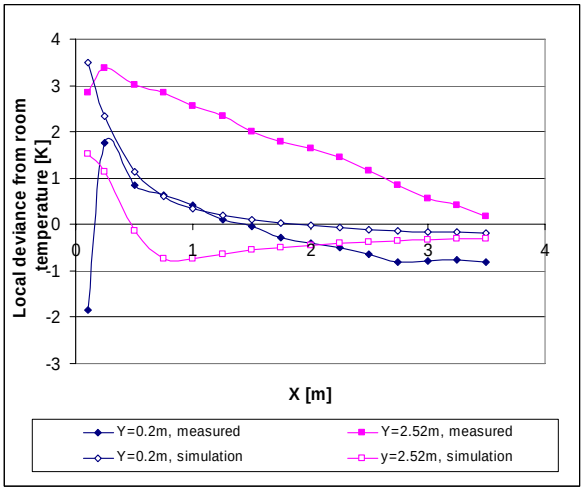

Fig. 3. Measured and simulated local deviances from room temperature; pig simulators positioned adjacent to wall, horizontal profiles Y = 0.2 m and Y = 2.52 m above floor level

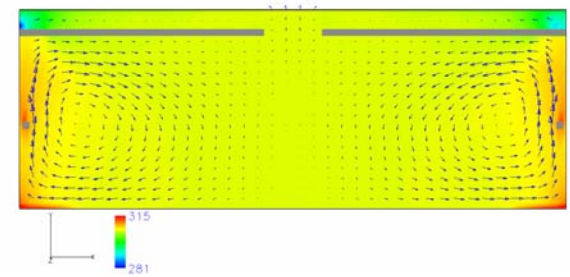

Fig. 4: Airflow velocity distribution in 2D simulation with wall floor heating and finned pipe heating

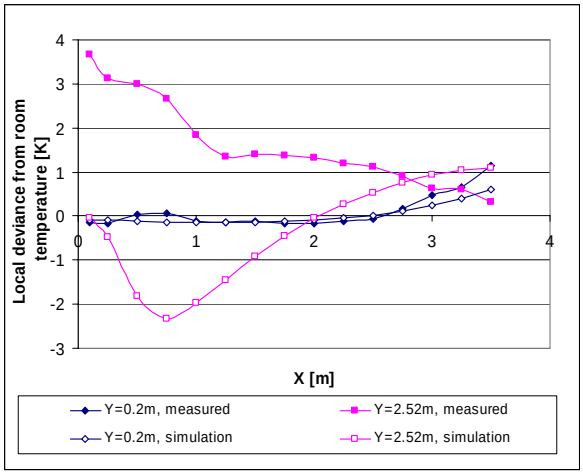

Fig. 5. Measured and simulated local deviances from room temperature. Pig simulators positioned adjacent to aisle, horizontal profiles Y = 0.2 m and Y = 2.52 m above floor level

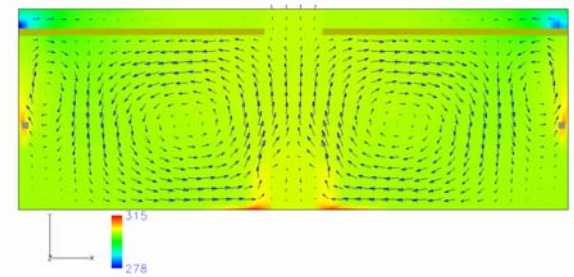

Fig. 6. Airflow velocity distribution in 2D simulation with aisle floor heating and finned pipe heating

Measuring results: Assuming that the measurement values are normally distributed and independent, the confidence interval of each measuring point can be calculated. The maximum and minimum 90% confidence interval (CI) values for each horizontal temperature profile measurement are shown in Table 1 to give an impression of the confidence interval span of the measuring points in the temperature profile. The measuring point CI value ± measuring value gives an interval in which there is a 90% probability of finding the measuring value. If the simulation value is within this interval, the similarity between the measurements and the simulation results will be significant, although, the variations in the measurement values, and as such the confidence interval, is the consequence of random measuring errors and not of the systematic measuring errors. But the absence of systematic errors is assumed.

Table 1: Max. and min. values of 90% confidence interval of horizontal temperature measurement.

Heating setup	Horizontal measuring position, Y	n	CI_{max}/CI_{min}, 90%
	m		K
Wall	0.20	170	0.021/0.014
Wall	2.52	76	0.046/0.030
Aisle	0.20	58	0.094/0.075
Aisle	2.52	42	0.29/0.083

Simulation results: The airflow patterns in Figs. 4 and 6 are in good agreement with the visualization results found in the experiment.

Aisle heating setup: The visualization showed a very complex and transient flow pattern, which is difficult to reproduce with a steady state solver. The flow directions at the ceiling observed in the visualization cannot be reproduced in the simulation. The flow direction at the floor is similar in the simulation and the visualization.

Wall heating setup: The flow visualization showed a simple and steady flow, and the simulation reproduces this flow pattern meticulously.

Comparing the measurement results of two different heating setups with the simulation results at floor level, Y = 0.2 m, and at ceiling level, y = 2.52 m, the deviance between the measuring values and the simulation values at ceiling level, Y =2.52 m, is obvious. The simulated air temperature below the ceiling deviates up to 5K from the measured temperature. Only two ceiling measuring points at the aisle heating setup have simulation values within the confidence interval (X, Y) = (2.75, 2.52) and (X, Y) = (3.0, 2.52). Looking at the difference at Y = 0.2 m, 67% (10/15) of the simulated values at the aisle heating setup is within the confidence interval. At the wall heating setup, Y = 0.2 m, two of the simulation values are within the confidence interval (X, Y) = (0.75, 0.2) and (X, Y) = (1.0, 0.2).

Conclusions

The conclusions of this experiment cover the following two aspects: control and simulation.

Seen from a control point of view, the measurements show that the deviances from the room temperature are less than ±2K at floor level in both heating setups. This means that the central measurement in the given heating setup gives a good impression of the temperatures in the occupational zone at floor level. This result, however, cannot be transferred to the comfort perception of the animals. The temperature conditions may be acceptable, but the air velocity and the irradiation are equally important in evaluating the thermal comfort of the animals. The temperature simulation and the measurements show good agreement at floor level in both heating setups. At ceiling level or close to the inlet, the agreement is very poor. The reason can be the absence of radiation in the simulation model. An introduction of radiation in the simulation would result in a heated surface on the diffuse inlet and an increase in the air temperature at the boundary layer below the ceiling. In the STORMCFD2000 code, the radiating wall boundary condition cannot be applied to inlets, outlets and porous boundaries.

The simulation is 2D, and the 3D experimental room is not axially symmetric. This may influence the thermal conditions more at the ceiling than at the floor, where the flow is inhibited by pen partitions.

References

[1] Benzinger, T.H., 1979. The Physoiological Basis for Thermal Comfort. Proceedings of the First International Indoor Climate Symposium, Danish Building Research Institute, Copenhagen, Denmark.

[2] Test report No. 936, 2001. Isover diffusrulle til diffus ventilation. (Isover Mineral Wool for Diffuse Air Supply) Danish Institute of Agricultural Sciences, Department of Agricultural Engineering, Research Centre Bygholm, Horsens, Denmark.

[3] EN ISO 7726:2001(E), 2001. Ergonomics of thermal environment Instruments for measuring physical quantities.

[4] EN ISO 7730:1994(E), 1995. Moderate thermal environments. Determination of the PMV and PPD indicies and specification of the conditions for thermal comfort.

INTERNAL PAPER:

Study of Coanda Effect and Non-Symmetric Flow Conditions in a Symmetric Enclosure.

Study of Coanda effect and non-symmetric flow conditions in a symmetric enclosure.

Flow condition in a room with symmetry boundary conditions is not always symmetric or static, even though the room boundary conditions is symmetric and the thermo and flow is at equilibrium conditions. The asymmetric and transient environmental conditions enhance the demands of documentation when accounting for the climatic conditions in ventilated room.

Several authors have found that transient conditions have a dominating influence on the flow systems of rooms. (Rees et al., 2001) studied the local transient conditions in a displacement ventilated room with chilled ceiling cooling and found that the quasi-periodic fluctuations take the form of lateral oscillations in the plumes above heat sources. Several heat sources were placed in the room and the measurements showed that the oscillations from the different heat sources was not independent. The results of the experimental data was reproduced with transient calculations. (Bjerg et al., 1999) measured 3D effects of airflow movement in a room with 2D boundary conditions. Numerical simulations showed that the room width to height ratio had significant influence on the development of tree dimensional effects of airflow where a increase in ratio increased the 3D effects. The effect of changes in room length to height was not investigated though. The use of symmetry plane in the simulations, where wall friction effects were exclude from the calculations, produced perfect 2D conditions in the room. It was concluded that 3D-effects are connected to wall friction. The measures SD of the flow direction was reversely proportional to the Reynolds number. It was assumed that this effect was caused by disturbances in the room that more readily affect the low velocity airflow (low Reynolds number).

(Zhang et al., 2000) found 3D effects in a room with 2D boundary conditions and concluded that in the present case the velocity conditions in the symmetry plane of a 2D room is not comparable to the velocity conditions at symmetry plane parallel to the symmetry plane. They found that the room air flow had transient character. In a equivilibrium condition the velocity on one side of the symmetry plane could be twice as high as the velocity in the equivalent position on the other side of the symmetry plane. This condition could interchange without any measurable interruption. The period of this interchange was not harmonic. Periods of down to 6000s was measured. To ensure 2D flow conditions in a room guide plates can be mounted in the room, longitudinal to the flow direction. (Bjerg et al., 2000; Zhang et al., 2000)

The attachment of fluid jets to walls, also known as the Coanda effect, was studied by (Triboix and Marchal, 2002). The separation distance, the distance from the slot inlet to where the jet detaches from the wall, were calculated using an stability analysis of the equilibrium of a layer that is denser than the ambient fluid. It was found that the separation distance is a function of the slot opening height and the Archimedes number of the blowing jet.

Understanding the effect of wall attachment or Coanda effect is closely connected to understanding the conditions of pressure around a jet flowing into an infinite room. When the jet discharge from the inlet fitting, the velocity of the jet is at core velocity equivalent to the flow profile in the inlet fitting. When the jet departs from the fitting there is a change of boundary conditions from a solid wall (with a non-slip boundary condition) to a infinite room with a principally full slip condition on the core surface. The boundary condition is satisfied with the formation of a mixing boundary layer at the surface between the jet core flow and the room. The flow acceleration or entrainment at the mixing boundary layer of the jet develops a pressure drop that is

proportional to the change in velocity. Over time an entrainment zone with recirculation flow develops at the side of the jet, and because the zone facing the wall is restricted in space a pressure drop develops that drags the jet flow towards the wall (Chen and Srebric, 2001). When isothermal conditions prevail this effect is independent on the gravitational field. At non-isothermal conditions the density difference between the jet and the room air will affect the jet in vertical direction. From the above it can be derived that flow systems can have several stable solutions. These solutions can be both spatially and dynamically distributed in the room enclosure. Even if a room is geometrically symmetric the symmetry condition in the flow system may not be found outside the symmetry plane. The wall “friction” plays an important role, although it is not investigated weather the friction is dependent on surface roughness or other surface parameters. The room dimensions ratio also has an significant effect on the formation of 3D flow systems. The small flow disturbances in the room effect the airflow in the room more dominant at low Re numbers than at high Re. The flow disturbances can affect the flow into what could be interpreted as transient flow when the dominating flow direction changes in the room without measurable stimulation. The equilibrium conditions of kinetic and thermal energy may have an influence on the jet attachment to the wall. The Coanda affect of flow attaching to the wall is the effect of a spatially restricted entrainment zone and a resulting pressure drop in that zone.

Example

Some expansion sections in a flow channel can be an example of a flow system that attaches to the wall. Expansion or diffusor sections is used in many flow channel systems where a flow velocity reduction is anticipated.

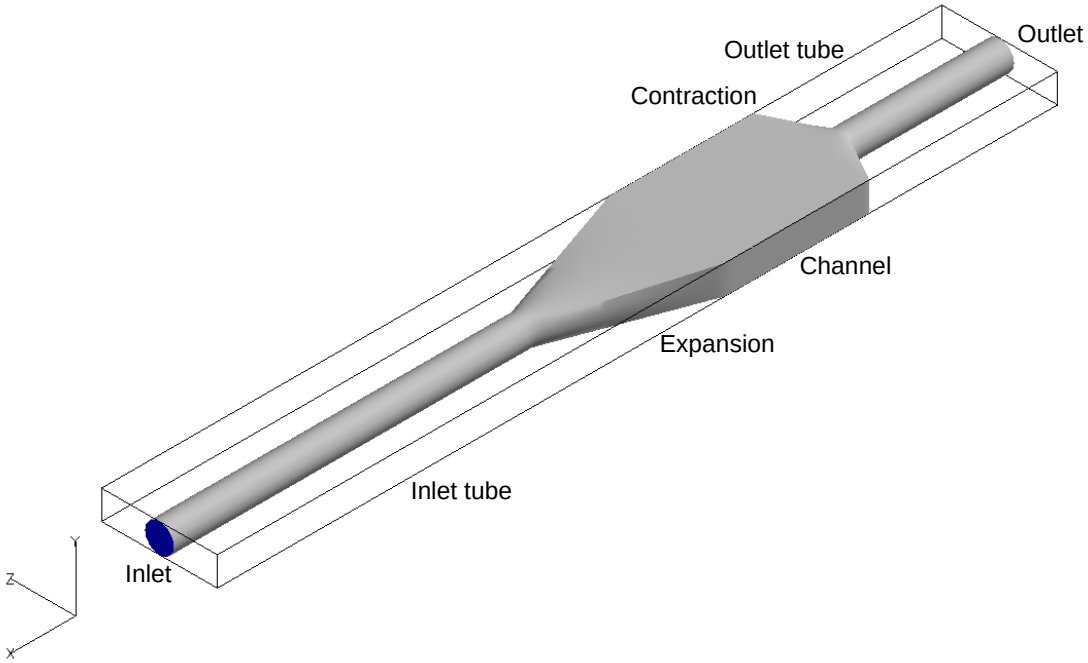

Figure 1: The two dimensional flow expansion channel. Coordinate system is placed at the central symmetry axis. Outlet x=0m.

The expansion flow channel is shown in Figure 1. A numerical simulation of the expansion flow channel is performed. The channel is (x*y*z) 12*0.4*1.6m and is divided into 4160 computational cells. The expansion channel consists of an inlet tube, expansion, channel, contraction and a outlet tube -section. The channel is perfectly symmetric in the y=0m- and z=0m-plane and have the dimensions 1.6*0.4*1.6 the outlet opening is at x=0m. The purpose of the channel is to obtain spatially and temporal uniform and symmetric flow velocity gradients around the symmetry planes in the channel section. The channel is intended to simulate the flow in a diffuse inlet section under non isothermal conditions or the surface diffusion and evaporation from a slurry gutter at isothermal flow conditions where well defined flow conditions are anticipated. Hence non-symmetric velocity gradients, transient conditions and flow attaching to one side of the wall is not intended and desired. To investigate the flow in the expansion flow channel simulations was performed. The test conditions were an inlet velocity of between 0.5-1m/s, equivalent to a flow filling

time of less than 45s. The iteration time is 1000s. Two simulations at 0.5m/s and 1m/s inlet velocity are shown in Figure 2 and Figure 3. At both inlet velocities there is an attachment to the wall and the Coanda effect is obvious.

.

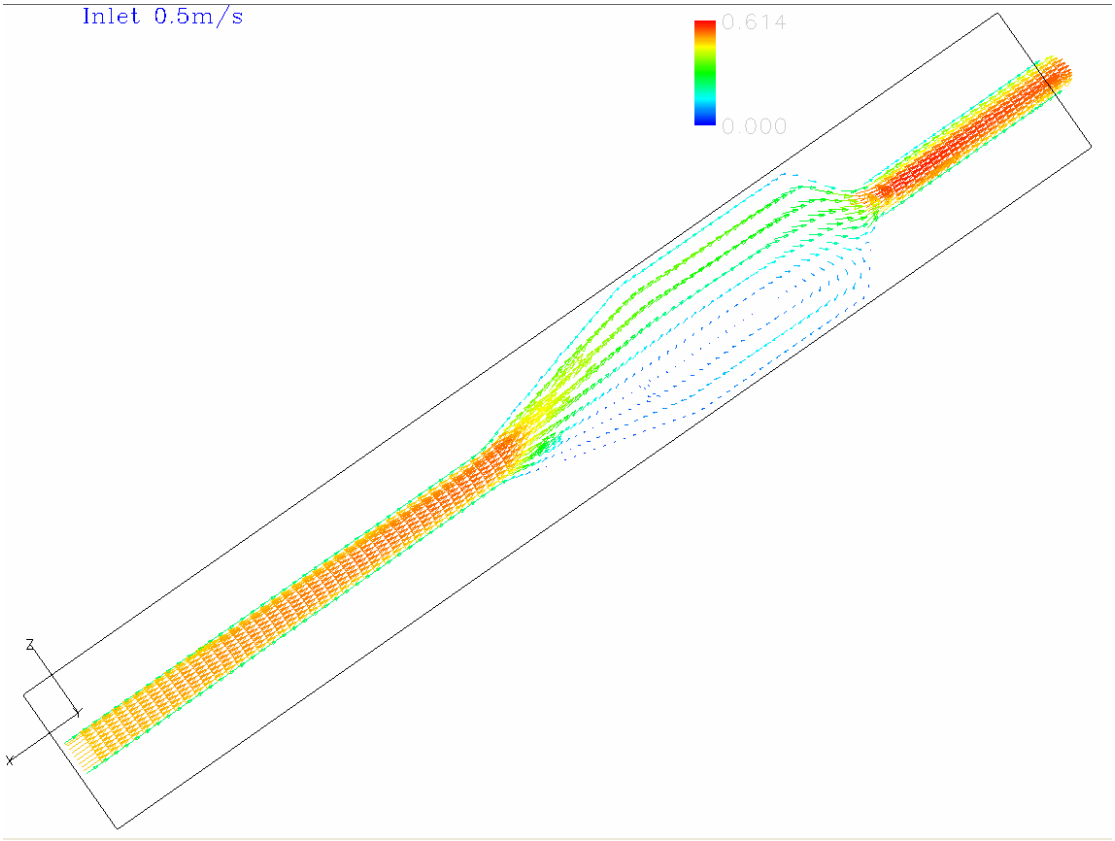

Figure 2: Simulation of inlet velocity 0.5m/s, cross section plane illustration at y=0m

The attachment wall is different in the two simulations at 0.5m/s Figure 2 and 10.m/s Figure 3 inlet velocity. This indicate that the boundary conditions have a influence on the wall attachment effect, and that the attachment formation is determined by the initial conditions.

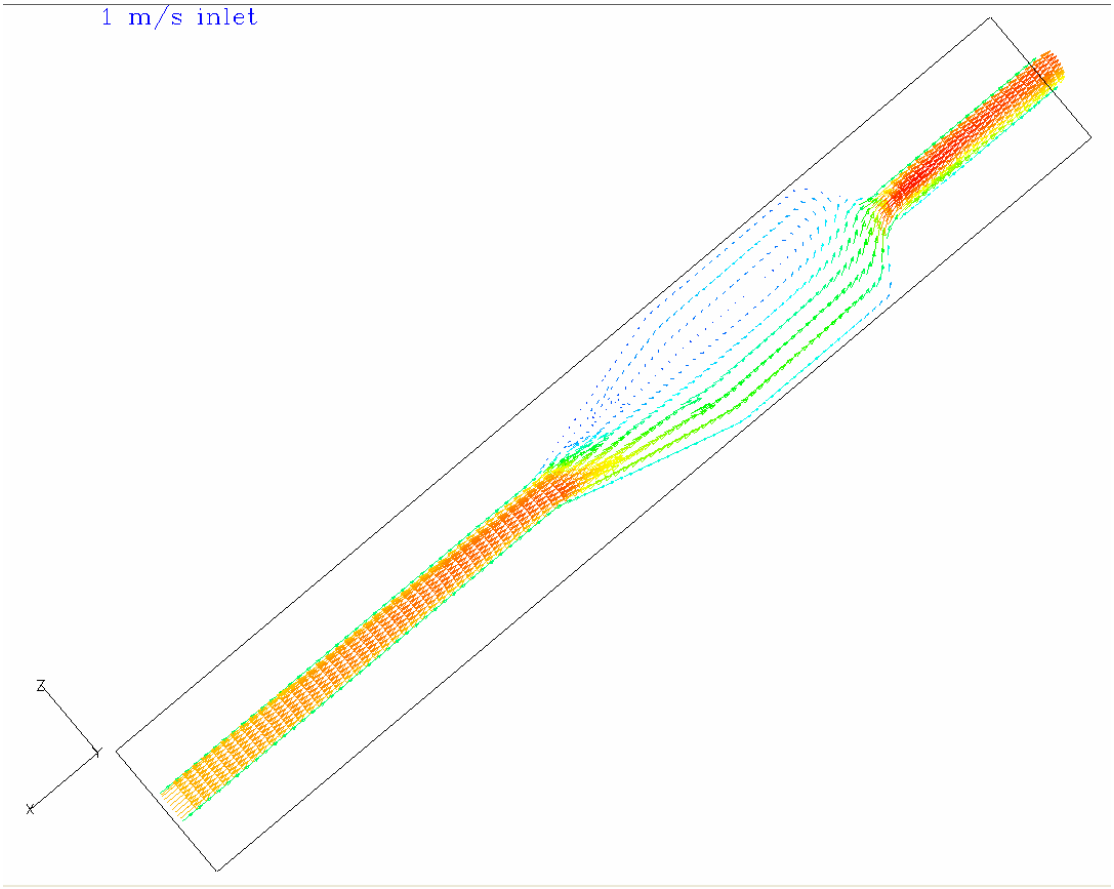

Figure 3: Simulation at inlet velocity 1m/s, cross section plane illustration y=0m

As mentioned above changes in room dimension ratio can have a significant effect on the formation of 3D flow systems. To investigate if the length of the channel system may have any influence on the attachment effect the length of the channel section is increased with 1.6m, the dimensions of the other sections are unchanged. The total expansion flow channel is now 13.6 m long, and the computational grid has 6336 cells.

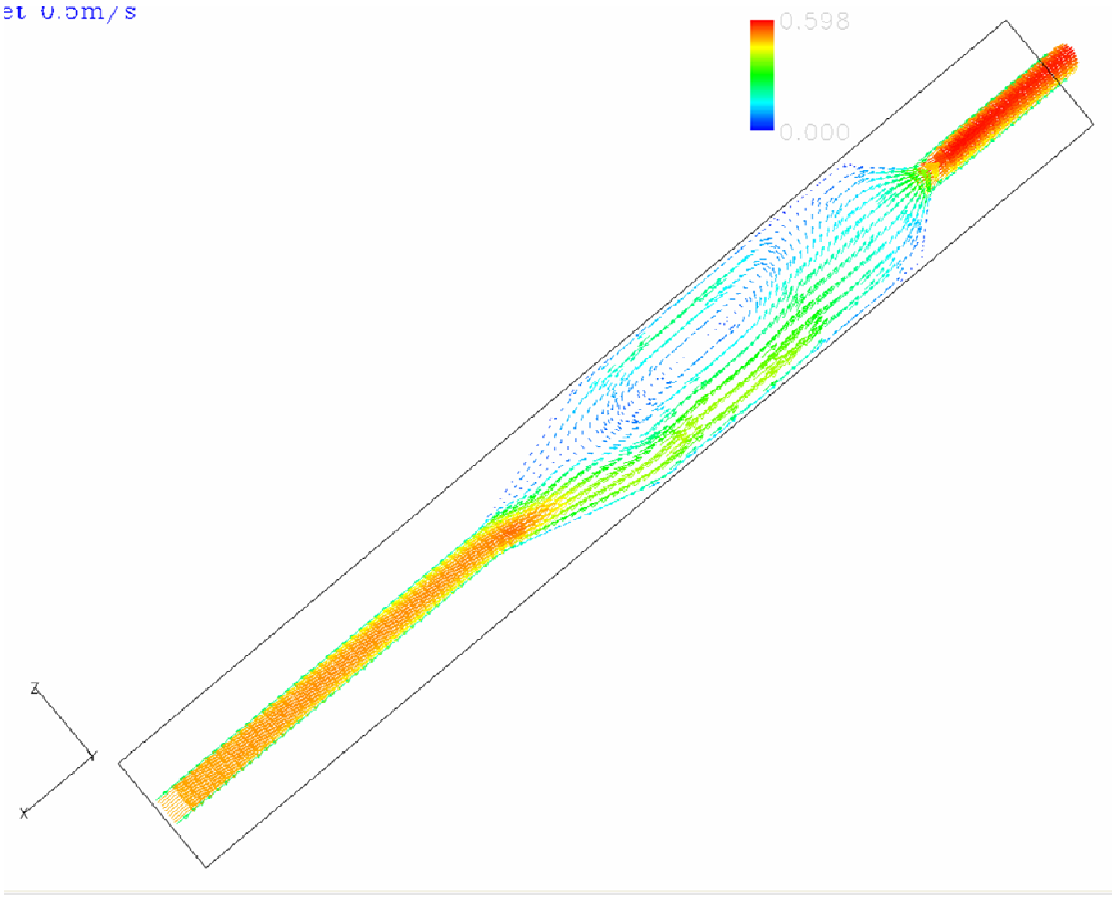

Figure 4: Extended channel section. Simulation inlet velocity 0.5m/s illustration at cross section plane y=0m,

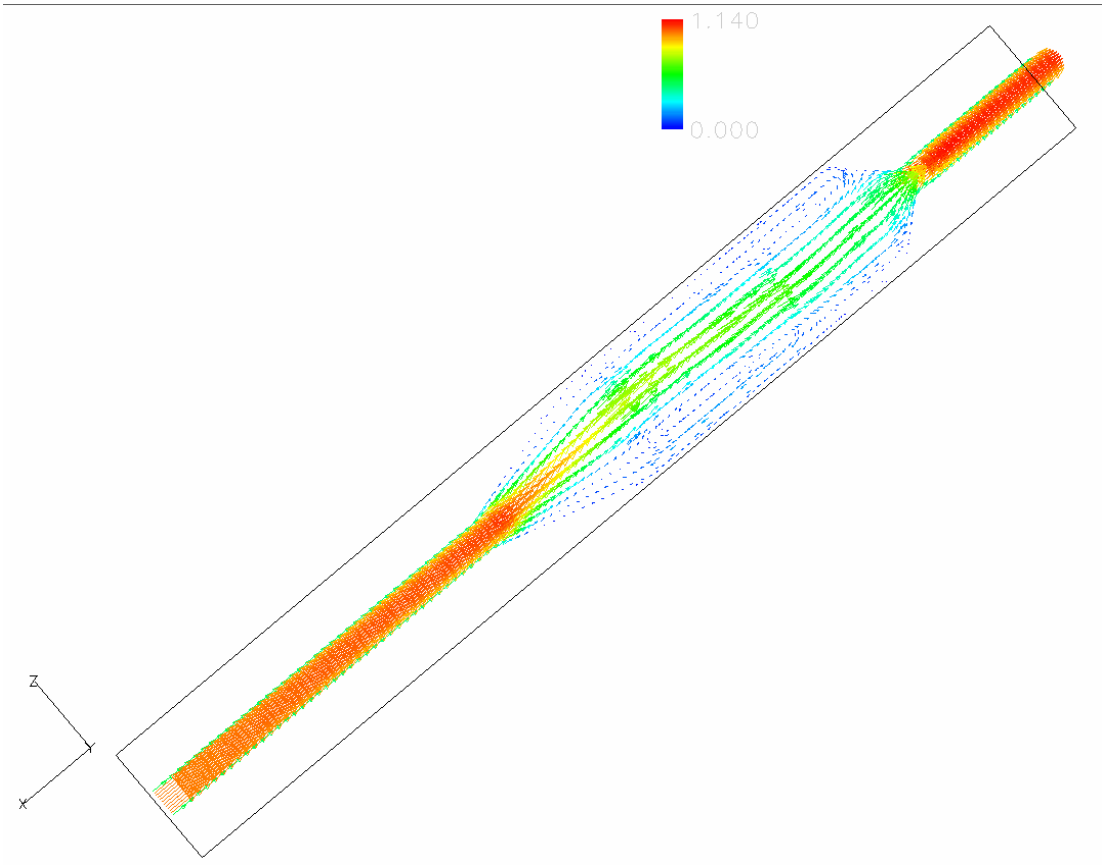

Figure 5:Extended channel section. Simulation inlet velocity 1m/s, illustration at cross section plane y=0m

From the simulations, Figure 4 and Figure 5 it is seen that the flow in the plane y=0 have a jet formation extending from the inlet tube to the outlet tube. In Figure 4 there is a Coanda effect of attaching the jet to the wall and a recirculation flow in the channel section. In Figure 5 there is a jet flowing through the centre of the channel, where a slight disturbed flow is observed. Since the flow is isothermal the Coanda effect, under the given circumstances, can not be dependent on thermal equilibrium conditions. More likely the wall friction induce a Coanda affect that is apparently dependent on the inlet velocity as well as the room dimensions because it appears at inlet velocity 0.5m/s but is not present at 1m/s. The dependency on room dimensions because there is a significant difference on attachment effect with the extension of

channel section Figure 3 and Figure 5. The short channel section attaches to the wall and the long channel section has a jet flowing in the centre of the channel section.

Amendments have to be made in the flow channel to realize the required uniform flow conditions. A flow diffuser is inserted in the cross section between the expansion and channel section, x=6.6m. The diffuser material was assumed mineral wool with a permeability of 5 e-5 m^2 0.1m thick.

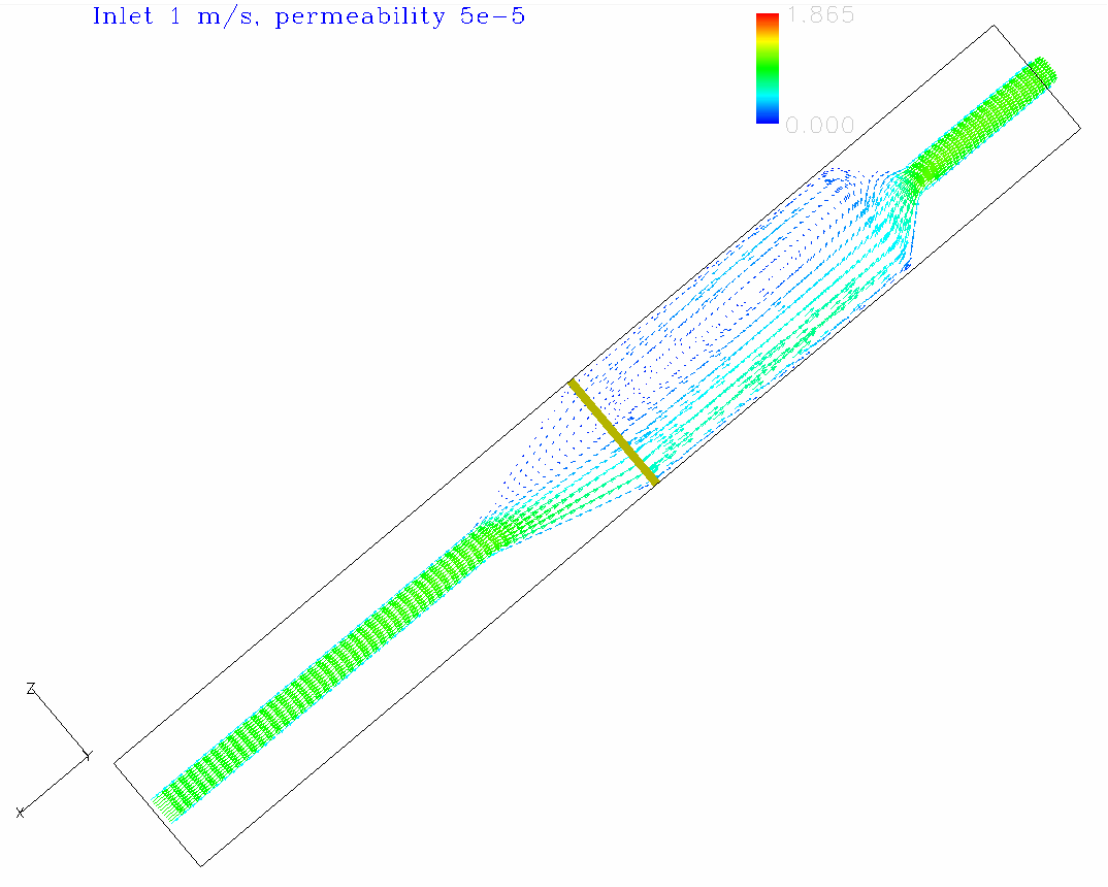

Figure 6:Flow difusor inserted in expansion section. Simulation inlet velocity 1 m/s, illustration at cross section plane y=0m.

As discussed in the above the Coanda effect of a jet entering into a enclosure is dependent on the pressure conditions. The diffuser establishes a pressure increase in

the expansion channel that extends over the entire cross section; this should give a reduction in velocity and a slowing down of the jet core and possibly a more uniform velocity. The change in pressure in the central axis is shown in Figure 7, there is a significant pressure increase in the expansion channel with diffusor.

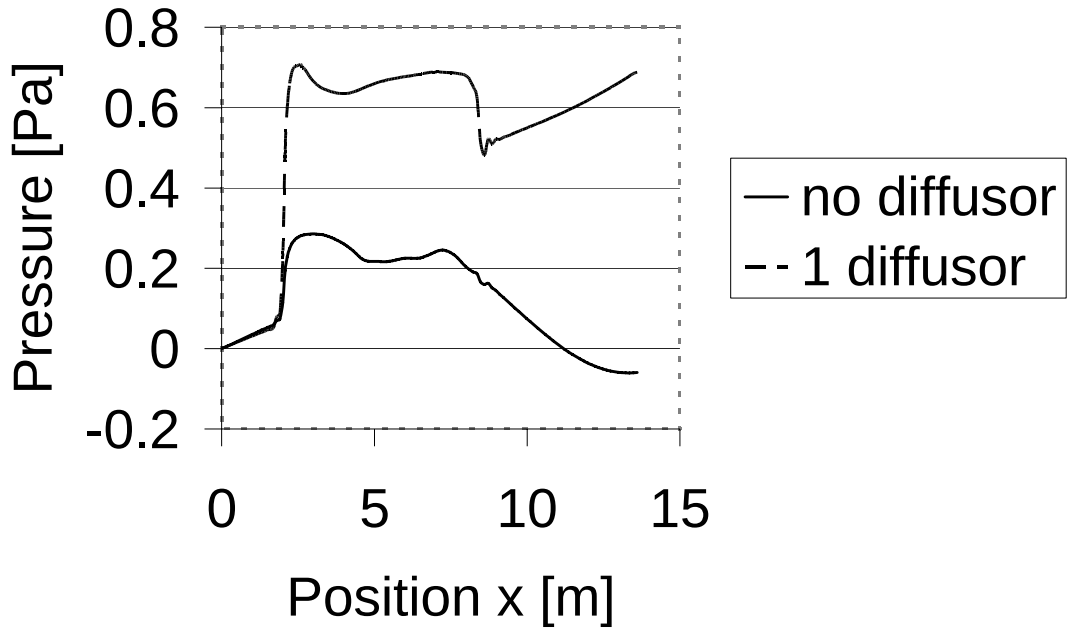

Figure 7: Pressure profile in plane (x,y,z)=(0-13.6,0,0) with and without diffuser between the expansion and channel section. Channel section 3.2m long. Outlet x=0m.

The introduction of a diffuser material induces a Coanda flow attachment to the wall and recirculating flow zone in the channel section, at inlet conditions of 1m/s Figure 6. The flow pattern is now equivalent to the flow pattern at inlet velocity 0.5m/s Figure 4 without the diffuser. An alternative to slowing the velocity down with a flow diffuser could be inserting flow guides in the expansion- and cannel-section. At the junction between the flow in the inlet section and the expansion section the flow is divided into separate flow systems by the flow guides inserted in the expansion channel. The flow guides extend into the channel section but only in the upper half of

the channel height. The channel section dimensions are changed to the original 1.6*1.6*0.4m the number of computational cells is 30208, the iteration time is 400s. In Figure 8 the effect of installing flow guides is shown in plane y=0. The flow guides clearly inhibits the formation of wall attachment but the velocity in the central region around the symmetry axis is elevated compared to the velocity close to the wall region. At the junction between the inlet tube and the expansion section the flow profile in the inlet tube is divided into 8 separate flow systems but with the initial conditions of flow profile of the inlet tube. Boundary layer formation in the vicinity of the flow guides is distinct. To reduce the velocity in the inlet section a pressure increasing diffuser is inserted in the junction between the expansion and channel section. The diffuser material has a permeability of 5e-10 m^2 and is 0.1m thick. The velocity profile of the plane y=0 of the expansion channel with flow guides and diffuser is shown in Figure 9. The insertion of a diffuser improves homogeneity of the spatial flow velocity in the channel section. The flow profile now complies to the demands of spatial and temporal uniform flow velocities.

Repeating the simulations of channel length x=12m and inlet velocity 0.5m/s, Figure 2 with unsteadu flow conditions does not indicate that the formation of the wall attachment should be unstable. During a iteration time of 10000s no a change in attachment position is observed. This supports the assumption that boundary conditions initiate the attachment formation and the flow is steady.

Discussion

The construction changes that have been applied to the expansion flow channel to provide a spatial and temporal uniform flow is quite extensive. One could say that the flow channel is not designed for its purpose and should be redesigned, but to novices

of fluid dynamics, the channel in the original presentation should present no impediment to produce the desired airflow.

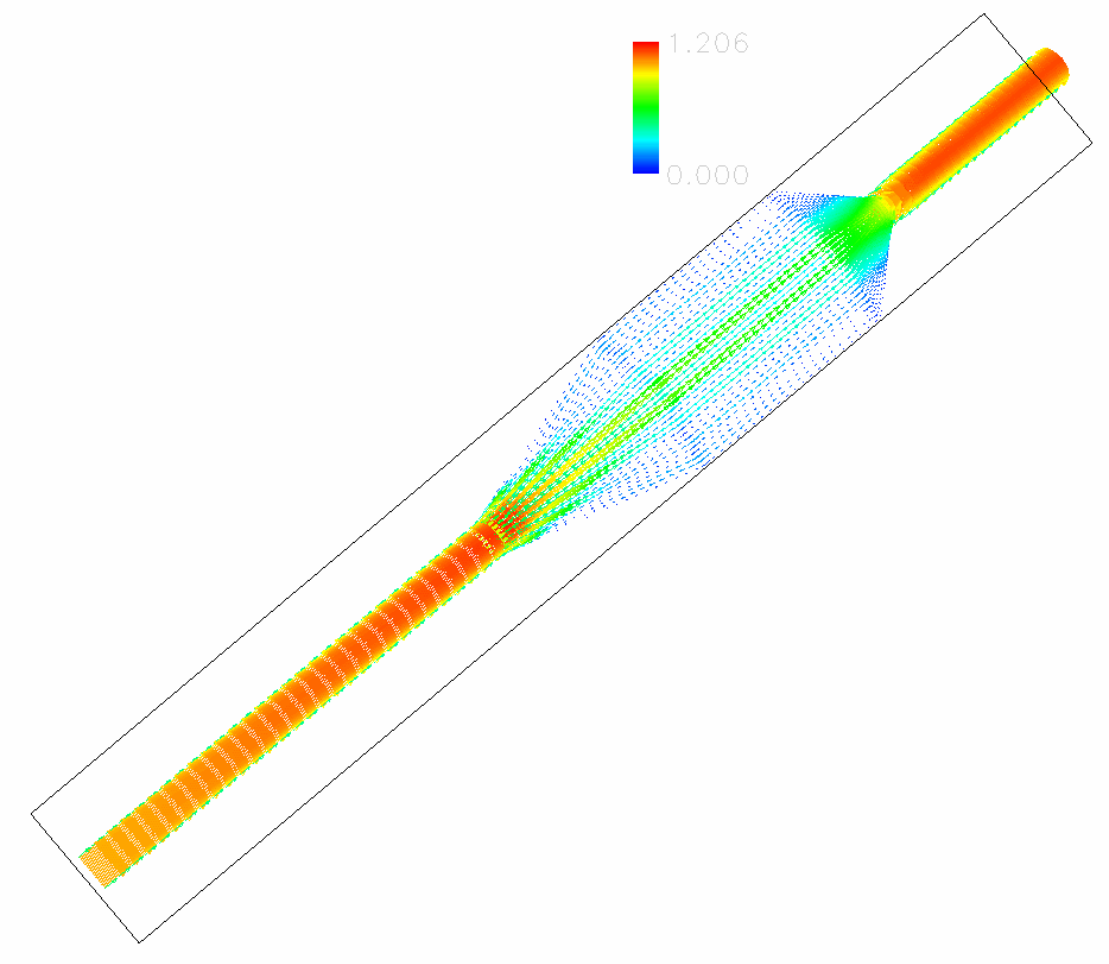

Figure 8: Expansion channel with flow guides. Simulation inlet velocity 1 m/s, illustration at cross section plane y=0m.

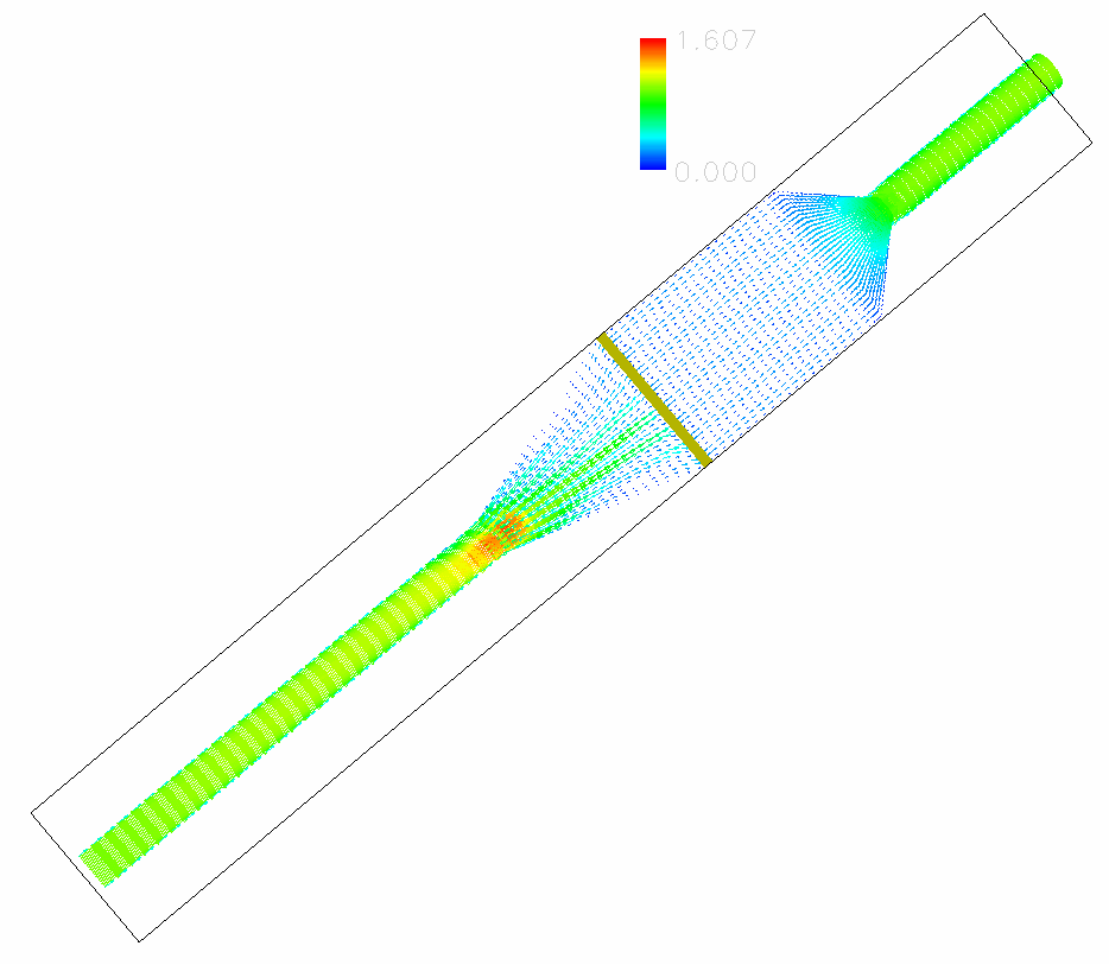

Figure 9: Flow guides and flow diffuser. Simulation inlet velocity 1 m/s, illustration at cross section plane y=0m.

The interesting problem is how to predict the formation of wall attachment. The formation is dependent on the development of a spatially restricted entrainment zone hence the jet distance from the attachment wall, the jet inclination to the wall and the formation of a jet mixing boundary layer may be some of the important parameters. As seen from the above the inlet conditions and room dimensions are also vital parameters to the formation of wall attachment or Coanda flow. The unsteady flow simulations show that the attachment formation is a steady condition in the room geometry investigated here.

Applying the knowledge of Coanda flow effect to understand the development of 3D flows in symmetric flow geometry is reasonable. Although the general flow in a room

does not have jet character, every flow movement is subject to the same principal physical conditions of mixing boundary layers and entrainment flow. The governing equations are the same if its jet flow or full scale flow in a room. The pressure conditions that onset the formation of jet attachment to the wall may be locally retrieved in the buoyancy driven flow in a occupational room.

Reference List

Bjerg, B., S. Morsing, K. Svidt, and G. Q. Zhang. 1999. Three-dimensional airflow in a livestock test room with two-dimensional boundary conditions. *Journal of Agricultural Engineering Research* 3:267-274.

Bjerg, B., K. Svidt, G. Q. Zhang, and S. Morsing. 2000. The effects of pen partitions and thermal pig simulators on airflow in a livestock test room. *Journal of Agricultural Engineering Research* 77:317-326.

Chen, Q. and J. Srebric. Simplified diffuser boundary conditions for numerical room airflow models. RP-1009, 1-178. 2001. Atlanta, ASHRAE.
Ref Type: Report

Rees, S. J., J. J. McGuirk, and P. Haves. 2001. Numerical investigation of transient buoyant flow in a room with displacement ventilation and a chilled ceiling room. *International Journal of Heat and Mass Transfer* 44:3067-3080.

Triboix, A. and D. Marchal. 2002. Stability analysis of the mechanism of jet attachment to walls. *International Journal of Heat and Mass Transfer* 45:2769-2775.

Zhang, G. Q., S. Morsing, B. Bjerg, K. Svidt, and J. S. Strøm. 2000. Test room for validation of airflow patterns estimated by computational fluid dynamics. *Journal of Agricultural Engineering Research* 74:141-148.

INTERNAL PAPER:

Testing the Solution Accuracy of CFD2000 on the Two Dimensional Test Case.

Testing the solution accuracy of CFD2000 on the two dimensional test case.

The experimentally well proven test case in Nielsen (1990) is used to run some quality control tests in the simulation software CFD2000. The focus of the simulation is to reproduce some of the findings in Sørensen et al.(2003) concerning changes in number of grid cells and differencing schemes order of accuracy. According to Sørensen et al. (2003) the effect should be:

1. for a given grid size, higher order schemes are superior to lower order scemes
2. the additional accuracy obtained by increasing the grid size increases with the order of the sceme.

A supplement to the testing of the above hypothesis the effect of a non homogeneous resolving gradient cell sizes are tested.

In CFD2000 the simulation solution is only obtainable in the cell center. If the exact same geometrical point for the reference point is acquired for comparison of different solutions at different grid size solution cell must be either frozen or the solution must be calculated using linear interpolation between neighboring cell centers.

If the cellsize is frozen sizing inhomogenity to the surrounding cells will occur. This can give an error with dispersivity of the solution. (changes in numerical diffusion)

Methods:

Table 1: Specification of simulation parameters for the 4 different testcases. 2 similar tables at 2. and 3. order convection differencing schemes exist, of which results are presented.

Test Case	Gridpoints	Diff. Order	**Test Case** Reference cell	Reference cell center coordinate (x;y;z) [m]	Reference cell dimension ($x_1;y_1;z_1$) [m]
1.a.1	209	1	Floating Point	(5.7;0.4;0.05)	(0.6;0.16;0.1)
1.b.1	800	1	Floating Point	(5.55;0.336;0.05)	(0.3;0.096;0.1)
1.c.1	3000	1	Floating Point	(5.5;0.36;0.05)	(0.2;0.048;0.1)
1.d.1	12000	1	Floating Point	(5.45;0.324;0.05)	(0.1;0.024;0.1)
2.a.1	240	1	Frozen cell	(6.05;0.53;0.05)	(0.1;0.1;0.1)
2.b.1	861	1	Frozen cell	(6.05;0.53;0.05)	(0.1;0.1;0.1)
2.c.1	3116	1	Frozen cell	(6.05;0.53;0.05)	(0.1;0.1;0.1)
2.d.1	12231	1	Frozen cell	(6.05;0.53;0.05)	(0.1;0.1;0.1)
3.a.1	240	1	Frozen cell	(6.005;0.485;0.05)	(0.01;0.01;0.1)
3.b.1	861	1	Frozen cell	(6.005;0.485;0.05)	(0.01;0.01;0.1)
3.c.1	3116	1	Frozen cell	(6.005;0.485;0.05)	(0.01;0.01;0.1)
3.d.1	6161	1	Frozen cell	(6.005;0.485;0.05)	(0.01;0.01;0.1)
3.e.1	12231	1	Frozen cell	(6.005;0.485;0.05)	(0.01;0.01;0.1)
4.a.1	209	1	Interpolation	(5.4;0.32;0.05)*	(0.6;0.16;0.1)**
4.b.1	800	1	Interpolation	(5.4;0.32;0.05)*	(0.3;0.096;0.1)**
4.c.1	3000	1	Interpolation	(5.4;0.32;0.05)*	(0.2;0.048;0.1)**

4.d.1	12000	1	Interpolation	(5.4;0.32;0.05)*	(0.1;0.024;0.1)**

*The cell center is frozen and is not the geometrical center of the four surrounding interpolation cells.

**the four cells used in the interpolation all have the same dimensions.

The grid are stretched towards the wall in the x direction of the domain, with a stretching factor 1.4. All other grids are equidistant. An example of a grid is shown in fig 1.
The domain is divided in 3 or 4 sections in both the x and y direction. The number of cell divisions in each section is shown in table 2.

Table 2: Number of cell divisions in each section of the grid.

Gridpoints	X1	X2	X3	X4	Y1	Y2	Y3	Y4
240	7	5	1	7	3	1	5	3
861	15	10	1	15	5	1	10	5
3116	30	15	1	30	10	1	20	10
6161	40	20	1	40	15	1	30	15
12231	60	30	1	60	20	1	40	20
209	7	5		7	3		5	3
800	15	10		15	5		10	5
3000	30	15		30	10		20	10
12000	60	30		60	20		40	20

5000 iterations was used in all tests.

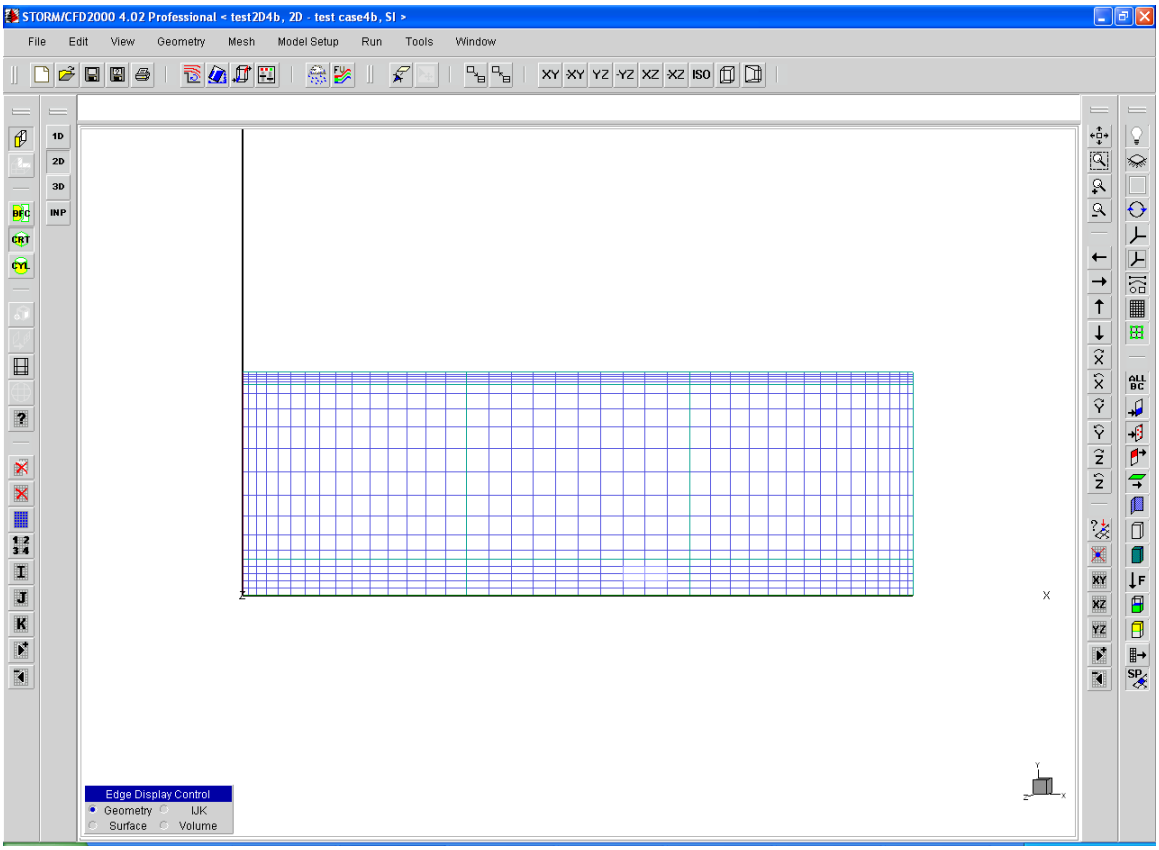

Fig. 1: Screendump presentation of griddistribution of test case 4.b.

Results.

The Test cases are evaluated using the grid convergence index (GCI)

$$GCI = F_s \left| \frac{f_2 - f_1}{1 - r_{12}^p} \right|$$

where F_s=3, $r_{12} \rangle 1$, f_2 and f_1 represents the solution of the coarse respectively fine and p is the formal order of accuracy of the differencing scheme. If $r_{12}=r_{23}$ then

$p = \ln\left(\frac{f_3 - f_2}{f_2 - f_1}\right) \Big/ \ln(r_{12})$ but not if the asymptotic convergence has been reached because

then $p \to 0$ and the solution of GCI gives a infinite number of solutions. We use p=1.

$r_{12} = \frac{h_2}{h_1}$ where h_2 represents the grid spacing (m) of the coarse grid and h_1 represents the grid spacing of the fine grid thus. In the analysis the calculation h_2 is substituted by the number of gridlines in the coarse grid and h_1 is the number of gridlines in the fine grid shown in table 2. r_{12} is in the range between 1.5-2.14. If the definition of r_{12} is

$$r_{12} = \frac{n_1}{n_2}$$

where n_1 is the number of cells in the fine grid and n_2 is the number of cells in the coarse grid r_{12} is in the range between 3.75-4.00. Because the test exercise are to evaluate the effect of inhomogeneous cell and frozen cell size the definition of r12 based on cell number is utilized.

A very intruding problem with CFD2000 is the program inability of stating more than 3 decimal. This is crucial when the residuals of f_1 and f_2 are in the 10^{-9} the GCI are zero or no solution to the GCI are found. Using the residual as a indication of the last significant digit it is possible to estimate a better solution in the asymptotic convergence area.

The solution and the GCI is calculated only for the u-composant of the velocity.

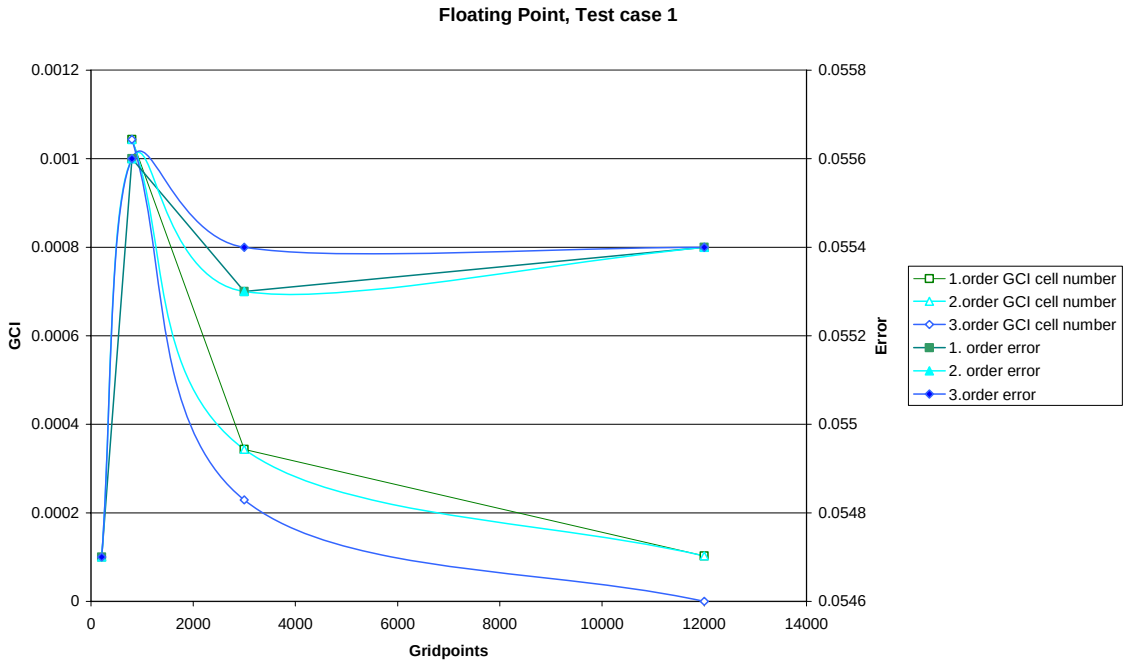

Fig.2: Test case 1. Floating point reference cellcenter.

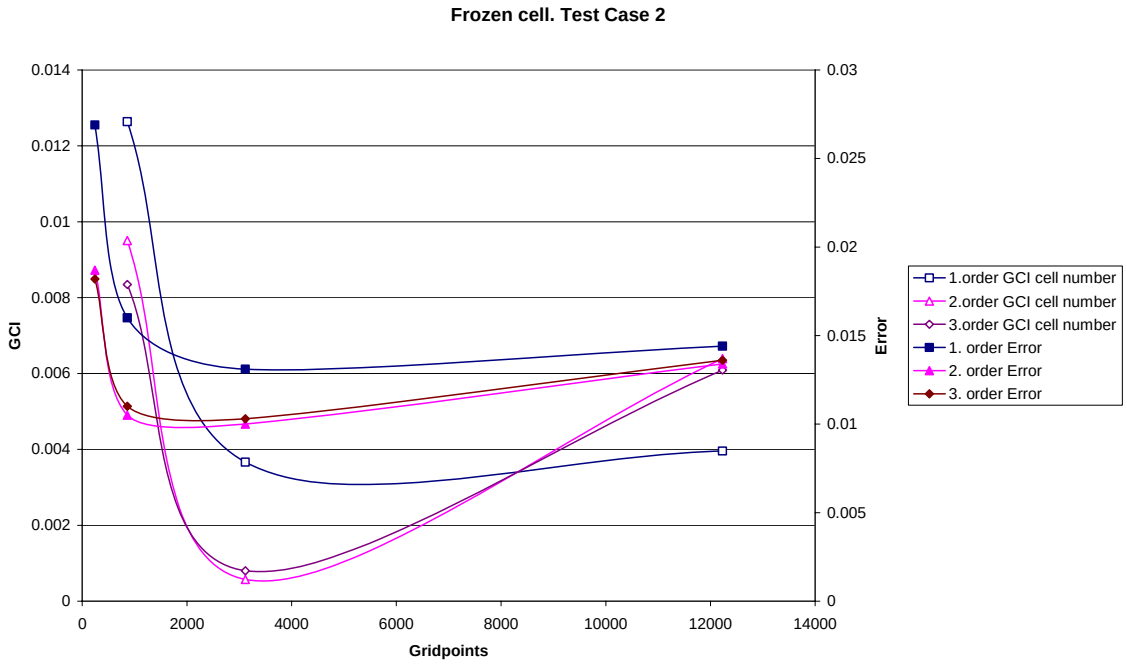

Fig. 3: : Test case 2. Frozen cell dimension (0.1,0.1,0.1)

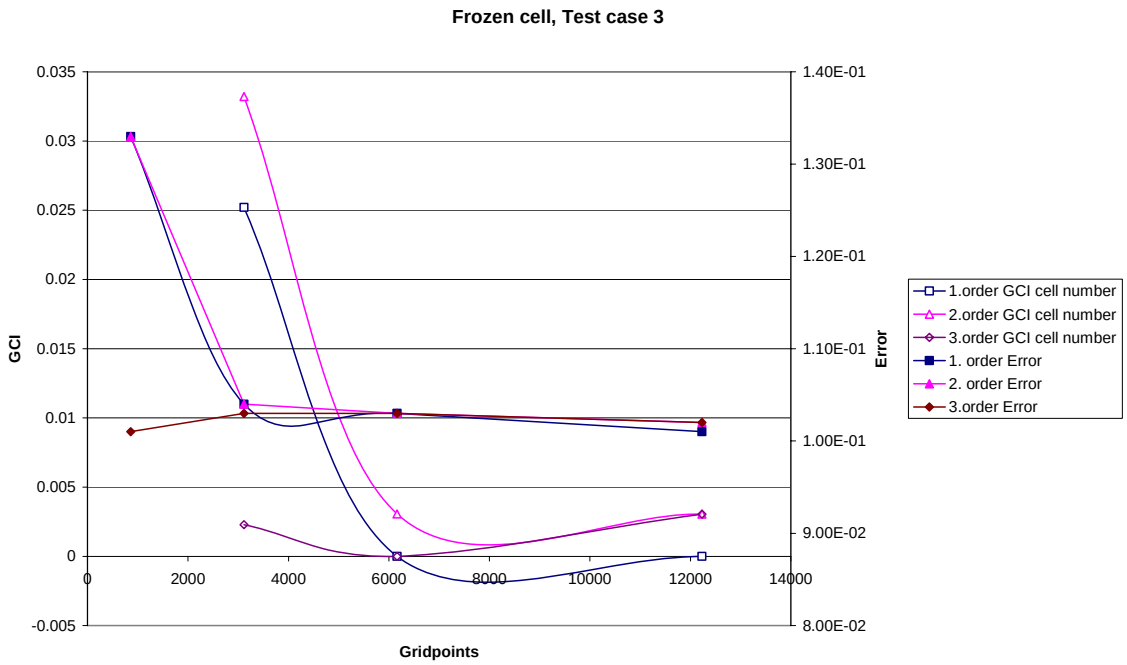

Fig. 4: Test case 3. Frozen cell dimension (0.01,0.01,0.1)

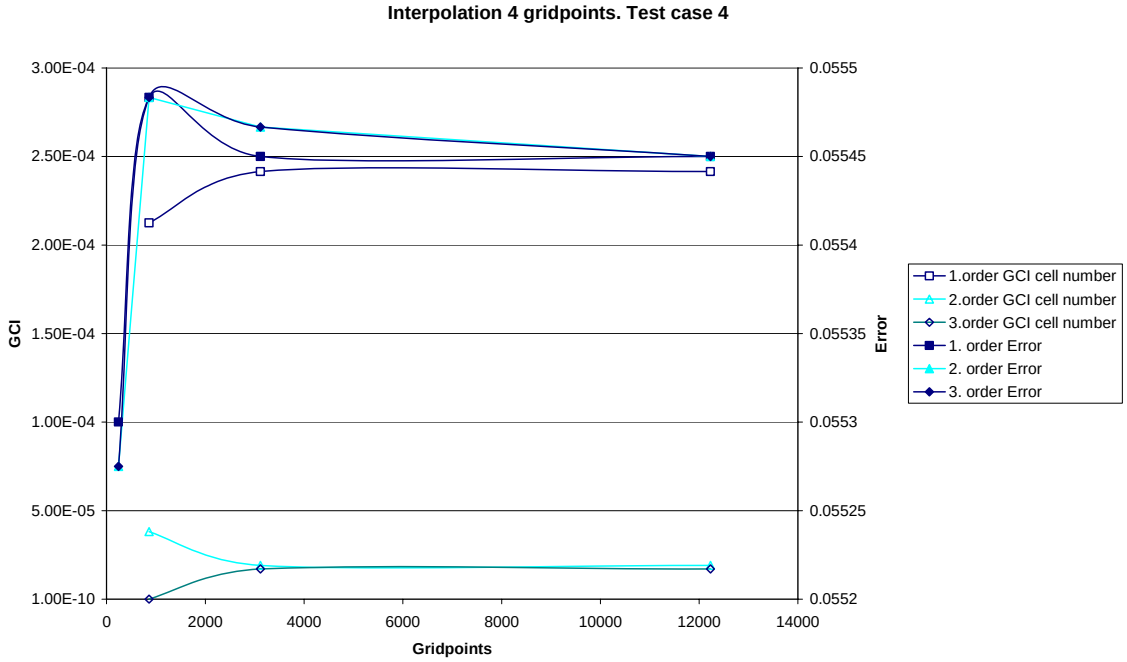

Fig. 5: Test case 4. Interpolation of 4 neighboring cellpoints.

Results

In the grid refinement study the number of gridlines are increased by a factor 2 at each succeeding test sequence according to recommendations in Sørensen et al. (2003). But the solution in test case 3 at 240 gridpoints the solution diverge, assumingly because if the large sizing inhomogeneity of the cells at small gridpoint numbers. Because of this an additional test sequence of 6161 gridpoints are added. There are some overlapping of the results of different runs, primarily 1. and 2. order differencing schemes. This is marked by using both a linear and a smoothed line between the datapoints.

Test Case	1	2	3	4
ΔGCI_{800}	0	4.3e-3	3.1e-2**	2.1e-4
ΔGCI_{12000}	1.0e-4	2.4e-3	3.0e-3	2.2e-4
$\Delta Error_{200}$	0	8.7e-3	3.2e-2*	2.5e-5
$\Delta Error_{12000}$	0	1.0e-3	1.0e-3	0

*at ~800 gridpoints, ** at ~3000 gridpoints

Table 3: Max. difference between value of GCI and Error at max and min value of gridpoints.

Table 3 show that the increase in gridpoints independently of the differencing scheme will reduce both the difference between the error estimate of the grid convergence index and the actual error in all cases except test case 1.

In fig. 2 both the CGI and the error have a converging tendency although the error estimate increases at low gridpoint numbers. Changing to a frozen cell monitoring point

and a inhomogeneous grid distribution in fig 3 and 4 the actual error and the GCI show a converging tendency in all but the GCI for the 2. and 3 order diff. scheme in test case 2 (fig. 3) . This could be because the frozen reference cell is large compared to the surrounding cell dimensions and therefore gives an increase in error at the fine grid. The convergence tendency in test case 3 supports this assumption. In test case 3 (fig. 4) at the coarse grid the actual error and the GCI of the 3. order diff. scheme are substantially lower than the equivalent at the 1. and 2. differencing scheme. Apparently the 3. order differencing scheme deals much better with inhomogeneous grid layout than the lower order differencing schemes. Test Case 4 has the best converging tendency of the for tests and the GCI estimate of the higher order diff. schemes are very low. The result indicates that it is very important for the evaluation of the actual error and the GCI that the grid layout have a homogenious structure.

Reference List

Nielsen, P. V. (1990) "Specification of a two-dimensional test case.". International Energy Agency, Energy Conservation in Buildings and Community Systems, Annex 20:Air Flow Pattern Within Buildings.

Ref Type: Report

Sørensen, D. N. and Nielsen, P. V. (2003) "Quality control of computational fluid dynamics in indoor environments.", *Indoor Air*, **13**, 2-17.

Ref Type: Journal